LIGHTNING DATA STUDY IN CONJUNCTION WITH GEOSTATIONARY SATELLITE DATA

A Final Report to

National Aeronautics and Space Administration

Contract NAS 8-35981

University Account #144-U650

for the period of

June 23, 1984 to December 22, 1987

Prepared by

Brian Auvine
David W. Martin

Space Science and Engineering Center
at the University of Wisconsin-Madison
1225 West Dayton Street
Madison, Wisconsin 53706
(608) 262-0544

for

George C. Marshall Space Flight Center
Huntsville, Alabama 35812

December 1987

ABSTRACT

During the summer season of 1985, cloud-to-ground stroke lightning from the NSSL and NASA-Marshall networks of LLP and the North Central States network of LPATS were collected and made available on McIDAS, along with improved analysis software. Using the LLP data, 30 minute samples of lightning data were compared with GOES IR fractional cold cloud coverage computed for three temperature thresholds (213, 243 and 273 K) twice daily (morning and evening). Results for the two networks were comparable, with the fraction of cloud colder than 213 K and the minimum cloud top temperatures having the best correlation with flashrate, especially of positive flashes. Little lightning occurred for samples where minimum cloud top temperatures were warmer than 243 K. Regression shows from 47 to 66% of the flashrate variance explainable at NSSL using all three fractional cloud coverages and the minimum temperature. Statistics for all flashes in our samples showed about 3.4% with positive polarities and an average of 2.2 return strokes per flash. Three times as many flashes occurred in our evening as compared to our morning samples. However, strokes magnitudes were generally greater in the morning at NSSL.

The LPATS data from two case study periods (Days 250-251, 251-252) were compared to minimum temperature and the rate of anvil expansion using GOES rapid scan imagery. Composites of flashrate, anvil area change and anvil minimum temperature show declines in temperature and increases in growth rate during the period of flashrate increases. After the peak flashrate, temperature either leveled off or continued to decline for another 30 minutes before beginning an upward trend. Rate of area change declined or remained steady. The lag of temperature behind the area change may be due to the combined effects of the later arrival of higher speed updraft velocities to anvil level and the failure of the IR sensor to revolve the overshooting tops until they had spread out over a large area.

Results of these study encourage the belief that changes in anvil temperature, area and cloud coverage are significantly related to flash rate and can be used to monitor or predict the amount of lightning associated with satellite observed infrared cloud.

ACKNOWLEDGMENTS

The authors would like to thank Mr. Steven Goodman, Manager of the NASA Marshall Lightning Network, Dr. Donald MacGorman, Manager of the NSSL Network, and Dr. Walter Lyons (R*Scan Corporation), Manager of the LPATS network data provided by Atlantic Scientific Corporation. These individuals not only granted access to their respective data sources, but also provided many helpful comments on the interpretation of the data and our final conclusions.

Significant contributions to this work were also made by Joseph Rueden, Ralph Dedecker, Raymond Lord, Gail Dengel, and Irwin Bitter (ingest software and hardware); Dave Santek (applications software); and Robert Gifford, Gary Krueger, and David Slezewski (programming and processing assistance), all of SSEC.

Finally, thanks is due to Mr. Andy Edman and Dr. Fred Mosher of NSSFC, Michael Meier of LLP, Inc. and Dr. Hugh Christian, NASA Project Monitor for providing much needed information and assistance in the course of this work.

TABLE OF CONTENTS

Lightning Data Study in Conjunction with Geostationary Satellite Data

1. Introduction

This is the final report on NASA Contract NAS 8-35981 - Lightning Data Study in Conjunction with Geostationary Data. The original contract proposed work in three main areas: expansion of the Man-computer Interactive Data Access System (McIDAS) database to include access to lightning data from multiple sources, development of tools on McIDAS to display and analyze lightning data in conjunction with geostationary satellite images, and the application of lightning data to understand and monitor thunderstorm processes. In the following sections of this report, activities and findings for each of these areas will be described. Section 4, covering the relation of lightning to some satellite-observed properties of thunderstorms, has been broken down into two parts. One, which we term climatological, is a study of averaged cloud-to-ground flash characteristics over a period of several summer months in relation to GOES infrared cloud cover. The other, our case studies, compares the behavior of storm anvils in the infrared with changes in lightning flash rates over periods of less than a day.

2.0 Formation and Expansion of a Cloud-to-Ground Lightning Database

2.1 Data Collection Efforts

During the time in which this contract has been active, the ground networks for cloud-to-ground lightning flashes have been in a state of great flux. Existing Lightning Location and Protection (LLP) systems have undergone relocation or expansion, difficult decisions about who should have access and at what cost have been implemented, processing and communications technology has changed, and an entirely new system for ground flash detection, Lightning Position and Tracking System (LPATS), has appeared on the scene as an alternative to LLP. In particular, planning for a national data archive and the creation of a National Lightning Demonstration Network have appeared as promising signs of a trend toward wider access to lightning data. These developments have necessitated modifications of our specific data collection objectives over the course of this project.

In general terms, however, we have continuously aimed at two main goals: to obtain data adequate for the analysis tasks proposed by this contract, and to enhance the ability of McIDAS to serve as a lightning data base. To fulfill the first objective, we hoped to obtain samples of data from a minimum of two distinct geographical areas. One of our scientific goals was to be able to compare averaged lightning behavior between regions that varied in topography and synoptic regimes, if possible.

Realization of our other objective, to make McIDAS a more effective lightning data base, meant not simply access to real time data but also provision of software and hardware resources needed for adequate access to and reduction of the data. It was our hope that McIDAS would offer aid to SSEC scientists as well as other research groups working in the same general area.

Essential to all of these aims was access to at least some of the existing

lightning network databases. Of these we considered five possibilities: the Bureau of Land Management (BLM) fire prevention network, covering most of the Western U.S.; the State University of New York at Albany East Coast LLP network managed by Dr. Richard Orville; the Marshall Space Flight Center LLP network in northern Alabama; the National Severe Storm Laboratory LLP network in Oklahoma, Kansas and Nebraska; and the North Central States LPATS network. Beginning in early 1985, we attempted to establish real-time or near real-time access to all of these networks. Ultimately we were successful with all but the first two on this list.

The problems with the BLM were primarily bureaucratic. Although SSEC had installed ingest boxes for real-time access to BLM data in the summer of 1983 without difficulty, the BLM had since decided to institute user charges for any agency outside the BLM. Because the mechanism for these user charges would not be operational until late in 1985, the Bureau essentially closed all real-time access to its network in the meantime. Even supposing the proposed user fees had been instituted, it is doubtful that this program could have afforded access. At a 5¢/acre for the six month season, individual states would have cost an average of $3000 and the entire ten state network around $30,000 (telephone conversation with Mr. Lonnie Brown, 3/20/85).

It also proved impossible to work out a practical arrangement with Dr. Orville regarding access to the East Coast network. Although dial-up links already existed between Albany and SSEC, we needed technical cooperation from Albany programmers to test out communications and ingest software. Beginning in February, these matters were discussed in detail, but in late May (letter dated May 23, 1985), Dr. Orville finally decided that he could not commit the time or energy needed to complete the technical tasks of establishing a real-time link without further lengthy consideration. Since we were already well into the lightning season, we judged that further delays negated any advantage we might

obtain from access.

Connecting into the NSSL network proved to be relatively simple, despite some hardware problems. First, the ingest boxes used in the earlier NASA funded project with BLM needed to be refurbished to deal with differences in the NSSL raw data stream. At the end of April and with the consent and assistance of Dr. Don MacGorman at NSSL, an engineer was sent to Norman to install the box. Subsequent operation from late May through to the end of September resulted in a collection of data from all three of the Oklahoma direction finders, with some data holes caused by a fluctuating power source at Norman. This data proved useful in testing the methodology of the scientific tasks of this project, and in laying the groundwork for other real-time network access. A nearly complete set of 1985 NSSL data was later obtained on magnetic tape to give us a large and nearly continuous sample for our climatological study.

Access to the Marshall Space Flight Center Network was conceptually straight-forward. Links between the McIDAS IBM and the Marshall IBM and Harris systems were scheduled to be installed (using funds for another project) sometime during the spring of 1985. NASA budgetary problems, however, prevented work on the links and access to Marshall data was delayed until the beginning of August. Most of the data used in the scientific portion of our study came from lightning files on magnetic tape sent from Marshall by Mr. Steven Goodman.

Finally, our tie-in with the North Central LPATS network occurred in two phases. At the invitation of Dr. Walter Lyons of R*Scan Corporation, the company marketing the LPATS system, we accessed the files of real-time data being brought into the National Severe Storms Forecast Center (NSSFC). As in the Marshall situation, communication links were not completed until August and we subsequently obtained most of the data used in our study via magnetic tape archives. The second phase of access began in February of 1986 when a letter of agreement between SSEC and R*Scan Corporation allowed Center access to the raw

North Central network data in exchange for providing space on our roof for an LPATS antenna. Since then, the antenna and a multiplexor have been installed, an ingest program has been written (the only task for which funds from this project were used), and the data have been made available on a real-time basis for any research and developmental uses on McIDAS. Access is expected to continue indefinitely.

2.2 Lightning Database and Software Users

Primary users of the database collected via real-time and supplemented with archive tapes have been the participants in this project. Real-time data has been useful in testing the research methodologies of this study, choosing data sets for the case studies, acquiring general knowledge of lightning behavior, and developing new software. More recently, the real-time LPATS data have become generally available to undergraduate and graduate students in the UW Department of Meteorology for use in synoptics and thesis research.

During the course of this study, our facilities for handling lightning data have proved useful to NSSL, NSSFC and MSFC. We have converted over a year's worth of raw magnetic tapes to meteorological data (MD) files for use in the joint NSSL-NSSFC comparative study of LLP-LPATS data and developed a variety of ingest and analysis utilities, some of them in response to specific outside inquiries. These resources should continue to be useful long after the termination of this project.

2.3 Some Conclusions on Lightning Database Collection

Based on our experience with the data collection aspects of this project, we have some general conclusions about the technical and political aspects of lightning data collection. We also have some recommendations for any future efforts in this area.

It is not technically difficult to access data from several lightning networks simultaneously. Even with the now outmoded ingest box technology, total cost for accessing three networks as described above ran around $5000.

Communications cost for transmitting the data once the installation is complete can be expensive for a large lightning network, such as the East Coast or BLM networks (probably on the order of several thousand dollars a month on a dial up line). For small networks such as NSSL, the cost of a dial up line for the entire summer was around $1000. Where dedicated lines already exist (i.e. between SSEC and Marshall or SSEC and Kansas City), communications costs, of course, are covered under general operations with little difficulty since the volume of lightning data compared to other data transfers is small.

The current proprietary nature of lightning data collection presents the greatest obstacle to bringing such data on line for research and operations. Contributions to this maze of difficulties come from several sources: (1) there are two competing and conceptually different lightning detection systems currently on the market. While LLP, Inc. had a head start in sales and deployment, LPATS "arrival time difference" technique offers certain theoretical advantages in accuracy and ease of operation (Lee, 1986). Competition for market position between the two companies assures continued uncertainty over the future character of lightning detection networks. Charges for purchase of, or access to data, or technical assistance from these two companies is also unpredictable. (2) Quality control of lightning data is far from standardized and the process by which it is done is laborious and untimely. While this difficulty is to be expected given the uncertainties connected with this new technology, the lack of standardized quality control has caused delays in the distribution of high quality data and an unevenness of quality over time and among the various networks. (3) There are substantial differences among the existing networks in design, use, and public access.

In large part due to the factors above, some network managers hesitate to share their data or have not articulated a policy for use of their data. There is legitimate concern that a careless or naive user will apply the data in a misleading manner, making the data source or the basic instrumentation appear to be far better or worse than it really is. Basic ground rules for outside use and standardized and documented quality guidelines would be helpful in minimizing these concerns.

Perhaps the best hope for extending networks and increasing the use of ground based lightning data can be found in the current discussions on the formation of a national archive of lightning data taking place in the Office of the Federal Coordinator for Meteorological Services and Supporting Research. With the eventual deployment of a satellite-borne lightning mapper, there will be increased interest in and understanding of the utility of lightning stroke information and there will be more pressure to bring together the collective data resources we have in this area. The emphasis within the Earth Systems Science effort on the pooling and networking of geophysical data will have a similar effect.

Based on the experiences we have had in this project, we have these general recommendations on planning a large regional or national lightning archive for research and operations.

(1) A long lead time of a year or more is needed to construct an adequate archive plan and to bring together the people and resources needed to make an access plan work. The needs and requirements of each network manager should be written into the contract along with commitments to provide certain services (e.g. technical information on the network, quality control processing, interpretation of data). In addition, programmers and engineers need time to devise data transfer and ingest schemes.

(2) The users of the archive and their application of the data need to be

defined, at least in a general way. Given the differences in the networks described above and the absence of general ground rules, there needs to be a general understanding of what the current earth-based systems can and cannot do. At least at first, an archive might only be available to selected researchers and federal operations like NSSFC.

(3) If Steps 1 and 2 are followed above, then some important inputs into the design of the data transfer and ingest can be established; namely, the number of users, the amount and technical specifications of the data, and (through knowledge of the intended applications) the frequency and desired form of access for each user. Together, this information will help in choosing the format of the data archive and the modes by which it will be accessed.

(4) As with all efforts nowadays in the rapidly changing field of database management, adequate consideration needs to be given to the growth of microcomputer communications and networking. Lightning data might provide an ideal ground upon which to build a model archive system taking full advantage of current technology.

It is our general hope that in the near future the exciting operational and research possibilities inherent in ground-based lightning systems will become more generally known and supported.

3.0 Development of Display and Analysis Tools

At the beginning of this program, we had on hand some very basic facilities for processing and analyzing lightning data. Foremost among these is the IBM 4381 McIDAS which is capable of displaying and manipulating satellite data in conjunction with other data. Our first task was to develop the capability for lightning data to be received either directly through telephone dial-up or dedicated lines or indirectly via magnetic storage media. For each of the three networks described in the previous section, ingest software had to be written to decode the raw data parameters as they were transmitted from the source and translate them into a McIDAS-intelligible data stream for deposit in mass storage (MD files). Fortunately, basic similarities in the work involved for each network speeded the process along.

With the data on McIDAS, a user could obtain either sorted listings (using MDO) or plots (using LITPLT or MDX). This latter option allowed the display of lightning stroke locations on either a base map (state or national) or on a satellite image. Histograms or scatter plots of the basic variables [time, location, number of strokes per flash (LLP only) and polarity (LLP only)] were also allowed. Obviously these capabilities left a good deal to be desired. Especially needed was some way of extracting subsets of data based on their location or time, statistically summarizing these data and obtaining hard copy results. Described below are the software enhancements effected over the span of the program.

--In order to make real-time data readily accessible, the MD file structure was revised and the LITPLT command upgraded to find real time data automatically and display them with a minimum of user intervention. Data could be displayed over limited time or space domains as specified by the user;

--A decoding routine was written for converting raw LLP data tapes to McIDAS format. This capability allowed us to supplement our real-time data with

archive material and was also used extensively to move data from SSEC to NSSFC for their local use;

--A gridding utility was added to allow the sorting of lightning strokes into latitude-longitude grids. These grids could later be contoured or mathematically manipulated using general McIDAS routines; they could also be defined relative to the motion of a cell or other user defined axis, thus enabling a quasi-Lagrangian analysis;

--The McIDAS Area Statistics-related subroutines were revised to allow the extraction of lightning strokes falling within a user-defined outline and interval of time. These strokes could be counted or moved as a unit into a separate file (LW) for later use;

--Subsets of lightning data such as those obtained using the technique above could be recorded onto a floppy diskette (using a PC-McIDAS) and physically transported to an IBM PC-AT for further analysis;

--Basic and Fortran routines were written on the AT to edit files of stroke data and to average and map the data;

--Commercially available software (e.g. Statgraphics from STSC, Inc.) were used on stroke variables to obtain hard copy scatterplots, correlations, regression analyses, and many other statistical products.

In summary, software development for this project has been concentrated in two areas. The first of these has been in the creation of facilities allowing the easy transport of data from the raw data stream or tape to the appropriate computer cpu. The second area of development has been in tools for display and analysis of lightning data.

4.0 Studies of Ground Strokes and Satellite-Observed Cloud Behavior

4.1 Summer Season Ground Strokes and Infrared Cloud Cover

Ground stroke networks operating on a permanent basis are a relatively new phenomenon and accordingly, the averaged behavior of cloud-to-ground lightning is just beginning to be explored systematically. One of the goals of the experiment described in this section has been to present some information on the time-averaged nature of ground strokes over the course of a single summer season.

Another goal has been to test the idea that lightning behavior varies from region to region depending on, among other things, topography (e.g. Reap, 1986, Lopez and Holle, 1986) and synoptic regime (Kitterman, 1980). To add a regional perspective to the lightning climatology, we have used LLP data from both the National Severe Storms Laboratory in the Midwest and the NASA-Marshall LLP network in northern Alabama and southern Tennessee.

The final goal of this experiment has been to demonstrate the relationship between fractional cold cloud coverage as seen in infrared GOES satellite images to this same lightning activity. There are a number of reasons why we think this relationship is worth examining. Various studies have appeared in the literature showing a relationship between lightning activity and the coldest or highest cloud tops (Reap, 1986; Cherna and Stansbury, 1986). However, we do not know with what certainty satellite-observed cloud is associated with lightning nor do we have a means of deducing a flash rate estimate from the extent of cold cloud cover. Such information might prove helpful both operationally (in protecting aircraft, for instance) and scientifically, especially in respect to the physics of thunderstorms.

There is another way in which such information might be useful: in remote rainfall estimation. Journal articles over the past 20 years have given

plentiful indication that lightning has a strong relation to the occurrence and intensity of convective rainfall (Battan, 1965; Stansbury and Marshall, 1978; Piepgrass,1982). While we have not attempted a direct study of lightning and precipitation, our study does connect lightning with fractional cold cloud coverage, the variable upon which the reasonably successful precipitation estimation technique of Richards and Arkin (1981) has been based. Our hope is that such a beginning will eventually link satellite and lightning information together as a mean of better understanding convective precipitation processes and enhancing current techniques of remote rainfall estimation.

4.1.1 Data

The NSSL ground stroke network, one of the two data sources for this experiment, contains equipment manufactured by Lightning Location and Protection, Inc (Krider et al.,1976). Seven magnetic field direction finders with crossed loop antennas and waveform signal processors are positioned in Oklahoma and Kansas covering a four state area of northern Texas, most of Oklahoma and Kansas and southeastern Nebraska (see Figure 1). Within about a 300 km radius of the direction finders (DF's), the detection efficiency of ground strokes is about 70%. Errors in the location of strokes detected by the system are caused by errors in the azimuth angle at each DF. Mislocations result from random, site bias, rotation, and baseline errors. The random errors cannot be removed and are a consideration at all seven DF's. At 300 km radius from the center of the network, the average random error of about 1° leads to mislocations of up to 30 km (Mach, 1986). Errors are of course much less near the center of the network (as small as 1 or 2 km). Site errors vary depending on direction but average around 2 or 3°. These errors were removed from three out of the four Oklahoma DF's (Norman excepted) but are present at all the Kansas sites. Rotation errors, or misalignment of the

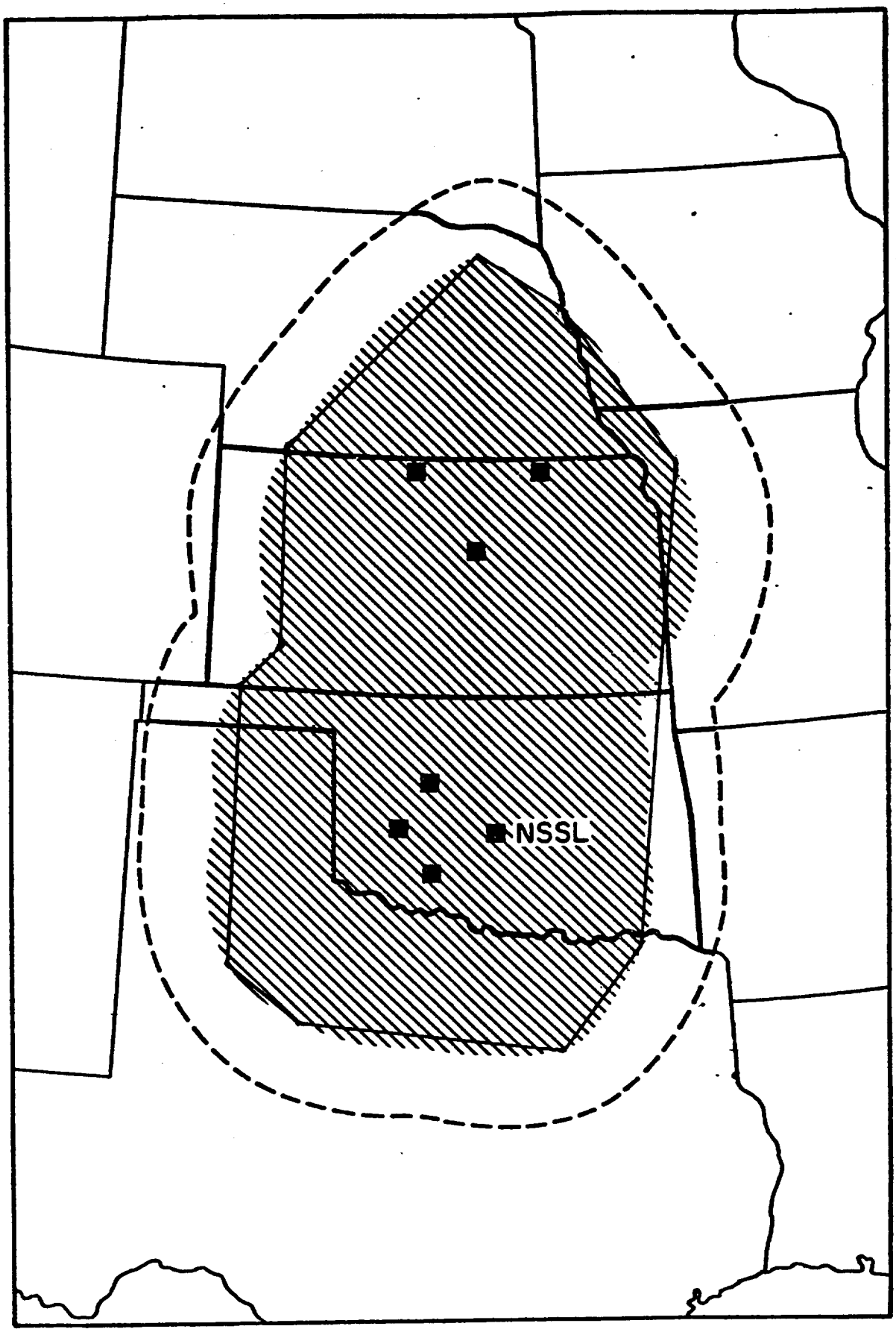

Figure 1

antenna with respect to true north were minor (<½°) except for one DF in Kansas (a 4° error). Finally, for strokes within 20° of a baseline between DF's, there may be significant inaccuracies. These strokes are located by a comparison of signal magnitude between the two stations, rather than the more accurate method of triangulation.

The combination of these errors in a given situation may result in fairly large location error, especially on the edges of the detection area. Fortunately, as we were looking only at the total numbers of strokes, our study was sensitive to location accuracy only along the boundaries of the network. Our procedure for handling these situations is detailed below.

For a definition of an analysis area we chose a boundary (delineated in Figure 1) that stayed almost completely within a 300 km radius. This minimized the azimuth errors (e.g. random errors were less than 30 km) and the bias in the calculation of average stroke magnitude resulting from a preferential recording of high intensity strokes (Orville, et al., 1987). We collected data from 15 May through 9 September 1985 (Julian Days 135 thru 252), with some breaks because of missing or rejected data.

On occasion the network was down due to communications failure or DF malfunctions. These days were easy to spot since there was a total absence of stroke reports over the network area (or a significant section)--a few spurious strokes are commonly seen even when a thunderstorm is not present in the network. Unless the satellite image showed a network area free of all cold cloud (less than 273K), other than a few patches of thin cirrus, such a case was not included in our sample. The data we did include was subjected to further quality checks. Since the data we used were all within ±30 minutes of a satellite image, the lightning stroke locations were plotted as overlays to an infrared image. In a few cases we found clusters of lightning strokes inside the analysis area evidently displaced from a cold cloud area located outside the

network. When there was no other nearby convective areas inside the network that could account for the activity, these strokes were not included in our sample. Also excluded were a few cases where, for reasons unknown, the lightning appeared to be randomly located with respect to the satellite cloud. As a final check on the validity of individual flashes, we examined each flash included in our original samples for magnitude and the number of return strokes. If either of these variables was zero because of errors in the data records, these flashes were not included in our statistics. In any given sample these rejected strokes were a few percent or less of the total number.

Our second source of data, the NASA-Marshall network, had many characteristics in common with NSSL because of its similar LLP technology. The detection efficiency, and azimuth errors were of the same magnitudes, although in this network, none of the DF's had been corrected for site errors. As shown in Figure 2, we defined the analysis area to be approximately 200 km in radius with an average error of about ±5 km error from all sources(S. Goodman, private communication). With the assistance of Steve Goodman, the network manager, we were able to obtain data from 11 July through 30 September, 1985 (Julian Days 192 through 273), with breaks due to missing or rejected data.

4.1.2 Methodology

Infrared GOES satellite images are available at least every 30 minutes. As a practical limit on the size of our samples, we decided to center our observations on just two times during the day. An early morning sample (12 GMT at NSSL, 11 GMT at Marshall) should give us a reading of activity when it is close to its minimum. Twelve hours later (00 GMT at NSSL, 23 GMT at Marshall), our second daily sample, there is diurnal peak at Marshall [which, according to Williams, et al.(1987) lasts from 20 to 23 GMT]. There should also be a significant increase in activity in the Midwest although Wallace (1975)

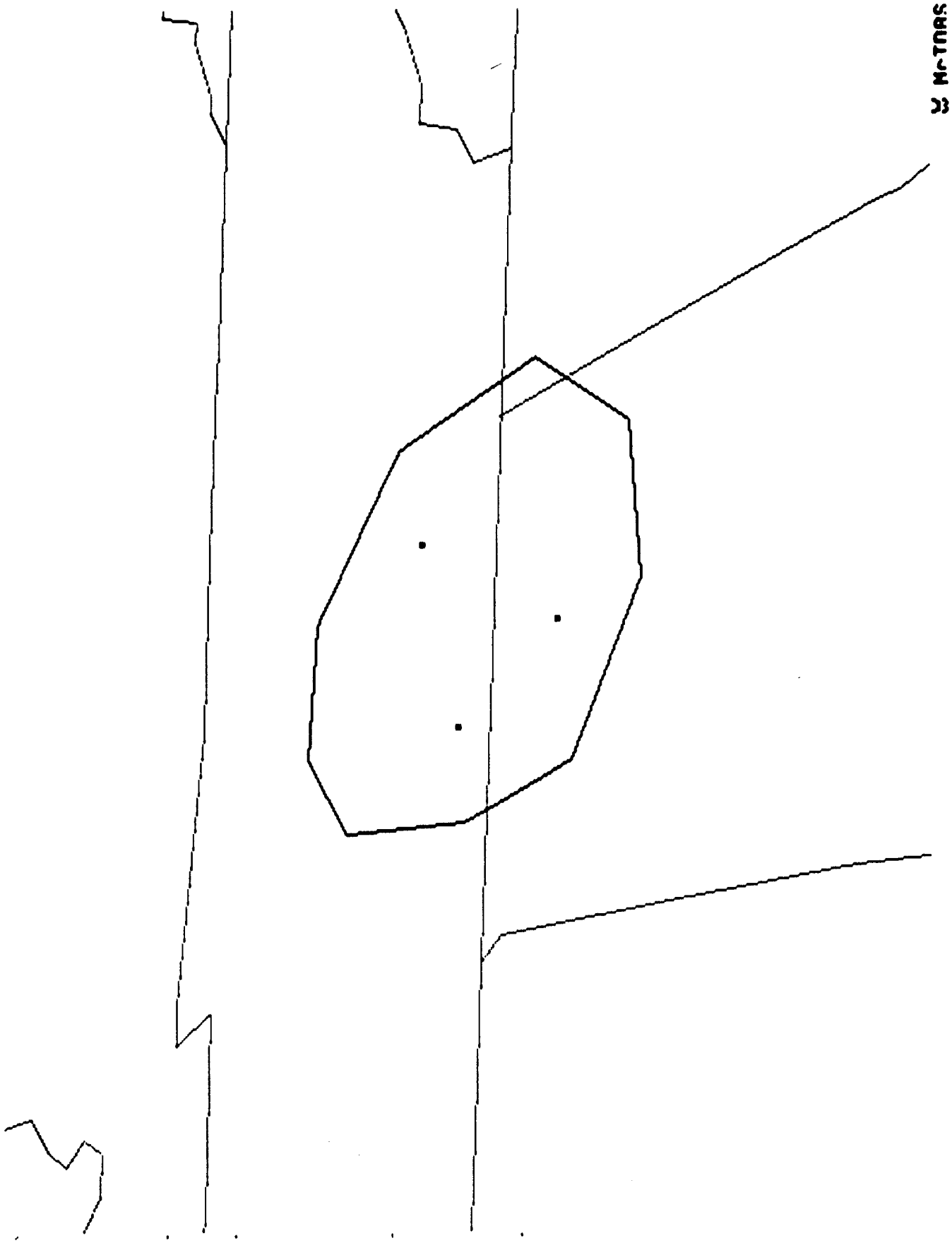

Figure 2

documents a thunderstorm rainfall maximum around 5 GMT at NSSL. Whether this is also the time of the maximum flash rate is unknown.

For each day, two images at the appropriate network time were displayed on McIDAS and checked for accurate navigation. The lightning flashes occurring within each area of coverage over a sixty and thirty minute period centered on the time of a satellite infrared image were overplotted on each image in accordance with the quality control approach detailed in the previous section. If the data were acceptable, the fractional cold cloud above certain thresholds was measured and recorded along with the minimum blackbody infrared temperature (*tmin*) and a measure of the average temperature gradient for cold clouds in the network (*gdmean*). Fractional cloud coverages were measured using McIDAS area statistics software which operates on parts of a satellite image defined by arbitrarily drawn outlines (in this case coinciding with our chosen analysis areas for the two networks). The coverage is expressed in percent of an area. The area statistics program corrects pixel area for small differences from image to image due to satellite orbital changes. The thresholds used to define cloud coverage were 273, 243, and 213K (designated as *f273*, *f243* and *f213*). The extremes were chosen in order to isolate cloud around the freezing level and the very coldest cloud tops usually associated with mature cumulonimbi. The middle threshold represents an environmental temperature near which many cloud-to-ground strokes can be expected to originate (Mazur et al., 1984 find most ground strokes coming from sources at 6 to 8 km; Ray et al., 1987 show a peak in major flash occurrence at 8 km, -30 C; Ziegler et al., 1986 demonstrate a peak charge transfer between -30 and -40 C). The gradient measure was defined as the average difference in temperature between adjacent pixels for cloud colder than 0C. We thought this parameter might distinguish between the flat gradients of non-convective cloud and steeper convective gradients, and in so doing help isolate lightning from non-lightning producing clouds.

The lightning data corresponding to 30 and 60 minute intervals centered on each image were also examined. Those flashes in the latter interval were simply counted (*n60*). Those in the shorter interval were filed and processed to reveal their total numbers (*n30*), the number of positive strokes (*n30*p), average range normalized signal strength for negative and positive polarities (*i30n* and *i30p*), and average number of return strokes (*nr*). Of course, with a detection efficiency of 70%, *n30* and *n60* are only a fraction of the actual number of strokes and should be corrected accordingly if actual flash counts are desired.

We obtained lightning data associated with a total of 162 images for the NSSL network and 148 for the Marshall network. The raw data are shown in Appendix A and B, respectively.

4.1.3 Basic Statistics and Distributions

In this section we will consider the non-relational statistical behavior of those variables we measured from the satellite images and the lightning networks. This will also give us an opportunity to compare the behavior of these variables between networks. As we have seen, the networks are similar in the technical nature of the instrumentation. Climatologically, too, they have similar annual flash densities--9 to 11 strokes/km^2, (MacGorman et al., 1984). The networks are somewhat different in the diurnal timing of thunderstorms, with the Midwest experiencing a nighttime maximum associated with the nocturnal jet. In addition, the thunderstorms in the two regions are typically the result of different forcing mechanisms. Maier and Krider (1982) in a comparison of Oklahoma and Florida thunderstorms show that most of the latter are small and numerous airmass types, whereas Oklahoma severe storms while less numerous, produce more lightning.

In respect to the present experiment, in spite of two months of overlap, the difference in periods observed may be significant. The most important

difference between the networks, however, is simply their size. The NSSL network is much bigger than the Marshall network, by 527,500 km^2 to 30,000 km^2 or nearly 18:1. The most important effect of this area disparity is the difference in sample size for most of the variables measured. There were more occasions at Marshall than at NSSL when no lightning or no clouds were in the network, and when they were present, their numbers were smaller. An example of this difference and an indication of the relative level of storm activity at each location can be seen in Figure 3, where *n30* has been ordered by magnitude. A glance at the y-ordinate for each plot shows show a difference of about five to one in the flash counts (2915 versus 610), two to one in the numbers of storms reporting lightning (115 versus 49) and nine to one in the total number of flashes over the entire sample (19,960 versus 2315). In proportion to the size of the analysis area, however, the Marshall total count is about twice as large as one might expect. The general shape of the distribution for both networks is roughly similar. Like many phenomena in nature, it follows an exponential distribution. Extreme lightning events can be potent indeed. The several large lightning events at NSSL are similar in magnitude to the large MCC-generated lightning outbreaks cited by Goodman and MacGorman (1986).

In Table 1 are some statistics by network for the basic variables used in this experiment. There is a surprising degree of similarity between the two samples, given the network size disparities. For instance, fractional cloud coverage is almost identical for the two locations, although, as the standard deviations suggest, the Marshall data were scattered over a considerably larger range.

The variable "*gdmean*", the average brightness difference between adjacent infrared satellite pixels, was consistently monitored only at the NSSL location. It became apparent after this first sample, that *gdmean* did not provide useful information on the lightning-producing capabilities of these storms; the few

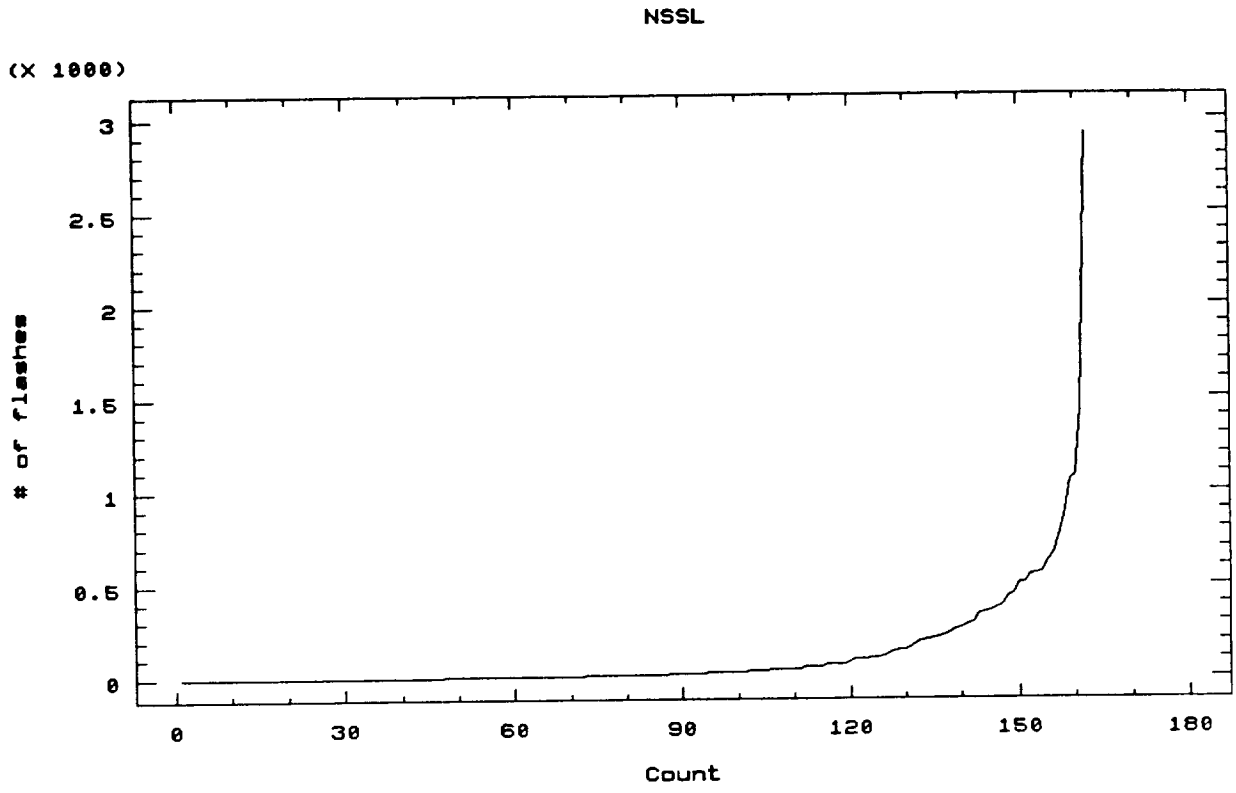
NSSL
(X 1000)
3
2.5
2
1.5
1
0.5
0
# of flashes
0
30
60
90
120
150
180
Count

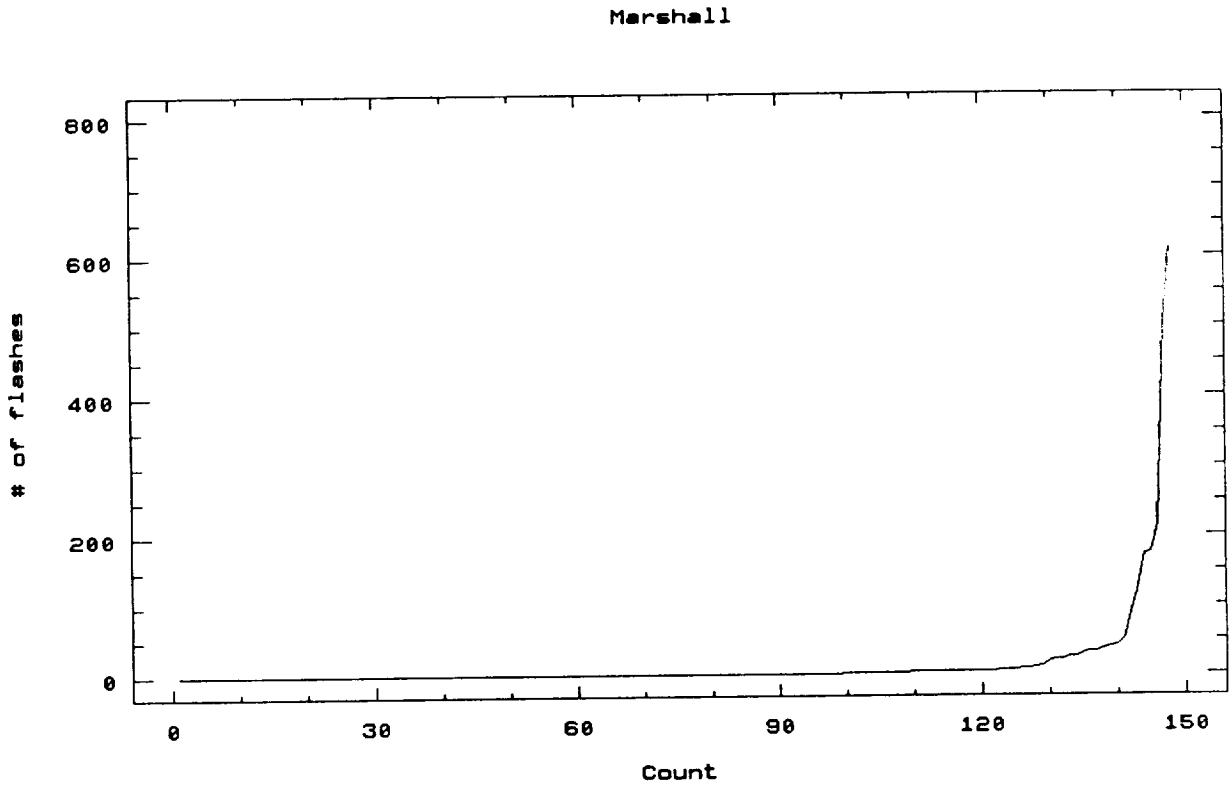
Marshall
800
600
400
200
0
# of flashes
0
30
60
90
120
150
Count

Figure 3

Statistics for Basic Variables

NSSL Network

	f273	f243	f213	gdmean	tmin	n60	n30	n30p	nr	i30n	i30p
units	%	%	%	count	°K	----flash----			stroke	relative mag.	
n	162	162	162	159	162	114	113	113	113	106	64
Mean	22.9	8.7	1.4	1.9	223	319	176	6	2.2	-138.1	222.1
σ	20.1	12.3	3.5	0.8	19.0	664	362	12	0.7	56.5	118.7
Max	87.8	70.6	26.0	6.6	277	5448	2915	71	4.9	-37.4*	552.6
Min	0.0	0.0	0.0	0.3	196	1	1	1	1.0	-449.0	46.9*

Marshall-NASA Network

	f273	f243	f213	gdmean	tmin	n60	n30	n30p	nr	i30n	i30p
n	148	148	148	N/A	148	62	48	48	48	48	12
Mean	23.5	6.8	1.0	N/A	258	67	47	0.7	2.1	-27.6	40.3
σ	32.2	17.2	5.0	N/A	26.2	191	118	1.7	1.0	27.6	26.5
Max	100.0	100.0	39.8	N/A	290	1103	610	9	4.5	-0.2*	87.7
Min	0.0	0.0	0.0	N/A	199	1	1	0	1.0	-148.5	10.4*

* = These minimum magnitudes were computed on the basis of only a few strokes and cannot be considered reliable.

TABLE 1

measurements made at the Marshall site did not warrant their inclusion in this table.

tmin is the coldest pixel or pixels found in the entire infrared satellite image analysis area. As expected, its value is generally colder at NSSL than at Marshall (223K vs. 258K), there being a higher probability of cold cloud within the larger network. The minimum *tmin* is also somewhat colder at NSSL. This 196K measurement was associated with the greatest lightning outbreak that we measured in the network, a squall line with a massive line of cumulonimbi. Among the coldest samples and largest lightning producers at Marshall, there were no well organized squall lines--only separate cells or clusters of cells (although some of them were very active and covered a large area). One of these cells, lying partly in the Marshall network, reported a minimum temperature of 199 K. However, it showed only moderate lightning in our sample because much of the lightning associated with this cell fell just to the south of the network boundary. The next coldest events at Marshall (201K and 206K), were more strategically located with respect to the boundaries and produced the two largest lightning outbreaks among our samples.

The averages for *n60* and *n30* are based on samples where at least one lightning flash was present during the 60 or 30 minute interval, respectively. The *n30p* average is composed of the number of positive strokes for samples when there was at least one flash (positive or negative) during the half-hour. As expected, positive strokes are comparatively rare; there were many cases where there were negative but no positive strokes. That positive strokes were only 3.4% of the total of negative strokes agrees with findings for the East Coast Network, where a 4% relationship was found (Orville et al., 1982). The flash counts for 30 and 60 minute periods illustrate in another way some points gleaned from Figure 3: there is a wide variation in flash rate from storm to storm and there is a higher flash density at Marshall than at NSSL. The average

number of strokes at Marshall is more than four or five times higher higher than would be warranted by its area. Finally, note that in the mean *n30* is from more than one-half to almost three-quarters of *n60*. This may be simply the result of imposing a condition of higher frequency on the 30 minute sample.

The average number of return strokes and the relative magnitudes of the first strokes in each flash are based on 30 minute samples with one or more flashes. The average number of return strokes (*nr*), their standard deviations, and their ranges are almost identical at both locations (around 2.1). Ogawa (1982), using a compilation of data, cites a values of 3 for the typical number of return strokes, although he shows individual samples that vary from 2 to greater than four. Clifton and Hall (1980) show about 2.6 strokes per flash for a small sample of 146 flashes.

The average relative stroke magnitudes at Marshall are for unknown reasons much smaller than at NSSL. This is true even if one accounts for the difference in range normalization used at NSSL compared to Marshall (100 versus 298 km). Correcting for this difference would still show *i30n*'s of about -138 versus -82 and *i30p*'s of 222 versus 120. Nonetheless, both networks indicate that negative strokes have only a fraction of the magnitude of the positive ones. This result agrees with Orville's findings for the East Coast Network (Orville et al., 1986). There he found a relative magnitude for summer negative strokes of -137 (compared to NSSL's -138) and positive strokes of 50% greater magnitude (205 versus NSSL's 222).

Frequency histograms of the basic variables shows the fractional cloud coverages and the flash counts to have exponential distributions; the minimum temperatures and the stroke magnitudes, lognormal distributions; and the return strokes, normal distributions. Lognormal distributions for peak stroke currents have been documented by several authors (Ogawa, 1982, Schütte, et al., 1987).

4.1.4 Interrelationships of the Basic Variables

In this section, connections between the variables we have examined will be established and discussed. It would first be helpful to look at the statistical correlations between our variables. These are listed in Table 2, where some of the more significant results can be seen in the shaded boxes.

A number of features stand out, one of which is the similarity of results between the two networks. Especially in those comparisons in which we are most interested--fractional cloud coverages and minimum temperatures versus flash counts--the NSSL and Marshall networks show similar coefficients. *f213*, the coldest cloud cover, is the best indicator of the flashcount, with a significant decline noted for warmer cloud. Interestingly, in respect to fractional cloud coverage the correlation coefficients for positive flashes are consistently better than those for negative polarities at both networks. This association of cold cloud with positive stroke occurrence may simply be a reflection of the fact that positive strokes originate at higher altitudes than do negative ones (Rust and MacGorman, 1981). This correlation may also reflect vertical wind shear which is thought to play a role in the creation of positive ground strokes (Brook et al., 1982), and may have the effect of increasing the fractional cloud coverages of the anvil. Note also for the NSSL storms the disproportionate jump in the *n30p-f243* coefficient from the *n30p-f213* value (an increase of 0.24). The change from f243 to f213, on the other hand, is only 0.11. Temperatures around 243 K seem to have significance to the occurrence of positive strokes.

Figure 4 shows a scatter plot for negative flashes relative to the coverage at each threshold (a series for positive flashes would appear very similar). The scatter is fairly great for the two warmer thresholds, whereas more linearity is evident for the coldest cloud. Note the single point near flash count 3000. This one storm produced nearly double the strokes of its nearest competitor and seems to lie to the left of a linear regression. There

Correlation Coefficients Between the Basic Variables
() = sample size

NSSL Network

	f273	f243	f213	gdmean	tmin	n60	n30	n30p	nr	i30n	i30p
f273	1.00 (162)										
f243	.84 (162)	1.00 (162)									
f213	.52 (162)	.77 (162)	1.00 (162)								
gdmean	-.45 (159)	-.29 (159)	-.19 (159)	1.00 (159)							
tmin	-.54 (162)	-.55 (162)	-.44 (162)	-.02 (159)	1.00 (162)						
n60	.31 (162)	.49 (162)	.68 (162)	-.08 (159)	-.40 (162)	1.00 (162)					
n30	.31 (162)	.50 (162)	.68 (162)	-.08 (159)	-.40 (162)	1.00 (162)	1.00 (162)				
n30p	.38 (162)	.62 (162)	.73 (162)	-.15 (159)	-.40 (162)	.60 (162)	.61 (162)	1.00 (162)			
nr	.12 (115)	.26 (115)	.27 (115)	-.01 (115)	-.40 (115)	.41 (115)	.41 (115)	.26 (115)	1.00 (115)		
i30n	-.19 (108)	-.16 (108)	-.10 (108)	.17 (108)	.29 (108)	-.10 (108)	-.09 (108)	-.06 (108)	-.31 (108)	1.00 (108)	
i30p	.23 (64)	.19 (64)	.13 (64)	-.43 (64)	.05 (64)	-.13 (64)	-.14 (64)	-.05 (64)	-.19 (64)	-.13 (62)	1.00 (64)

Marshall-NASA Network

	f273	f243	f213	gdmean	tmin	n60	n30	n30p	nr	i30n	i30p
f273	1.00 (148)										
f243	.70 (148)	1.00 (148)									
f213	.35 (148)	.64 (148)	1.00 (148)								
tmin	-.81 (148)	-.67 (148)	-.40 (148)		1.00 (148)						
n60	.28 (148)	.40 (148)	.59 (148)		-.40 (148)	1.00 (148)					
n30	.27 (148)	.39 (148)	.55 (148)		-.39 (148)	1.00 (148)	1.00 (148)				
n30p	.34 (148)	.56 (148)	.70 (148)		-.41 (148)	.80 (148)	.81 (148)	1.00 (148)			
nr	.32 (49)	.23 (49)	.17 (49)		-.37 (49)	.26 (49)	.26 (49)	.20 (49)	1.00 (49)		
i30n	-.38 (49)	-.23 (49)	-.24 (49)		.35 (49)	-.31 (49)	-.32 (49)	-.30 (49)	-.32 (49)	1.00 (49)	
i30p	-.15 (12)	.34 (12)	.45 (12)		.08 (12)	.04 (12)	.01 (12)	.49 (12)	-.20 (12)	-.05 (12)	1.00 (12)

TABLE 2

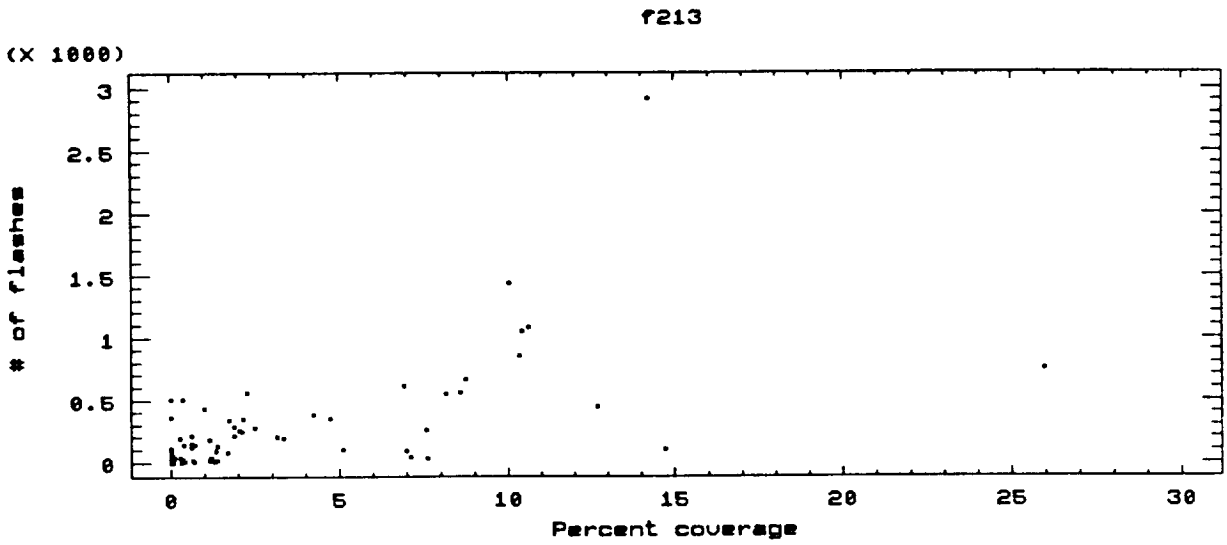
f213
(X 1000)
# of flashes
3
2.5
2
1.5
1
0.5
0
0
5
10
15
20
25
30
Percent coverage

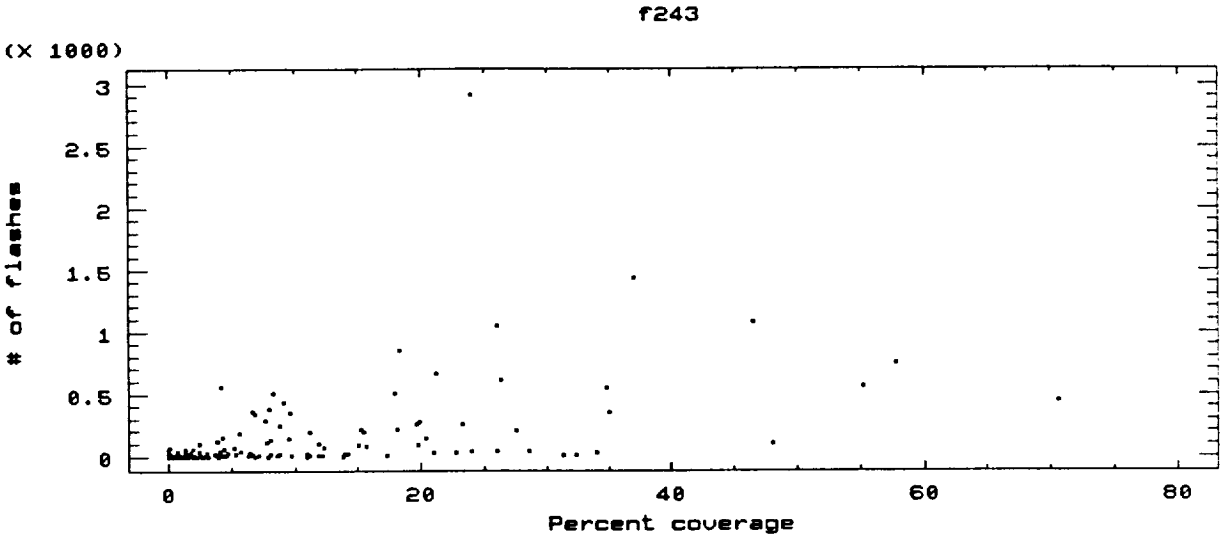
f243
(X 1000)
# of flashes
3
2.5
2
1.5
1
0.5
0
0
20
40
60
80
Percent coverage

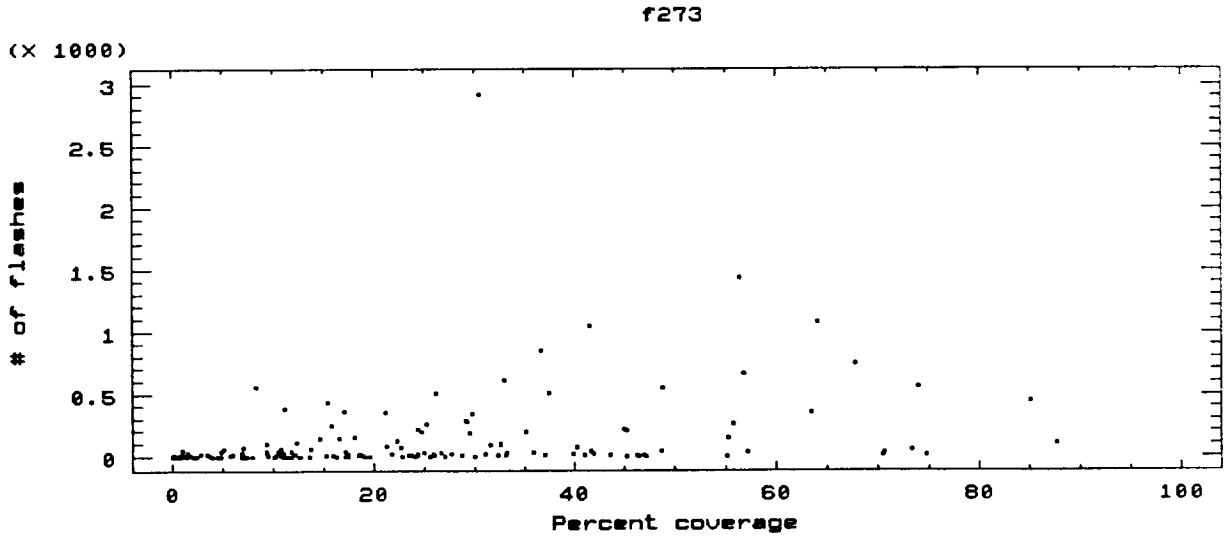
f273
(X 1000)
# of flashes
3
2.5
2
1.5
1
0.5
0
0
20
40
60
80
100
Percent coverage

Figure 4

is also an outlier just past the 25% coverage for *f213*. This storm (Day 155), although still a healthy producer of lightning, was a single large anvil just past its prime--it had experienced its peak flashrate an hour earlier.. At the time of our sample, it exhibited a large cold cloud shield, but a declining flashrate. This situation also points to one reason why correlations between cold cloud and lightning are not better than they are. As we will see in the next section, there is evidently a lag between the time when flashrates decline and the satellite-observed cold cloud shield begins to disintegrate. This lag would affect correspondence of *f213* and *n30* in this case and the quality of the correlation in general. Improved results could be expected if the cloud areas were measured at the time of the peak flashrate or if the maximum extent of the cold cloud areas were compared with the peak flashrates.

The *tmin*'s have a weaker but consistent connection with the flash count (around 0.4). That there is significance to this relationship can be more readily seen in Figure 5. For both networks there appears to be a threshold temperature for lightning. At NSSL no samples with more than 5 flashes occur at *tmin*'s warmer than 243K. At Marshall this situation occurs at 242K. By 210K nearly all samples show significant lightning activity. There have been a number of paper documenting lightning dependence on cloud or echo height (Cherna and Stansbury, 1986; Mazur et al., 1986). Reap (1986) notes a rapid increase in flash occurrence for cloud top temperatures below 238K in the Western states. Holle and Maier (1982) find that only one percent of the echoes in their sample produced lightning below 9 km (about 245K for a standard summer subtropical atmosphere). On the other hand, 80% of the echoes reaching 14 km (corresponding to about 210K) were lightning producers.

Positive flashes (Figure 6) appear to have a colder threshold than negative flashes. Significant activity appears only when minimum temperatures fall below 220K, at least at NSSL. At Marshall the positive flash counts were

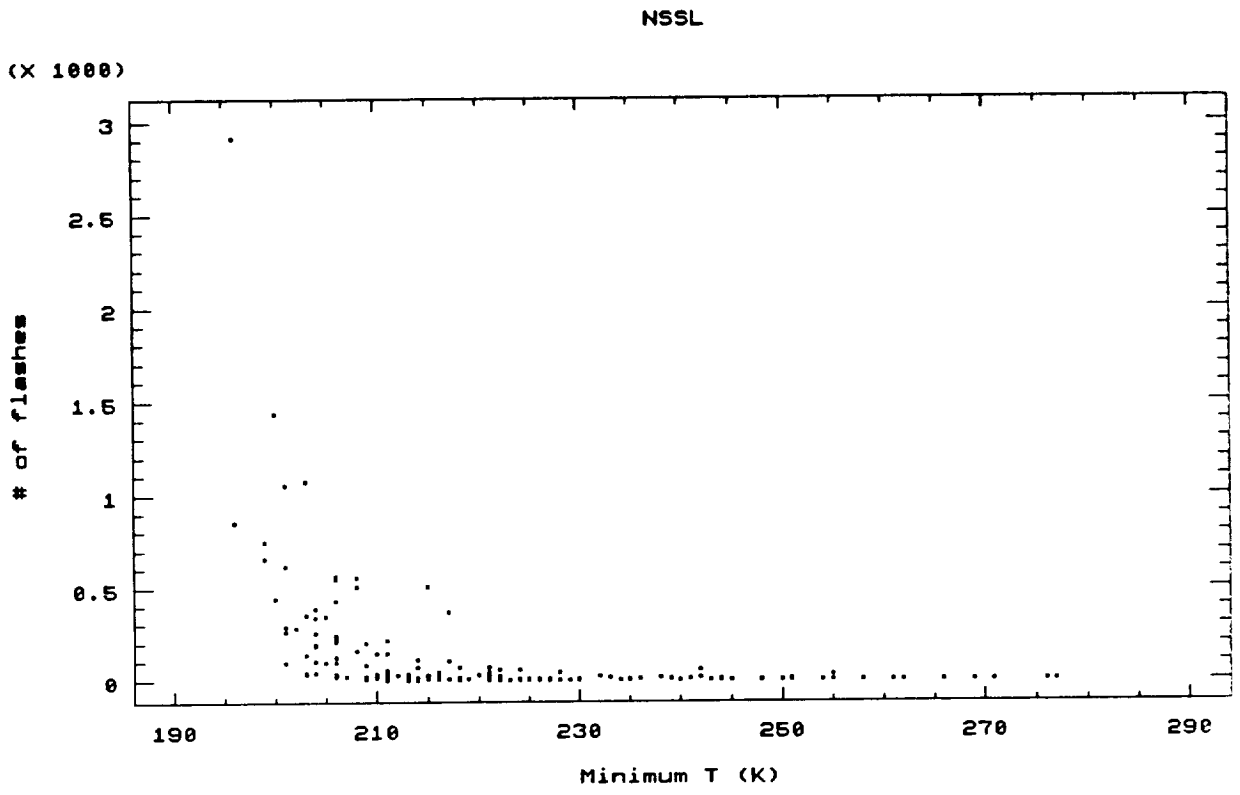
NSSL
(X 1000)
3
2.5
2
1.5
1
0.5
0
# of flashes
190
210
230
250
270
290
Minimum T (K)

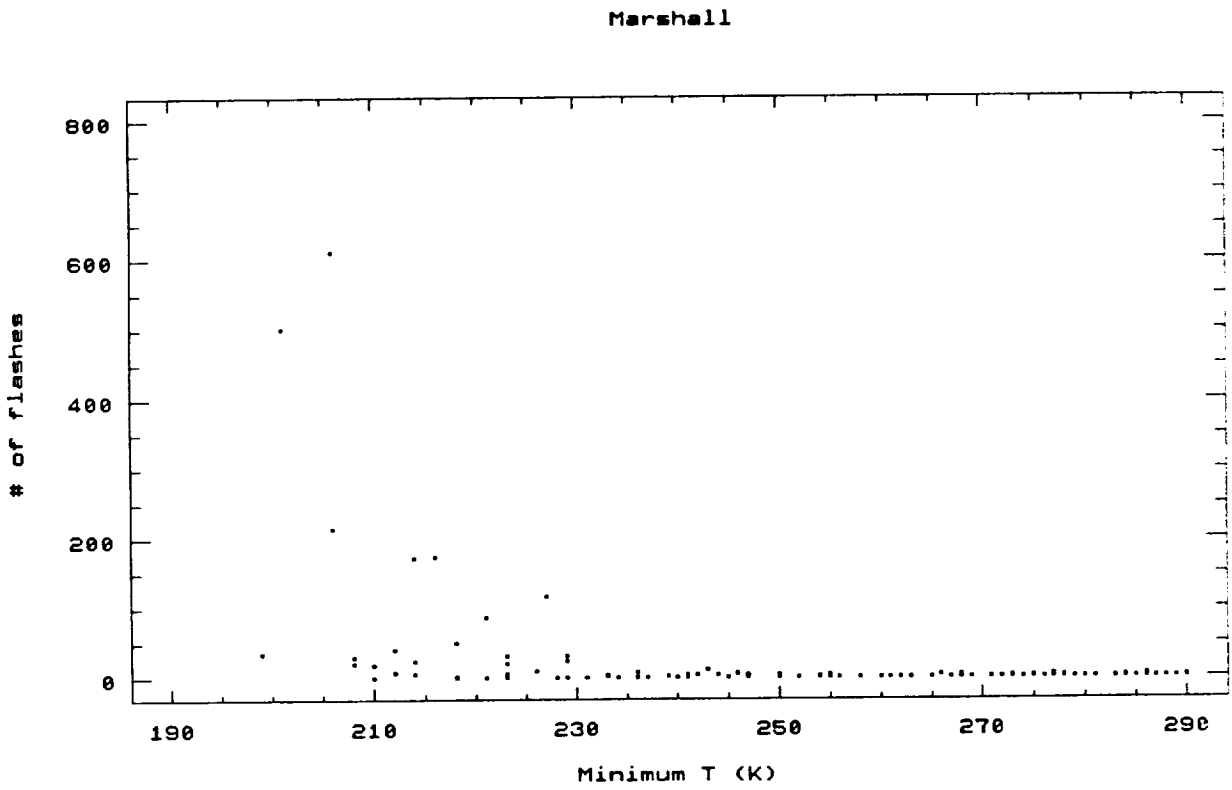
Marshall
800
600
400
200
0
# of flashes
190
210
230
250
270
290
Minimum T (K)

Figure 5

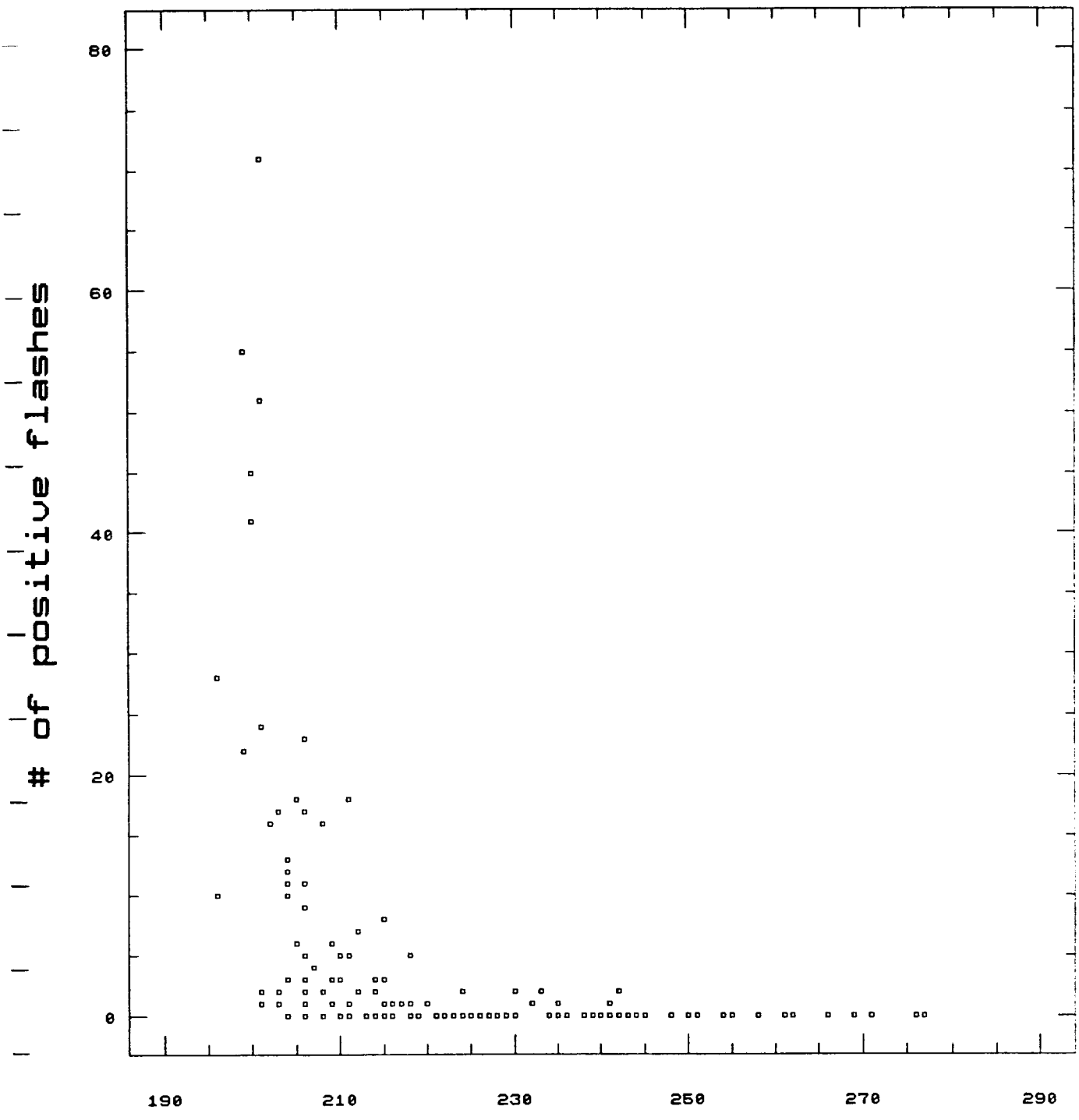
# of positive flashes
80
60
40
20
0
190
210
230
250
270
290
Minimum T (K)

Figure 6

so low (averaging 2) that a threshold determination was not considered reliable.

Our gradient measure, *gdmean*, showed no significant relationship with the flash counts. We had hoped that this gradient measure would be higher for convective than for layer cloud, thus serving as an additional predictor for the larger flash counts occurring when cumulonimbi are present in the network. Unfortunately, the measure of gradient chosen (average difference of infrared brightness between pixels on the same satellite scan line), does not make such a distinction. If anything, there is a tendency for higher flash counts to occur with lower values of *gdmean* (Figure 7). The distribution of layer and convective cloud and their associated gradients is evidently more complex than can be fathomed with this simple measure. *gdmean* might have been a more effective discriminator if its temperature trigger had been set lower than 0C. Otherwise a two-dimensional operator, such as that used by Adler and Negri (1987) to distinguish between stratiform and convective rainfall, might have been more effective.

Finally, there is some evidence of a positive relationship between the average number of return strokes per flash and the total number of flashes in the sample. Figure 8 show an interesting tendency for the larger storms to produce a higher *nr* although only up to values of 3.5 strokes/flash. Small lightning producers are much more likely to average two return strokes or less. According to Goodman and MacGorman (1986) the most electrically active storms produce return stroke averages between 3 and 4.

4.1.5 Regression

In the last section, results were presented which suggest that there are meaningful physical relationships between the variables measured in this study. This section examines the possibilities of using these variables as predictors of the flash count.

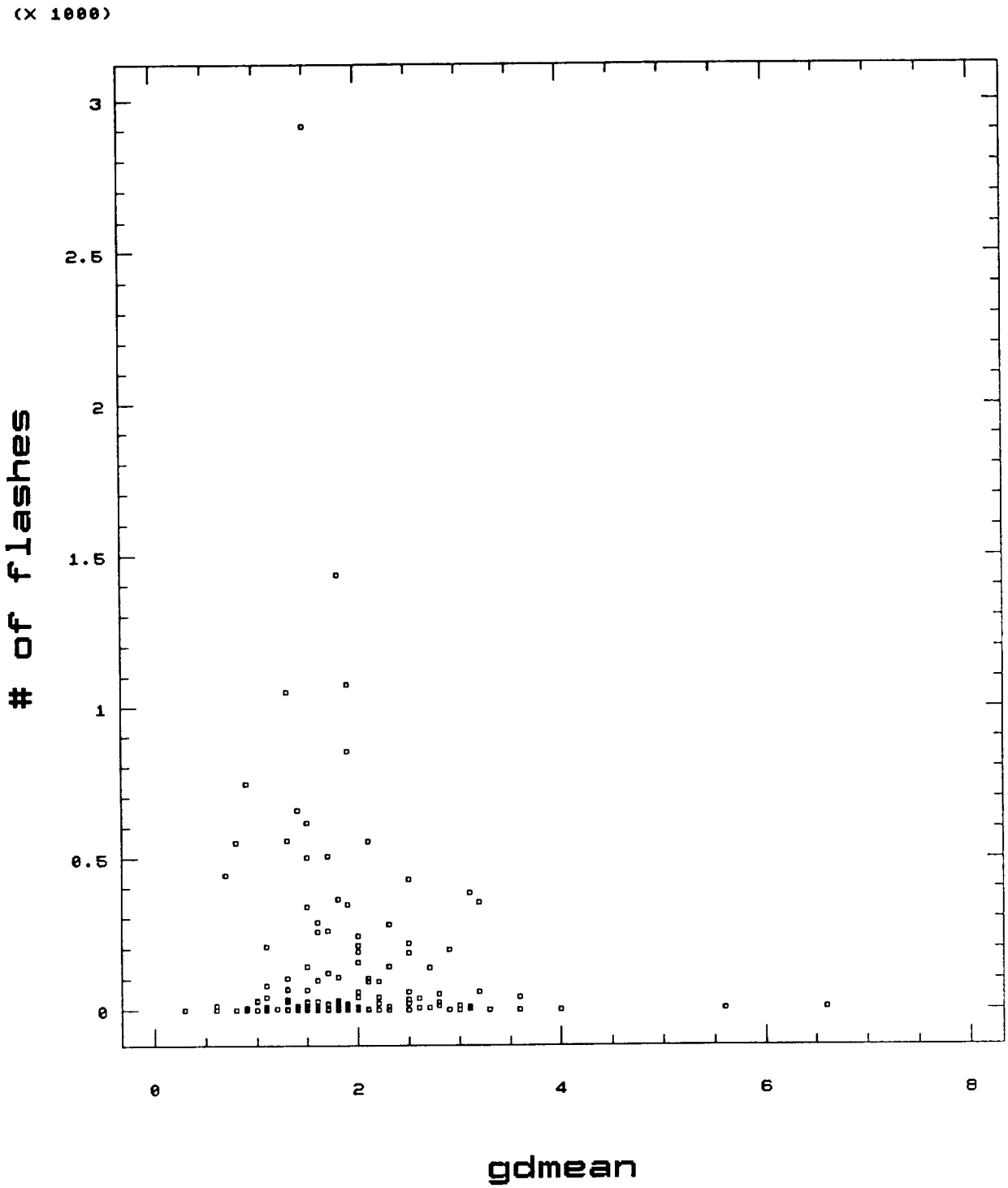

Figure 7

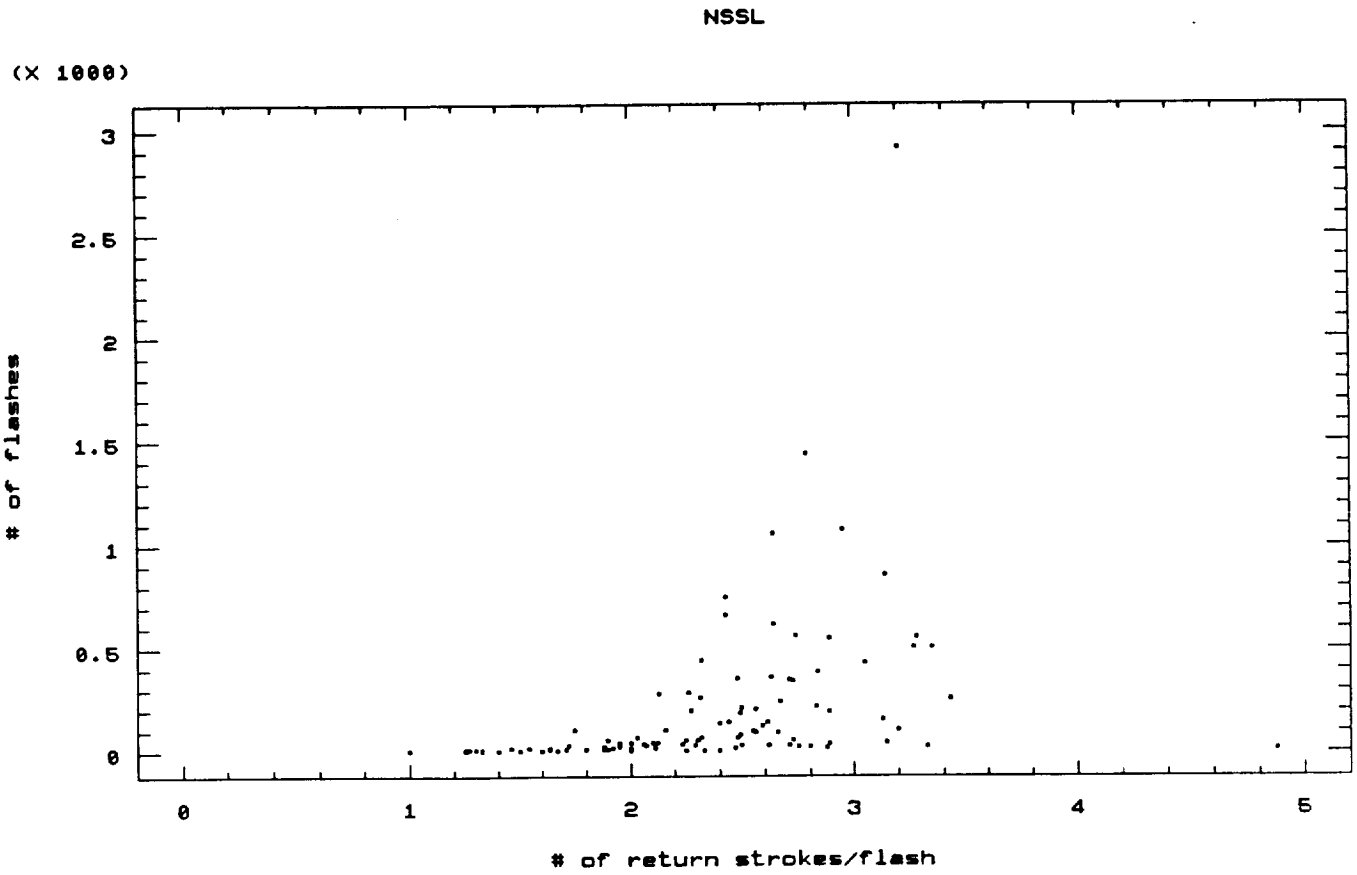
NSSL
(X 1000)
3
2.5
2
1.5
1
0.5
0
# of flashes
0
1
2
3
4
5
# of return strokes/flash

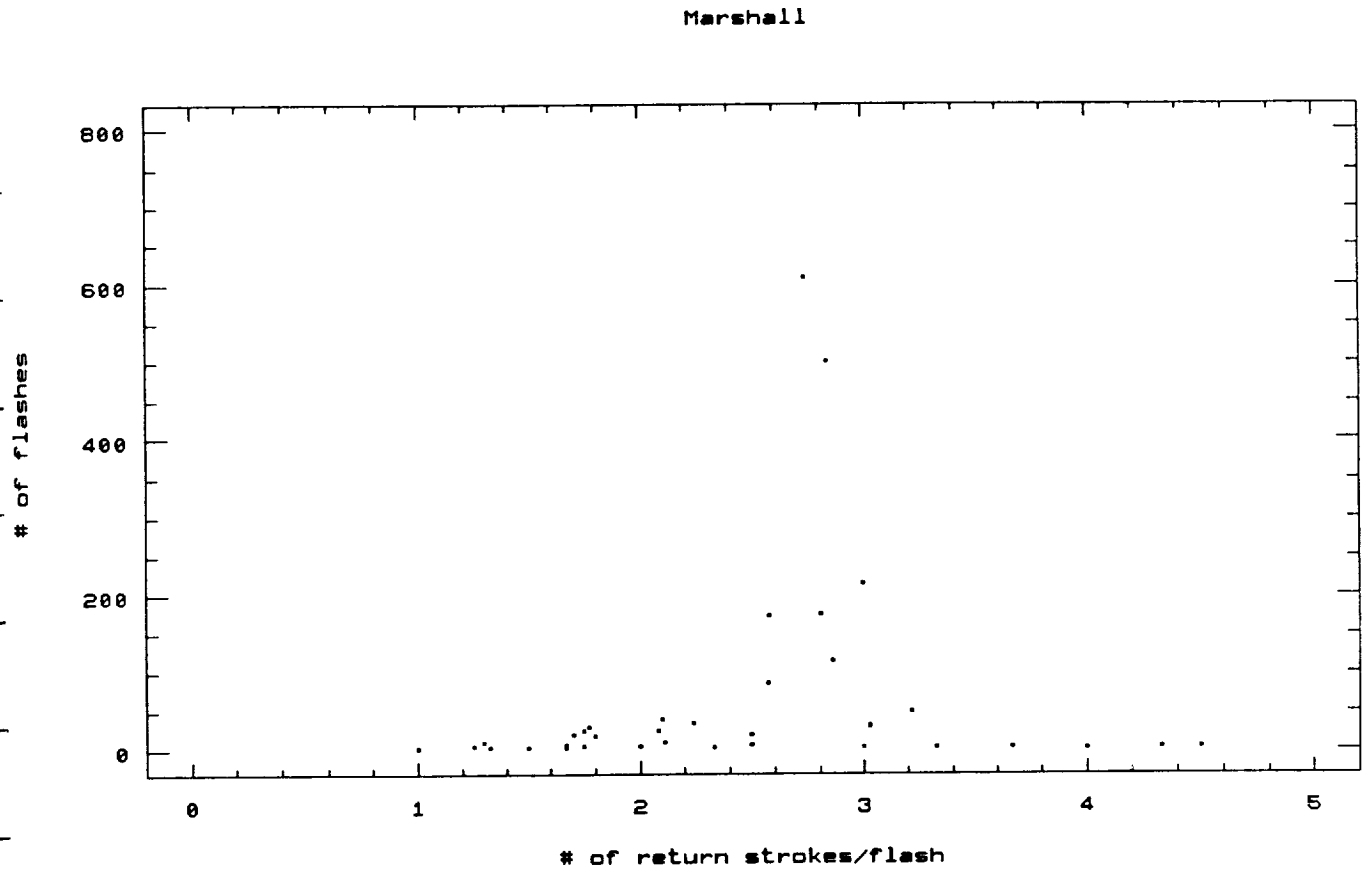
Marshall
800
600
400
200
0
# of flashes
0
1
2
3
4
5
# of return strokes/flash

Figure 8

We first tried fitting *n30* using stepwise linear regression on *tmin* and the fractional cloud covers. Because there is a high partial correlation between *f273-f243* and *f243-f213* (about 0.7), one would not expect that all three of these variables would have a useful predictive value. As it turns out, only *f213* was selected. *tmin*, on the other hand is only marginally correlated with *f213* (-0.2) and has significance in it own right.

The model selected using NSSL data has the following characteristics:

	Coefficient	Std. error
Constant	509.3	239.2
f213	55.6	5.7
tmin	-2.1	1.1

or:

n30 = 509.3 + 55.6 * *f213* - 2.1 * *tmin*.

For this equation, we have an r-squared (square of the correlation coefficient) of 0.47, meaning about 47 percent of the variability in *n30* is explained by the above equation.

Applying regression to the Marshall data, an equation with the same form results:

n30 = 150.7 + 6.6 * *f213* - 0.55 * *tmin*

with an r-squared of 0.33. Relative to the size of the *f213* and *tmin* coefficient, the constant is disproportionately large (compared with the NSSL form), but on the other hand *f213* and *tmin* have a greater variation and range in the smaller Marshall network than they do at NSSL.

Because the distribution of *n30* is exponential, we expected that we might be able to improve on these regressions by taking the square root or the natural log of *n30* (actually the log [*n30*+1] in order to avoid taking the log of 0) as our dependent variable. These transformations result in slightly improved correlations between the flash count and the fractional cloud coverages (for NSSL *f213* and sqrt(*n30*) an improvement from 0.68 to 0.71) and much improved

correlations with *tmin* (for NSSL *f213* and sqrt*n30*), from 0.40 to 0.60). We also included several modified variables in our model: the ratios of *f213* to both 243 and *f273* (*r213/243* and *r213/273*). Our rationale for creating these parameters was physical. These ratios can be expected to be high in the earlier stages of a storm when the proportion of the coldest cloud to the warmest is at a peak. This is also the time when a storm is most likely to be producing lightning (Holle and Maier, 1982).

Again applying stepwise regression to our NSSL results, we obtain:

	Coefficient	Std. error
Constant	28.6	6.8
r213/273	56.5	6.4
f243	0.14	0.044
tmin	-0.11	0.030

$$\text{sqrt}(n30) = 28.6 + 56.45 * (r213/273) + 0.15 * f243 - 0.114 * tmin$$

with a r-squared of 0.66. A plot of the observed versus the predicted sqrt(*n30*) for this regression is shown in Figure 9. There is a relatively even distribution of residuals, even for the extreme values of sqrt(*n30*).

For the Marshall network, we get a slightly different model:

$$\text{sqrt}(n30) = 39.1 + 42.0 * (r213/273) + 43.9 * (r213/243) - 1.1 * f213 - 0.16 * tmin$$

There is a r-squared of 0.56. Interestingly, both NSSL and Marshall equations show sqrt(*n30*) going to zero at almost the same temperature--251 and 246K, respectively. These values are close to the 242/243 K thresholds noted previously in comparisons of *tmin* with *n30*.

In summary, there appears to be some information about lightning activity attainable from access to satellite infrared images alone. Knowledge of minimum cloud top temperatures can offer a good indication of whether or not significant

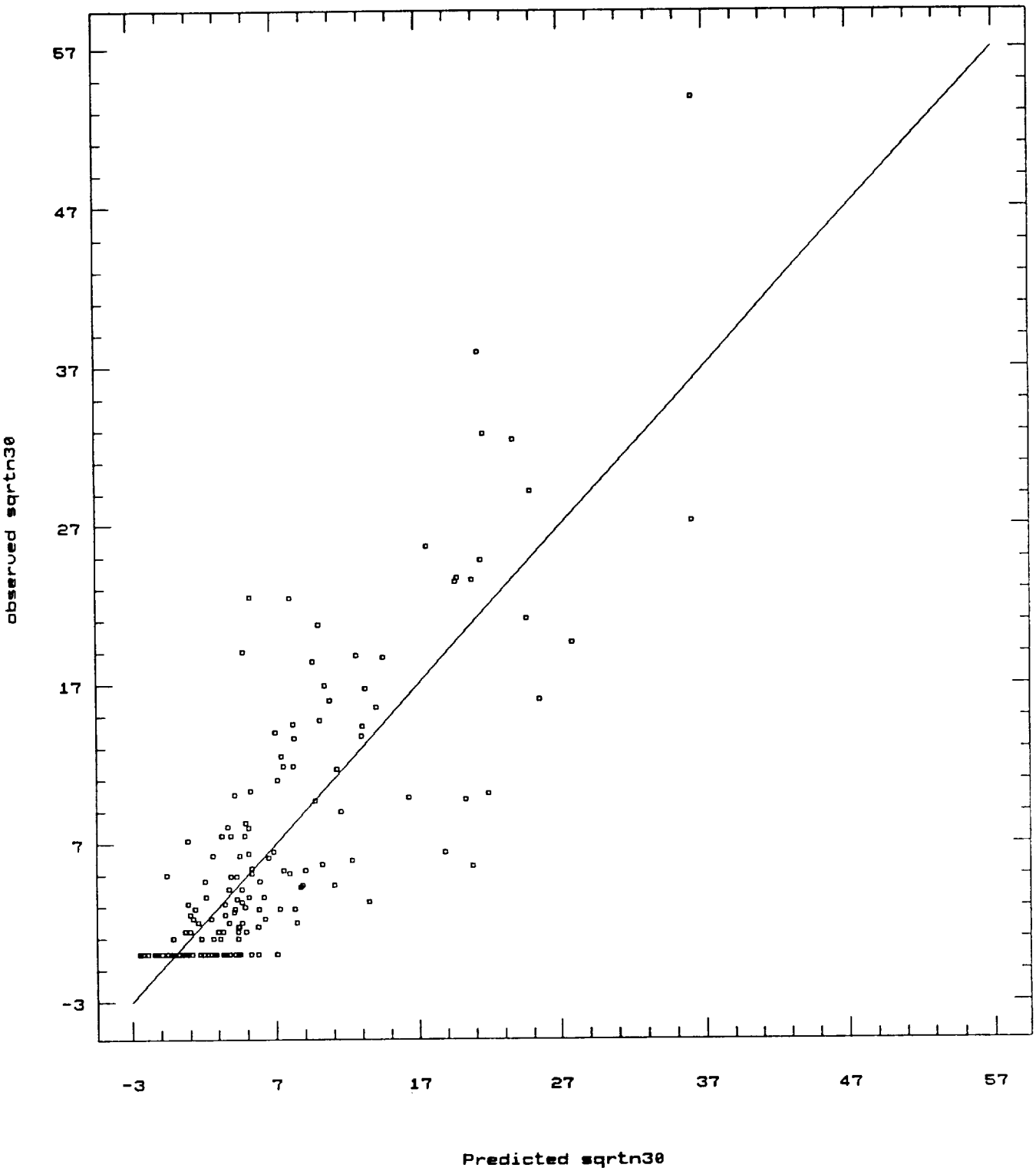
57
47
37
27
17
7
-3
observed sqrtn30
-3
7
17
27
37
47
57
Predicted sqrtn30

Figure 9

lightning is present in the cloud mass, although *tmin* alone does not provide a good prediction of the flash rate. Combined with information on fractional cloud coverage, however, we have been able to explain 47 to 66% of the lightning variability in the NSSL network and 33 to 56% at Marshall.

4.1.6 Diurnal Variations

The large diurnal variation in thunderstorm lightning is well known (e.g. Reap, 1976; Lopez and Holle, 1986). In our sample, too, there are large variations between the early evening and early morning. Figure 10 shows the dramatic variation in the sample size by time of day at NSSL. Table 3 gives a quantitative picture of these variations. By a factor of 2:1 at NSSL and 4:1 at Marshall, 7 PM local time flash counts outnumber 7 AM activity. Both locations also reported their single largest flash counts in the evening. A similar result holds true for positive strokes. Although the total numbers are small, flash counts vary by a factor of about 3:1 between the two times. Very little difference can be seen in the average number of return strokes, although there might be a slight tendency for larger *nr*'s in the evening.

The behavior of the relative stroke magnitudes varies between the two sites. At NSSL, there is a significant variation between the morning and evening samples (less than a 1% probability of the two distribution having the same mean according to the Whitney-Mann test), with the morning samples having the larger stroke magnitudes. Orville et. al. (1987) show a similar result for a seasonal comparison of stroke magnitudes. As the number of positive and negative strokes declines during the cold season, the average flash magnitudes increase.

While the Marshall data indicate an opposite conclusion, the sample size is smaller and the difference in the means is not found to be significant.

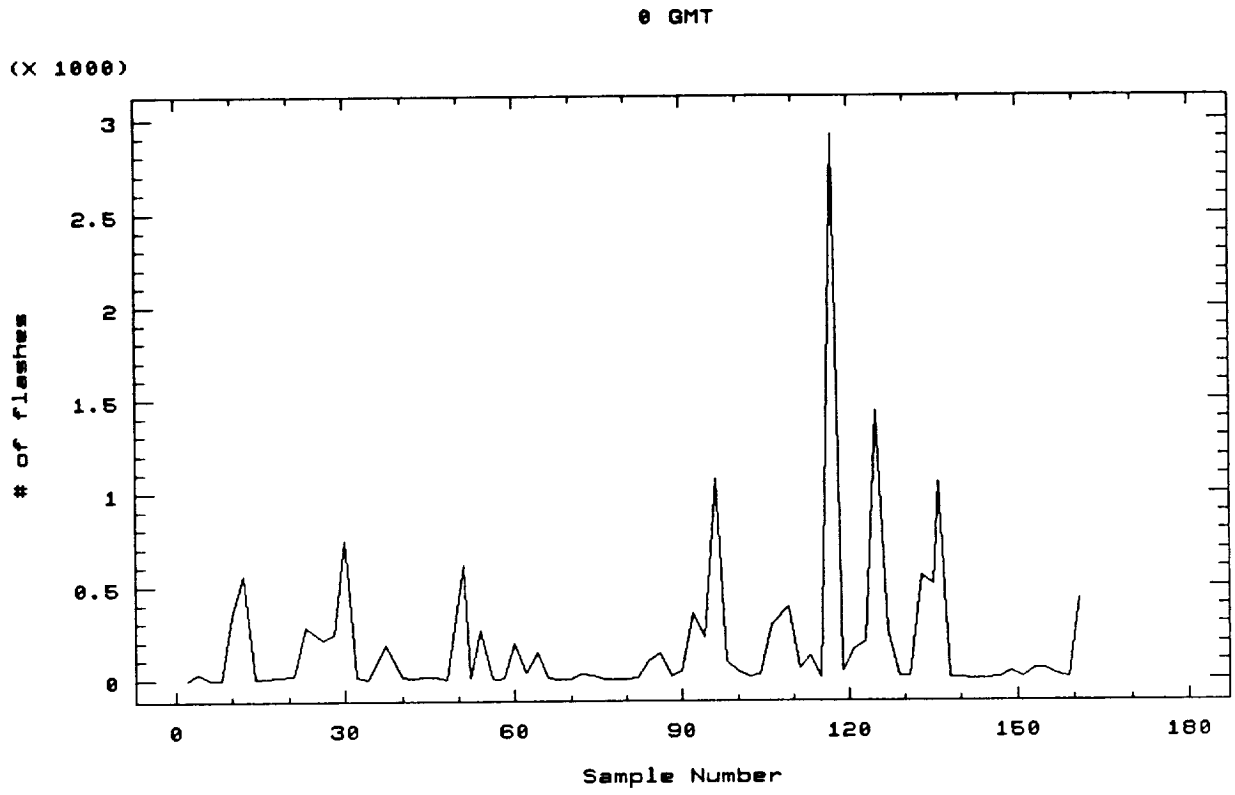
0 GMT
(X 1000)
# of flashes
3
2.5
2
1.5
1
0.5
0
0
30
60
90
120
150
180
Sample Number

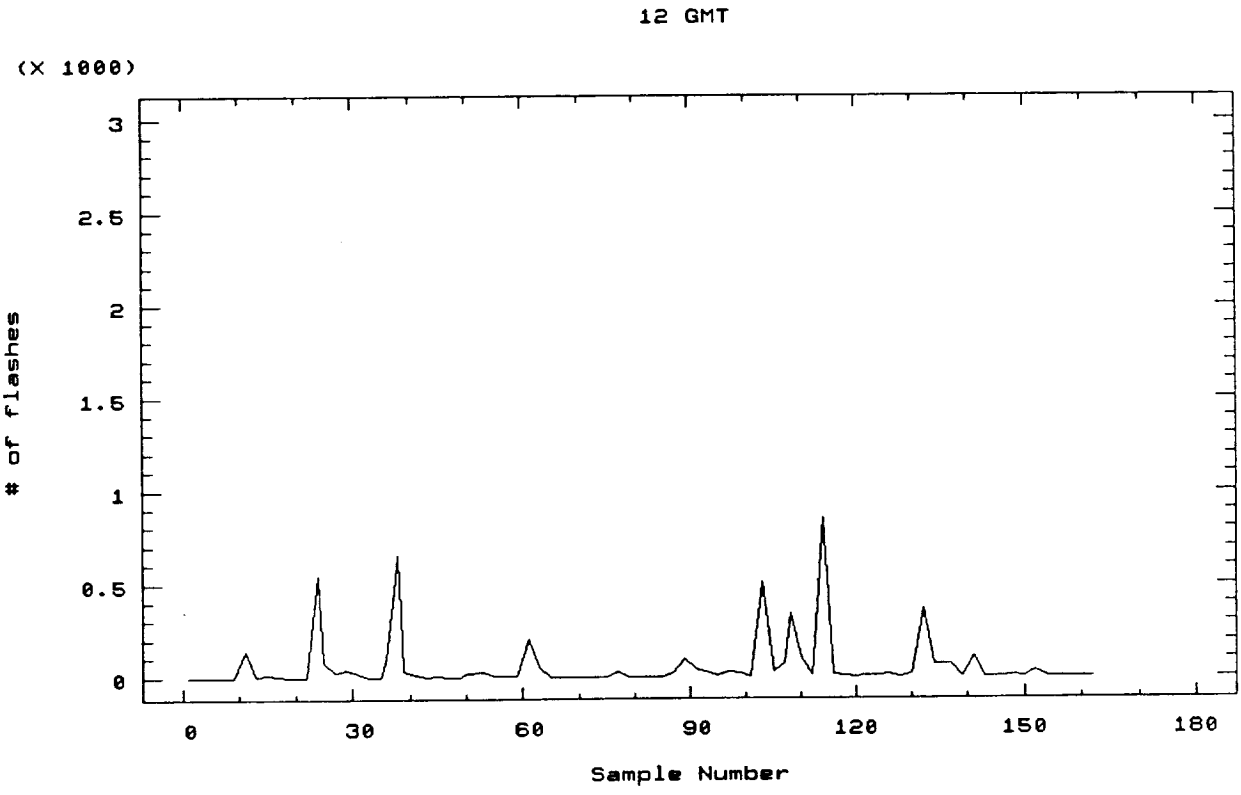
12 GMT
(X 1000)
# of flashes
3
2.5
2
1.5
1
0.5
0
0
30
60
90
120
150
180
Sample Number

Figure 10

Diurnal Variations of Basic Lightning Variables

NSSL Network

	n30 (count)		n30p (count)		nr (stroke)		i30n (rel. mag.)		i30p (rel. mag.)	
time	0 GMT	12 GMT	0 GMT	12 GMT	0 GMT	12 GMT	0 GMT	12 GMT	0 GMT	12 GMT
n	67	46	67	46	67	46	64	42	35	29
Mean	225	104	8	3	2.3	2.1	-127.3	-154.5	186.5	265.2
Max	2915	852	71	22	4.9	3.3	-38.7*	-37.3*	470.0	552.6
Min	1	1	0	0	1.0	1.0	-315.4	-448.9	55.1*	46.9*

Marshall-NASA Network

	n30 (count)		n30p (count)		nr (stroke)		i30n (rel. mag.)		i30p (rel. mag.)	
time	23 GMT	11 GMT	23 GMT	11 GMT	23 GMT	11 GMT	23 GMT	11 GMT	23 GMT	11 GMT
n	32	16	32	16	32	16	32	16	9	3
Mean	62	17	0.9	0.3	2.1	2.0	-29.0	-24.8	46.4	21.9
Max	610	172	9	3	4.0	4.5	-0.2*	-1.2*	87.7	34.0
Min	1	1	0	0	1.0	1.0	-67.3	-148.5	18.7*	10.4*

* = These minimum magnitudes were computed on the basis of only a few strokes and cannot be considered reliable.

TABLE 3

4.2 Case Studies of Anvil Temperature, Area Change and Lightning

Anvil growth as seen by satellite is one of the most dramatic evidences of deep convection. It is not surprising that anvil growth became an early diagnostic tool and has since been used by many investigators to study thunderstorm dynamics (e.g. Sikdar and Anderson, 1970; Lo et al.,1982) In particular, anvil growth has been used as a measure of volume flux into the upper troposphere and as an implicit indicator of updraft size and intensity. Infrared imagery also allows the measurement of blackbody cloud top temperatures. Obviously such temperatures are useful because they are closely related to the height of the cloud top of a storm through most of its life cycle.

In our second experiment in this study, we have undertaken to measure anvil growth and minimum temperature as it compares to lightning stroke rates. We have been encouraged in this approach by Adler et al. (1985) who by combining a view of anvil temperatures and growth were able to devise a reasonably accurate storm severity index. In a sense this index, by ignoring cloud-to-ground lightning, misses an important severe weather feature in itself, and a possible indicator of other severe weather phenomena. We hope, by relating storm temperature and growth to lightning, that we can begin to link lightning to the more traditional means of storm description and assessment.

In some respects, our approach complements what we have learned in our first experiment. In the previous section we sampled a wide range of storms in an attempt to relate temperature and cloud coverage to flash rates. While useful in giving us a climatological view, this approach tell nothing of the time dependency of these relationships for individual storms. Does flash rate increase with accelerating anvil expansion and a fall in cloud top temperatures? If so, is there a lag? Is flash rate qualitatively different in small cells with short lifetimes? Using data from two GOES rapid-scan image sequences and

lightning data for the North Central States LPATS network, we have attempted to answer these questions.

4.2.1 Data

GOES rapid scan infrared images, generally at intervals of from 5 to 15 minutes, were used for the two case studies included in this experiment. One of these case study days (hereafter referred to as "Study One") ran from 2130 GMT, Day 250 (September 7), 1985 to 0500 GMT, Day 251. In addition, half hour images were used to measure one anvil from 0930 to 1430 GMT, Day 251. "Case Study Two" began on 2130 GMT, Day 251 (September 8), 1985 and ended at 0500 GMT, Day 252. Although located close to one another in time, these cases were quite different from the standpoint of the kind of storms generated, as we will see in the following section.

The North Central States LPATS network (Dr. Walter Lyons, R*Scan Corporation--network manager) covers Minnesota, Wisconsin, Iowa and parts of surrounding states. It is a time-of-arrival system with four dual-whip antennas, each connected by a data link to a central analyzer. One of the antennas at each site receives the LORAN-C signal, while the other receives the electric pulse from the lightning strike. For a technical description of the LPATS system, see Lyons, et al. (1985).

At the time of this experiment, only ground strike locations were recorded by the network. There was no information on stroke magnitude and polarity, although the latter has since been added. Multiple strokes within one flash are recorded separately. Thus the stroke rates calculated in this experiment are not directly comparable to the flashrates used in the previous sections. A more accurate comparison could be made be dividing the stroke rates by the 2.2 strokes/flash calculated from the NSSL data. This correction would of course only be an approximation to the actual flash rate since, we have seen in Figure

8, there are sample variations in numbers of return strokes from 1 to 5, with a tendency for higher stroke rates in samples with greater electrical activity. Our sample of LPATS storms may vary significantly from the averages found in our LLP climatologies.

Location accuracy, calculated theoretically on the basis of likely timing errors, shows an error of less than 0.5 km near the center of the network (approximately where the borders of WI, MN and IA intersect). At the outer edge of the network, near a radius of 500 km, the errors are still generally 10 km or less; the lightning data taken for this experiment are within this radius. An estimated 0.5% of the strokes reported are considered bogus. There were a few samples where the strokes appeared to be randomly distributed or where significant numbers of strokes were entered into the file twice. These erroneous data appear to have been the result of miscommunications between the network and the computer on which they were being archived (at NSSFC in Kansas City). Fortunately, these errors were few and easily detected; all were excluded from the final data set.

4.2.2 Methodology

Since we intended to compare lightning to satellite-observed anvil growth and temperature, we first plotted stroke location as an overlay to the satellite infrared image. Strokes appearing in the plot had to occur between the image start time (corrected for the time the camera actually observed the latitudes of interest) and the time of the next image available. This lightning subset was chosen so as to center the stroke counts on the interval over which anvil area changes were to be measured.

Navigation of the image was checked relative to observable landmarks and the lightning was examined with respect to the presence of possible cumuliform clouds. We found stroke locations consistently clumped in proximity to the

coldest cloud, with these centers of electrical activity trackable over time. We also observed that at five minute resolutions the appearance of lightning often preceded the appearance of a recognizably growing anvil in the satellite image. A few cases, as noted above, stood out as essentially random distributions of strokes, and were excluded.

Anvils with which the lightning was to be compared were defined as cloud colder than 226 K with a period of rapid growth at least sometime during the period in which there was associated lightning. Except for lightning, these criteria are similar to those used by Adler et al. (1985) to identify thunderstorms in satellite imagery. In order to obtain a smaller scale record of lightning and cold cloud growth, two other empirically designated thresholds--210 and 206 K--were used to define cold cloud areas. These thresholds delineated small features which had good continuity over time. Furthermore, each cold cloud area was usually associated with a cluster of lightning in the immediate vicinity which also showed good time continuity and which appeared to follow the cold cloud area as it evolved.

Each image was processed as follows. First, digital enhancements corresponding to each threshold were applied to the infrared satellite image so as to allow the comparison of the anvil and cold cloud areas to centers of lightning. The lightning strokes falling within or in the immediate vicinity of each threshold-defined area and clearly not associated with any other separate cold cloud area were considered to have originated with that anvil or the colder area within the anvil. These strokes were counted and recorded with the help of a McIdas area statistics routine. The statistics routine was also used to measure the cold cloud area and the minimum blackbody temperature.

Sometimes, of course, separate anvils or cold cloud areas within anvils were seen to merge. As long as there was only a small region of overlap with respect to the size of the original areas and there was a clear separation

between the centers of lightning, an estimate of the boundary between the areas was drawn and separate statistics recorded. Sometimes (for three of the Study One anvils), the merger reached the point where the 226 K threshold no longer defined a unique anvil, but the colder thresholds still enclosed areas with distinct centers of lightning. We continued to measure these colder areas and associated lightning as part of the original anvil. We usually continued to measure the 226 K area as well, the exception being where cirrus debris from nearby decaying anvils made such measurements meaningless by masking growth in the active regions of the cloud. Usually, this combined entity was given a given a new number (likewise for anvils or cold cloud areas that fractured into several separate areas). An exception to this practice was observed for Anvil 1 in Study Two. At 22 GMT, and again at 00 GMT, two small cells formed on the edge of the main cloud canopy. The first cell was very small in relation to the total cloud area, had a short lifespan and generated few ground strokes. The second cell while still small quickly merged with the anvil where it remained for the rest of its lifetime.

From these measurement three statistics were calculated. These were the stroke rate, the area change [dA/dt] and the divergence [$(1/A)*(dA/dt)$]. Area change and divergence were calculated by counting satellite pixels and converting pixels to area (1 pixel $\approx$ 19 km^2). All statistics are referenced to the interval between successive satellite images.

For an anvil to be included in the final set of measurements there had to be at least ten images from which an area change, minimum temperature and lightning stroke rate could be computed. Fewer data points would have made inter-anvil comparison difficult, especially where compositing was applied.

4.2.3 Synoptic Setting and Comparison of Case Study Storm Character

The synoptic setting for the two case studies is illustrated by a series

of charts and a pair of soundings, all for 00 GMT on 8 September. Through the period of this experiment, a warm high lingered over the southeastern United States as a cool high dropped southeast out of western Canada. Driven by the southeastern high and a developing low in the central plains (Figure 11), moist air streamed out of the Gulf of Mexico, across the southern plains and into the upper Mississippi Valley (Fig. 12 and 13). At 500 mb (Figure 14), a shortwave trough was emerging from the central Rockies. In the upper troposphere the subtropical jet arched anticyclonically around the southeastern high from the American Southwest into southern Canada (Figure 15). Fronts and baroclinic disturbances lay along the northwestern and northern fringes of the southeastern high, in the central and northern plains and across the Great Lakes.

Several air masses were present in the upper Mississippi Valley and the western Great Lakes. At the surface, to the south of the Minnesota/Wisconsin/Michigan front was a warm, very moist mass of Gulf air. Equivalent potential temperature in this air mass was as high as 360 K (Figure 11). To the north of the front was a cooler, drier air mass of Canadian origin. Soundings at St. Cloud (not shown) and Green Bay (Figure 16) confirm that near its southern edge the Canadian air mass was overlain by the Gulf air mass.

As is shown by the sounding for Peoria (inset to Figure 16) the Gulf air mass, above about 800 mb, itself was overlain by drier air 250 to 300 mb in thickness. A distinct inversion in temperature separated the two air masses. Like the Gulf air mass, the drier air mass extended north of the front; unlike the Gulf air mass, at Green Bay it was less stable. As a consequence, near the front relatively little differential lifting across the interface between the two layers would have been sufficient to completely destabilize the layer above the surface inversion. Any perturbation then could have tapped the very large convective potential energy which is implicit in indices of -7 (lifted) and 54 (totals) for the Green Bay sounding.

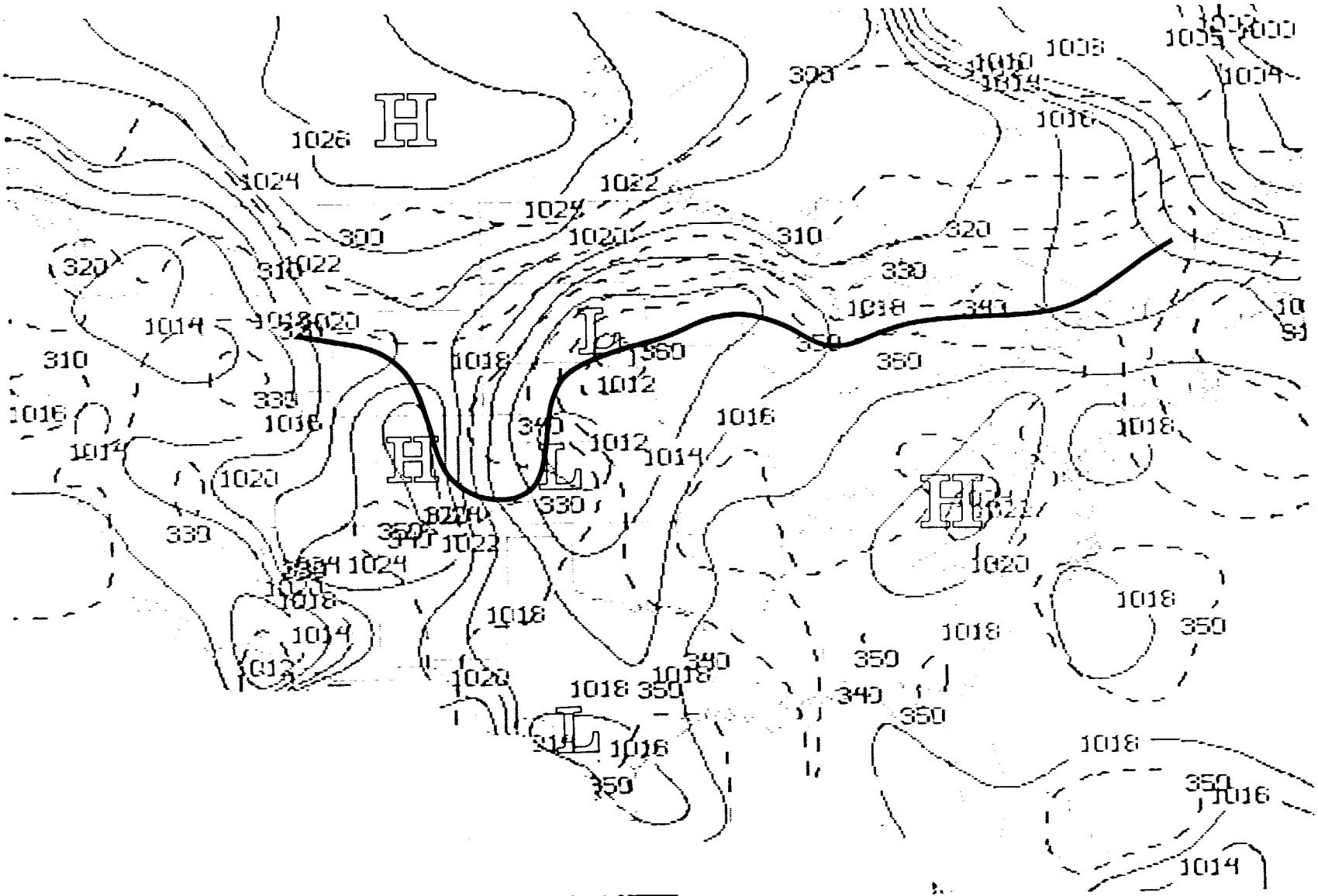

Figure 11

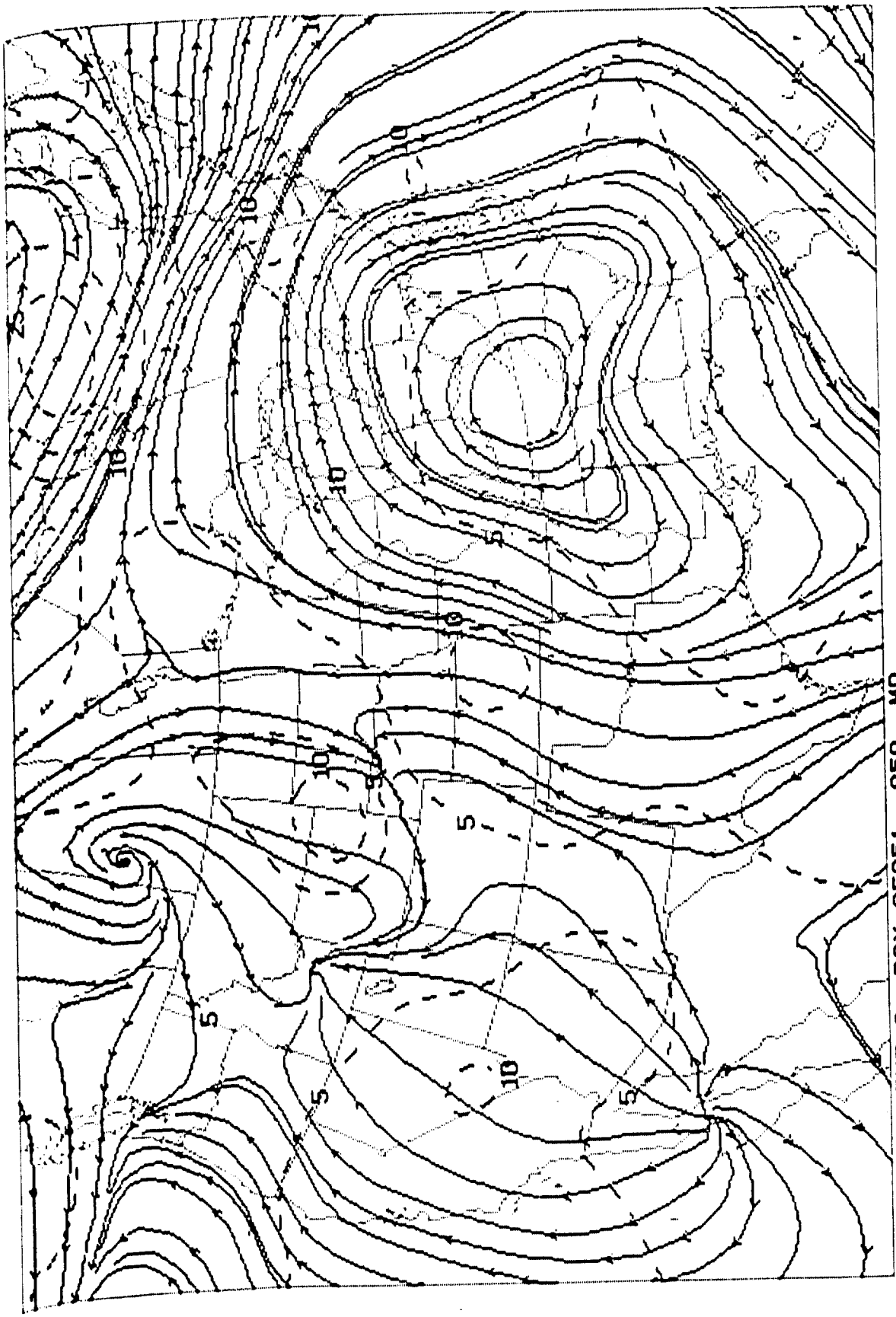

Figure 12

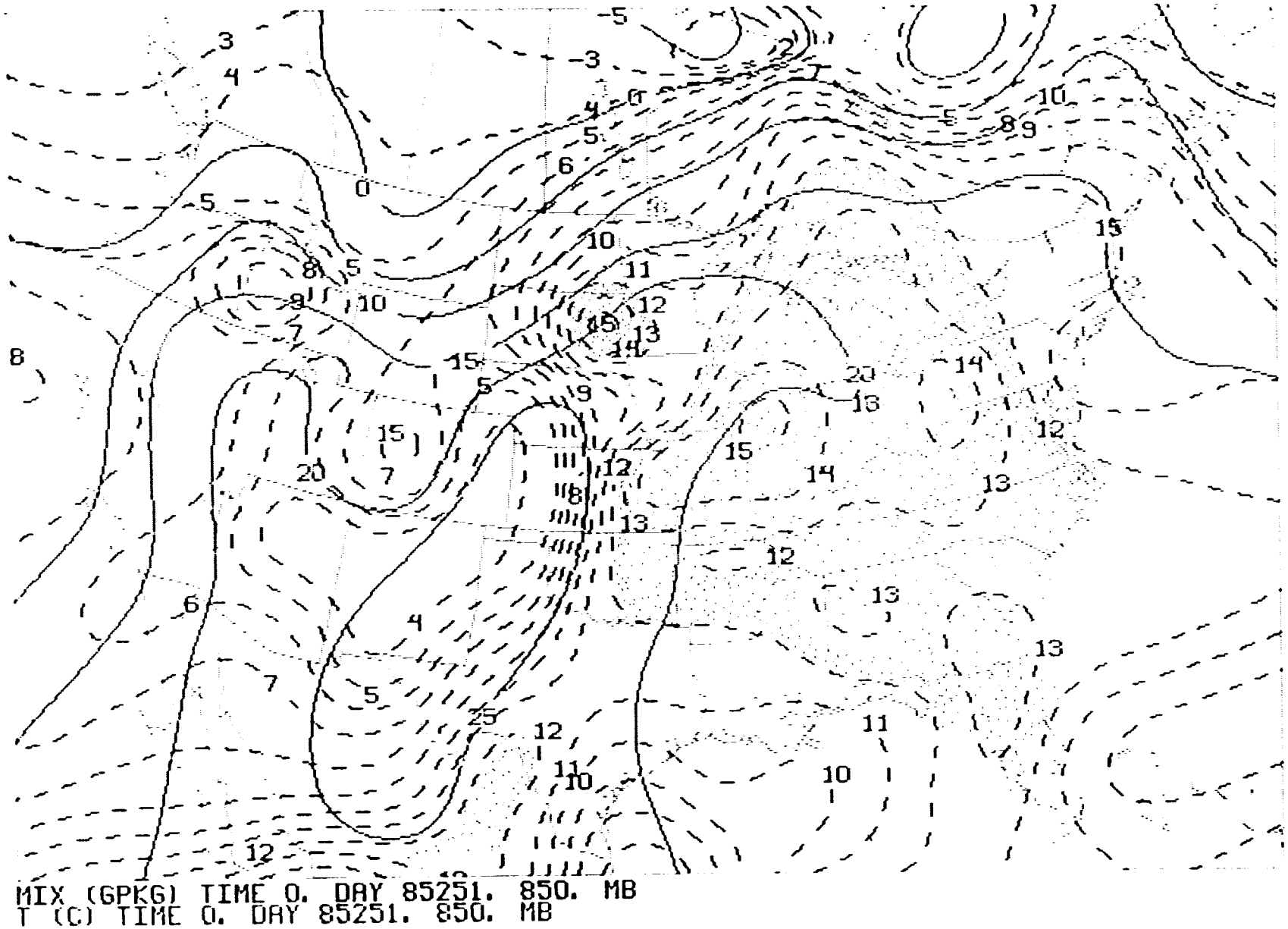

Figure 13

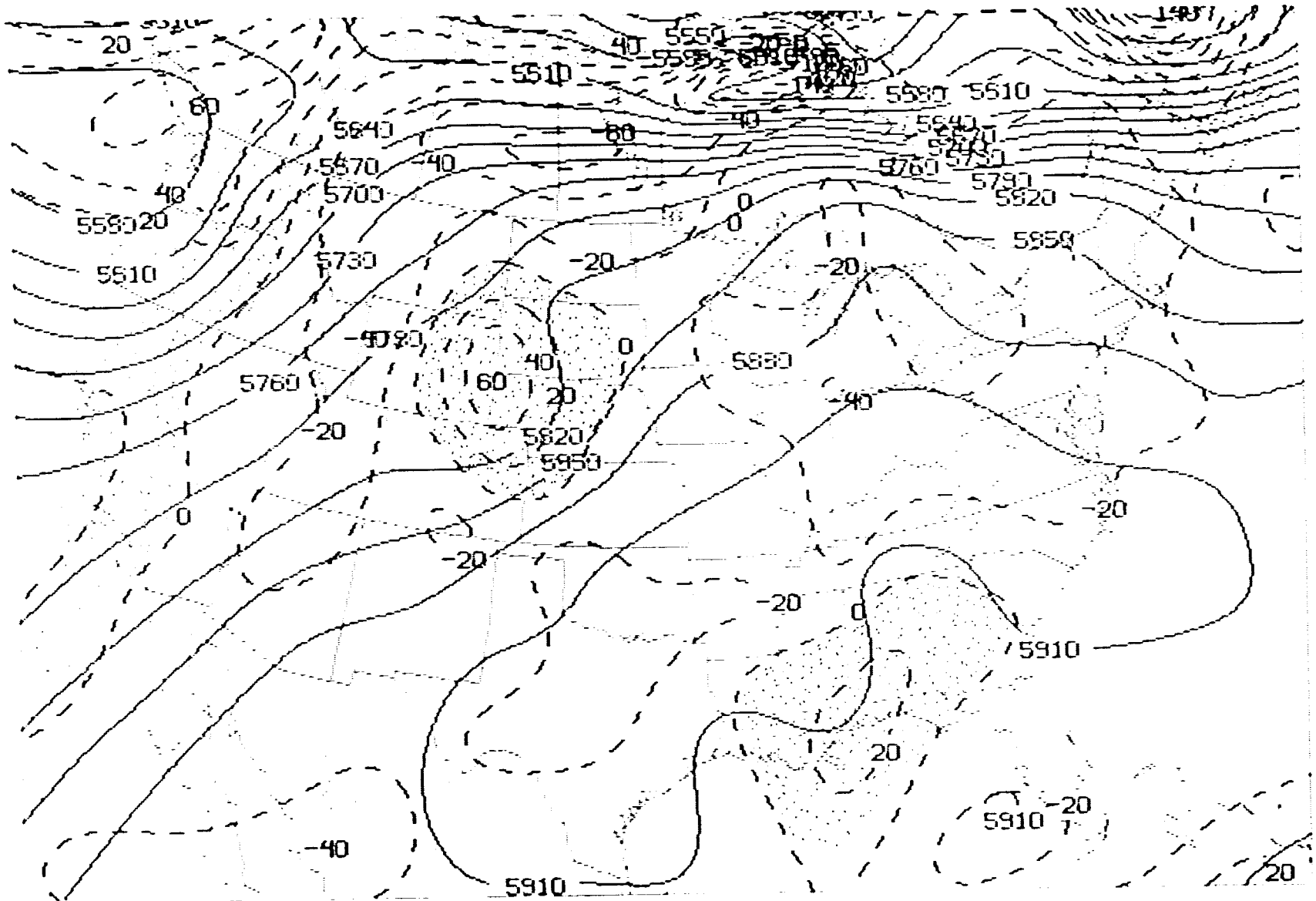

Figure 14

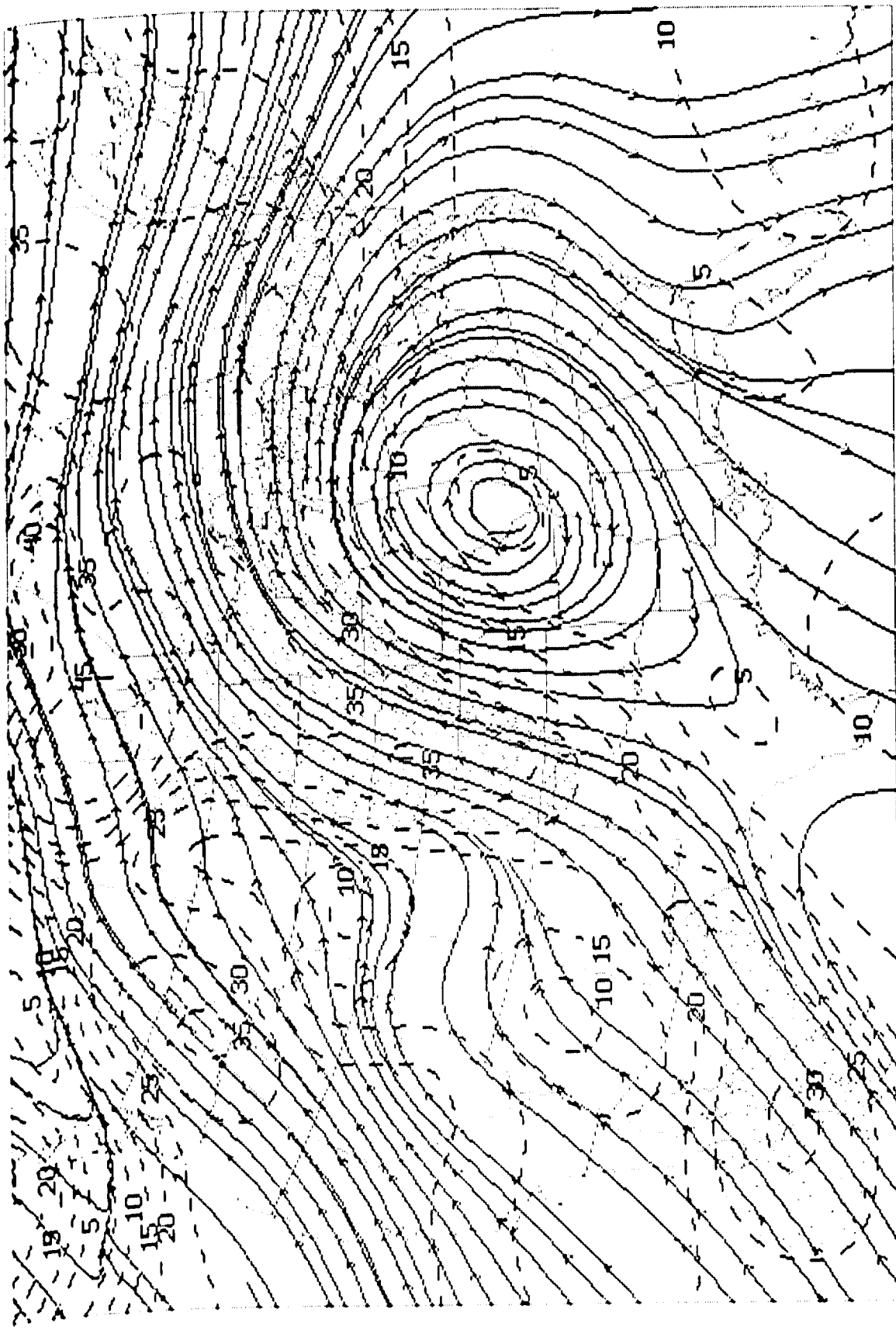

Figure 15

ORIGINAL PAGE IS
OF POOR QUALITY

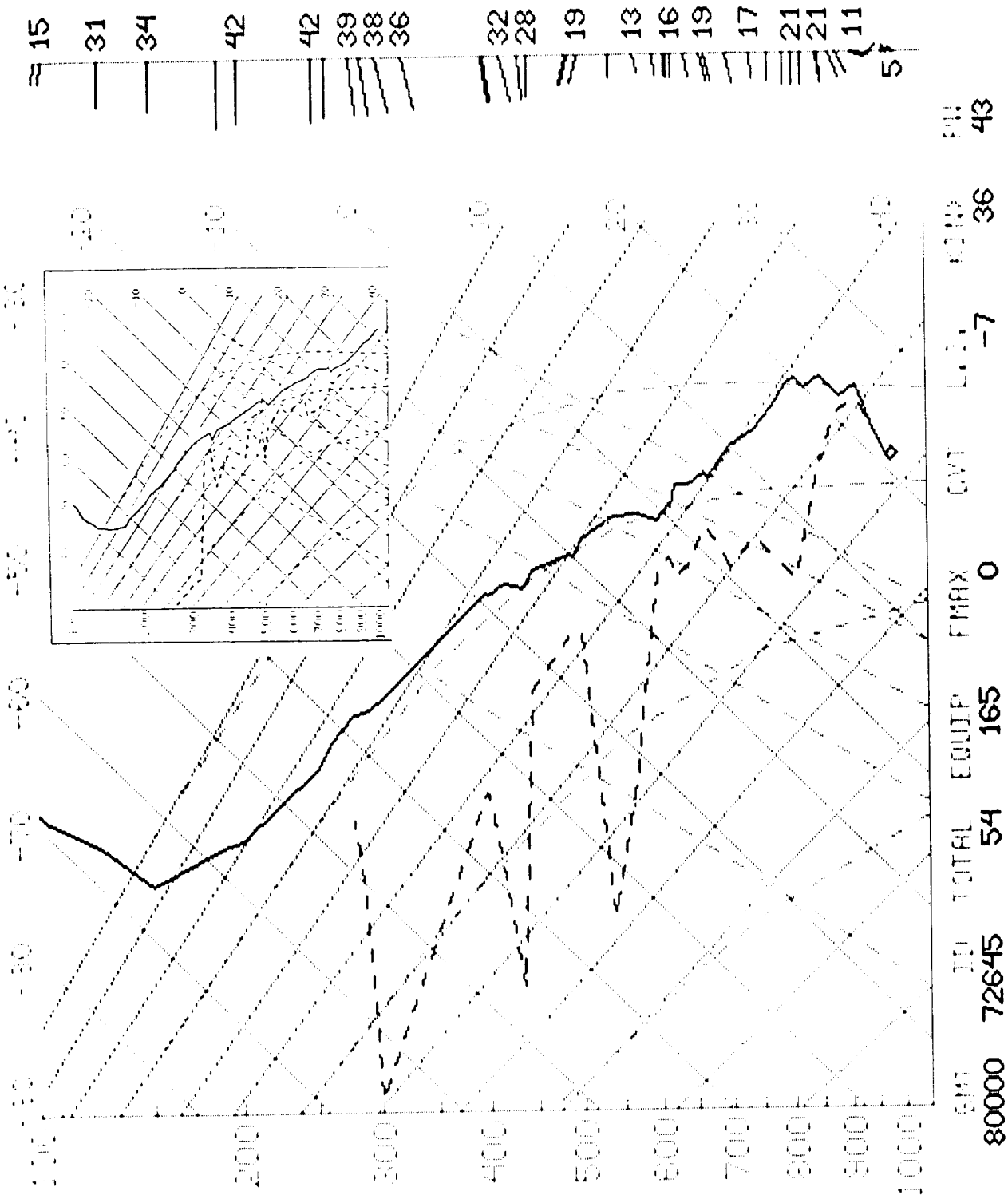

Figure 16

East of the Rocky Mountains and northern plains the tropopause was domed (Figure 17), with steepest gradients to the west and north. In the storm region, temperatures ran from -64 to -68 C.

During the last day of the study period the Minnesota/Wisconsin/Michigan front dropped to the southern border region of these states. Together with continued development of the central plains low, this produced a split in the Gulf airstream. The largest branch flowed east over Iowa and Illinois, but the smaller branch curled cyclonically from Iowa into southern Minnesota and the eastern part of South Dakota. Reflecting northeastward movement of the 500 mb short wave, tropopause temperature dropped 1 to 2 C.

Deep convection is summarized in Figures 18 and 19. In 18 a and b, which summarize the first outbreak of thunderstorms, we draw attention to the arc of cumulonimbus clusters which eventually extended from Michigan to the Dakotas. These clusters are numbered in order of their appearance: 1 (Michigan), 2 (Wisconsin), 3 (Dakotas), and 4 (Minnesota). Anvils for Study One were drawn from the western edge of cluster 1 (until they drifted outside the 500 km radius detection area), cluster 2 and cluster 4, covering a span of time from about 2130 GMT, September 7 to 1430 GMT, September 8. In general over the period of the study, deep convection shifted from east to west. However, individual clusters (and the cells within them) moved eastward. In contrast to those to the south, all of the arc clusters are more or less wedge shaped. West-pointing wedges imply a westerly shear through the troposphere. This is consistent both with the locations of cold centers, which tended to be on the west (upstream) sides of the clusters and with the airflow between 850 and 200 mb (Figures 12 and 15).

Figure 19 summarizes thunderstorms occurring over and near Wisconsin late on 8 September and early on 9 September. Of particular interest is cluster number 5, which was chosen for our second study and is identical to Anvil 1,

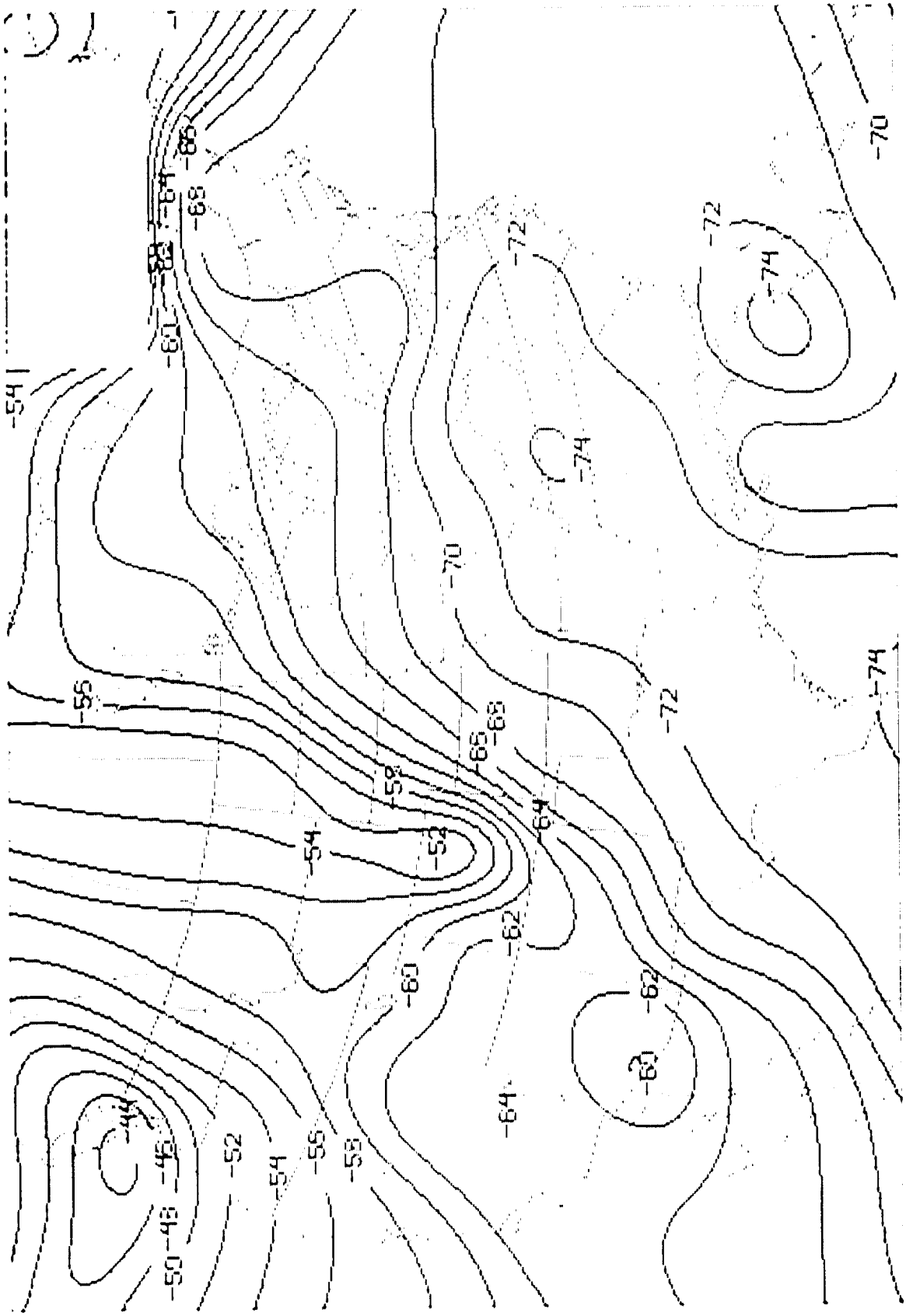

Figure 17

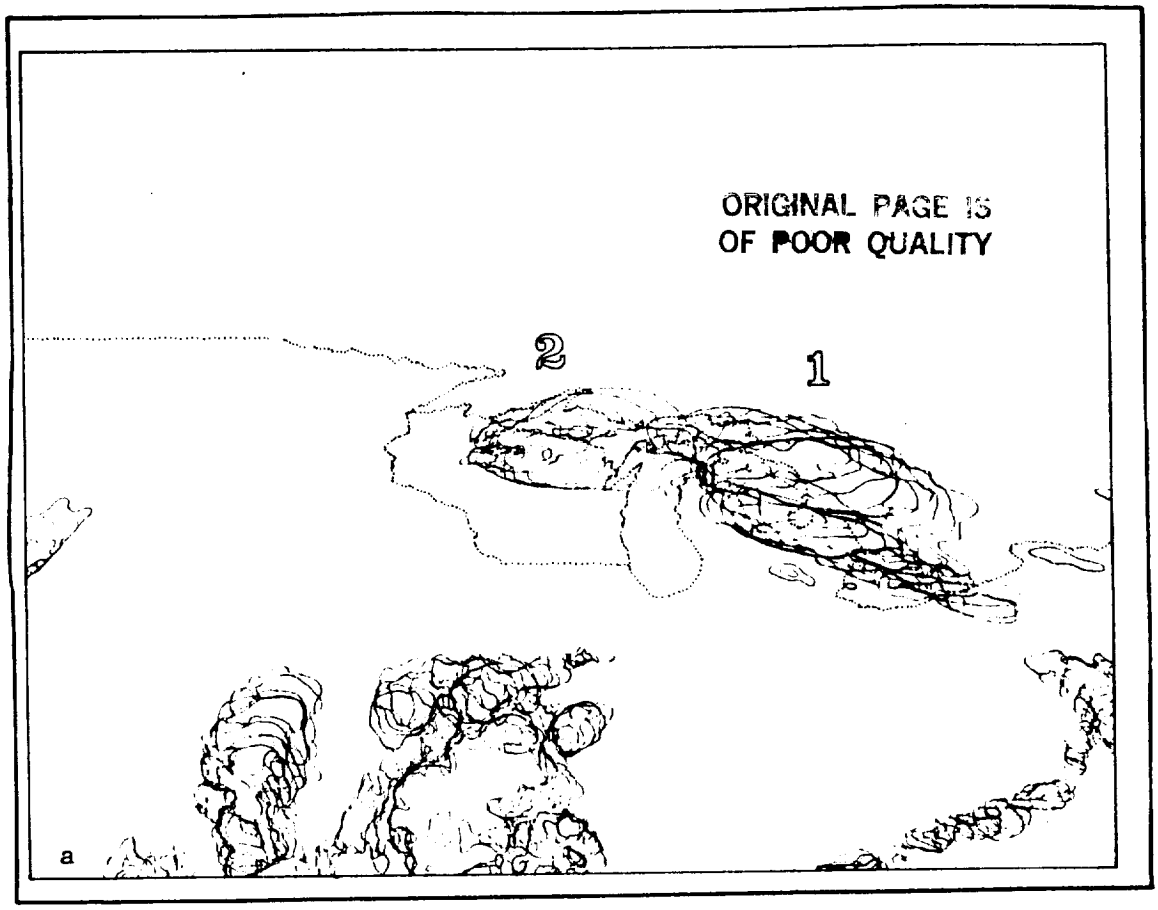

a

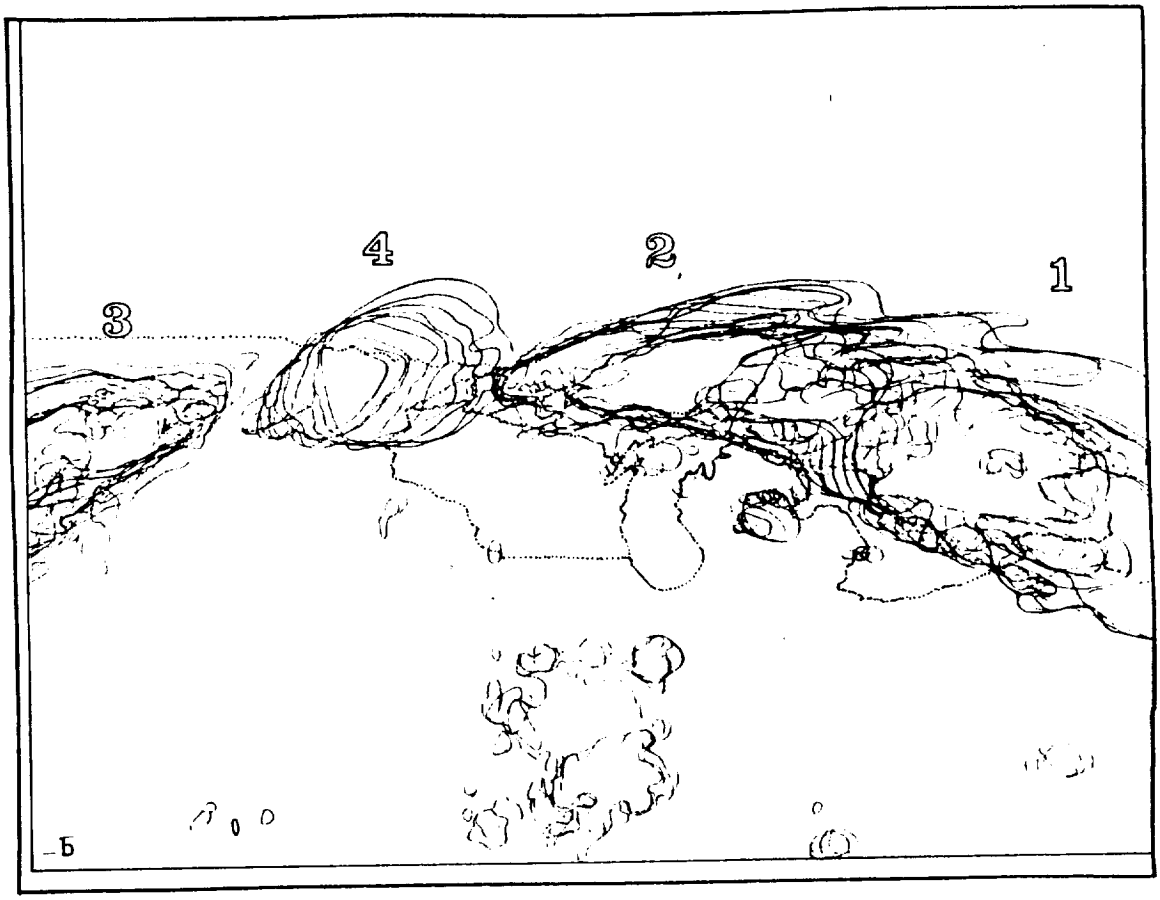

Figure 18

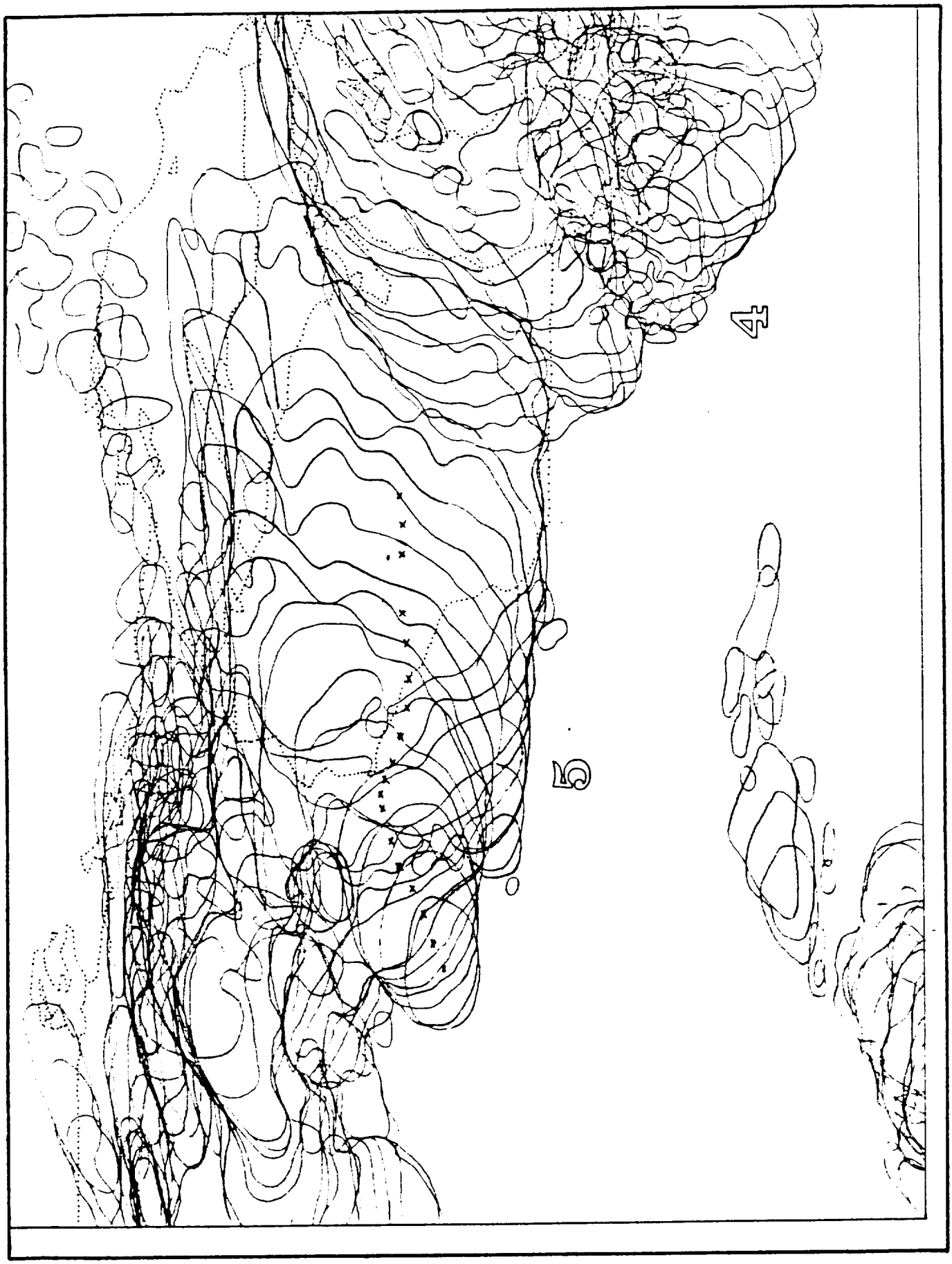

Figure 19

Study Two. We began its measurement around 2030 GMT, 8 September when it appeared as an cold oval cloud in central Minnesota. Shortly after 00 GMT, 9 September a small but rapidly growing cloud just west of Wisconsin formed and then joined with the larger anvil to the north. As it moved east, cluster 5 produced a memorable display of nighttime lightning over Madison. Tracking ended at 05 GMT, 9 September, due to the lack of additional rapid scan images.

Our two case studies exhibit significant differences from one another. Study One incorporated six different anvils drawn from three separate convective areas. Three of these anvils could be defined throughout their lifetime by the 226 K contour. The other three anvils were defined through all or part of their lifetime with the help of the 210 K contour because of merger at the 226 K level or the presence of decaying anvil debris. However, there was never any question of their distinct identity at the colder levels. Study Two, on the other hand, was based on the lifetime of a single convective area defined by the 226 K threshold. We also measured the areas enclosed by the colder contours and their associated lightning. Over the course of anvil measurement we found seven identifiable cold cloud areas ranging in lifetimes from one to over three hours. These measurements were useful in describing a more localized growth and stroke rate, especially for compositing in the later stages of the storm. However, the individual cold cloud areas within the anvil, unlike those of Study One, did not maintain clearly separate identities over long periods. Their proximity to one another allowed frequent interaction and transformation. While some of them did maintain a life-history of sufficient independence (continuity over ten or more images) to be used in this study, they are not presented here because they added little information that was not already included in the statistics for the whole anvil.

Table 4 illustrates the important characteristics of all anvils included in the final data set and their associated electrical activity. While there is

Case Study Anvil Measurement and Associated Electrical Activity

Case Study #	Anvil #	Start of Meas.	End of Meas.	Span of Meas.	Max. Size 226/210	Low Flash Rate	High Flash Rate	# of Peaks	Life-time Min.T	Comments
		GMT	GMT	h	km²	#/h	#/h		K	
1	1	2133 9/7	2303 9/7	1.5	39375 5505	29	1009	1	202	Passed out of network
1	2	2157 9/7	0203 9/8	4.1	19246 3661	0	98	2	208	No electrical activity after 0047 GMT
1	4	2303 9/7	0333 9/8	4.5	32115* 10676	65	655	2	202	Fragmented at 0333 GMT. Part is included in #10
1	6	0122 9/8	0333 9/8	2.2	- 2036	5	218	1	203	Dissipated after 0333 GMT
1	10	0333 9/8	0503 9/8	1.5	- 36041	212	780	1	198	Passed out of network
1	11	0933 9/8	1433 9/8	5.0	71402# 9107	0	647	1	206	Dissipated after 1433 GMT
2	1	2033 9/8	0503 9/9	8.5	87814 3213	239	2541	4	205	Still very active at time of last measurement

* Last 226 K threshold area measurement taken at 0122 GMT.
# Last 226 K threshold area measurement taken at 1103 GMT

TABLE 4

significant variation among Study One anvils, their average lifetimes, area extent and stroke counts, in comparison with the Study Two anvil, were small.

The Study Two anvil had a measured lifetime nearly double that of any other storm. It was still very active when measurement ceased. Although Anvils 1 and 10 were not followed through their entire lifetime either, both had only 90 minutes to their credit when they passed out of the network and for Anvil 10, lightning activity was in a marked decline during its last hour of measurement.

The Table area measurements are the number of square kilometers enclosed by the 226 and 210 K temperature contours. It was not always possible to measure both. Sometimes the 210 K contour did not yet exist. In other cases anvil merger or debris for nearby decaying anvils, prevented the use of the 226 K contour to define a unique anvil (as described in Section 4.2.2). Comparing first the 226 K areas, it would appear that at least three of the anvils (#1, 2, 11) were smaller than the Study Two anvil during their measured lifetimes. Anvil #4 probably never reached those dimensions either, although measurements of the 226 K threshold were terminated several hours before the anvil fragmented. Since the Study Two anvil was actively growing when measurement was terminated, it is therefore likely that it substantially outdistanced at least 4 of the 6 Study One anvils. Nevertheless the 210 K area of the Study Two anvil is intermediate. Four of the Study One anvils surpassed it, one (Anvil 10) by an order of magnitude. Under "Lifetime Minimum Temperature", a similar comparison can be made. We may conclude that while the larger anvil may have had a prolonged period of activity, it did not maintain anytime during its measured existence as large or as cold an area of active cloud tops as some of its more meteoric rivals.

Despite this failing, the Study Two anvil was an outstanding producer of lightning. Its peak flash rate (converted from stroke rate using the 2.2 strokes/flash average obtained from the climatological study) is three times

greater than the others. It also showed more fluctuation over time. Applying running means over three terms to smooth out short term variations, this anvil had 4 peaks (defined as relative maxima resulting from a steady increase and decrease of flash rate over at least a 40 minute period). In Study One storms there were either one or two maxima. We can compare these findings with Peckham et al. (1984), who have defined and studied three types of storms, which in ascending order of their lifetimes, flash rates and flash densities are termed single-peak, multiple-peak, and storm systems. The first two classifications were based on the determination of single groupings of lightning strokes over time which could not be decomposed into still smaller cells. Study One anvils appear to be such indivisible groupings, although Anvil 2 despite its multiple peak shows the lowest flash rate of all. The Study Two anvil, however, showed (as previously described) a complex history of seven proximate cold cloud areas which seem to fit the definition of a storm system ("two or more single-peak and/or multiple-peak storms that are related in space and time such that a non-directional lightning detector like a flash counter would view them as one overall storm").

Another way to characterize the Study Two anvil in comparison to Study One anvils might be through Goodman and MacGorman's (1986) definition of a Mesoscale Convective Complex (MCC)). While we did not use the same temperature thresholds to define our anvils and thus cannot make an exact comparison, the Study Two anvil appears close to meeting all the qualifications for size, shape, and longevity. Its peak flash rate of 2541/h (based on a 5 minute interval) or 2142/h (based on the actual number of flashes over a one hour period) and its more than five hours of continuous flash rates exceeding 1000/h (see Figure 20) compare well with the those storms found in the Goodman and MacGorman study. (Flash rates were still around 2300/h when measurement was terminated).

In terms of weather reported, however, none of our storms qualify as

notably severe. No tornadoes were reported anywhere in the study region. Until the early morning of 9 September, high winds (gust >50 knots, 25 m/s) were confined to the area east of Lake Michigan which included some of the Study One anvils. These same storms produced hail up to 1 3/4 in (4.5 cm) in diameter in Michigan and Wisconsin. Later the second Minnesota storm (our Study Two anvil) also produced hail and some high winds.

4.2.4 Anvil changes and lightning

If one plots the raw values of stroke rate versus minimum anvil temperatures and changes in anvil area, there appears to be little correlation. The minimum temperatures show gradual change but the stroke rate and anvil area changes are very noisy and fluctuate wildly between successive images, even those as close together as 5 minutes. Taking 3 term running averages on these two variables, however, to smooth out some of the smaller time scale fluctuations proves to be quite helpful. Figure 20 illustrates a comparison for anvil 1 of Study Two. In plot a, there is a general downward trend of minimum anvil temperature corresponding to a buildup of peak stroke rates and even some inverse correspondence over periods of about an hour. This conclusion is only partly sustained by the other anvils. Whereas four of the six Study One anvils showed negative correlations of -0.31 to -0.51, two anvils showed positive correlations of 0.39 and 0.08.

In part b of the Figure 20, we find, in contrast to the anvil temperatures, that the correspondence between the small fluctuations of anvil area change and stroke rate can be quite good. On the other hand, some major changes in *dA/dt* are opposed by stroke rate. Especially apparent is the sudden shift downward in dA/dt values around 23 GMT while the stroke rates shift upward. One might conclude that overall the absolute value of area change does not give a good indication of the stroke rate magnitudes. This suspicion is

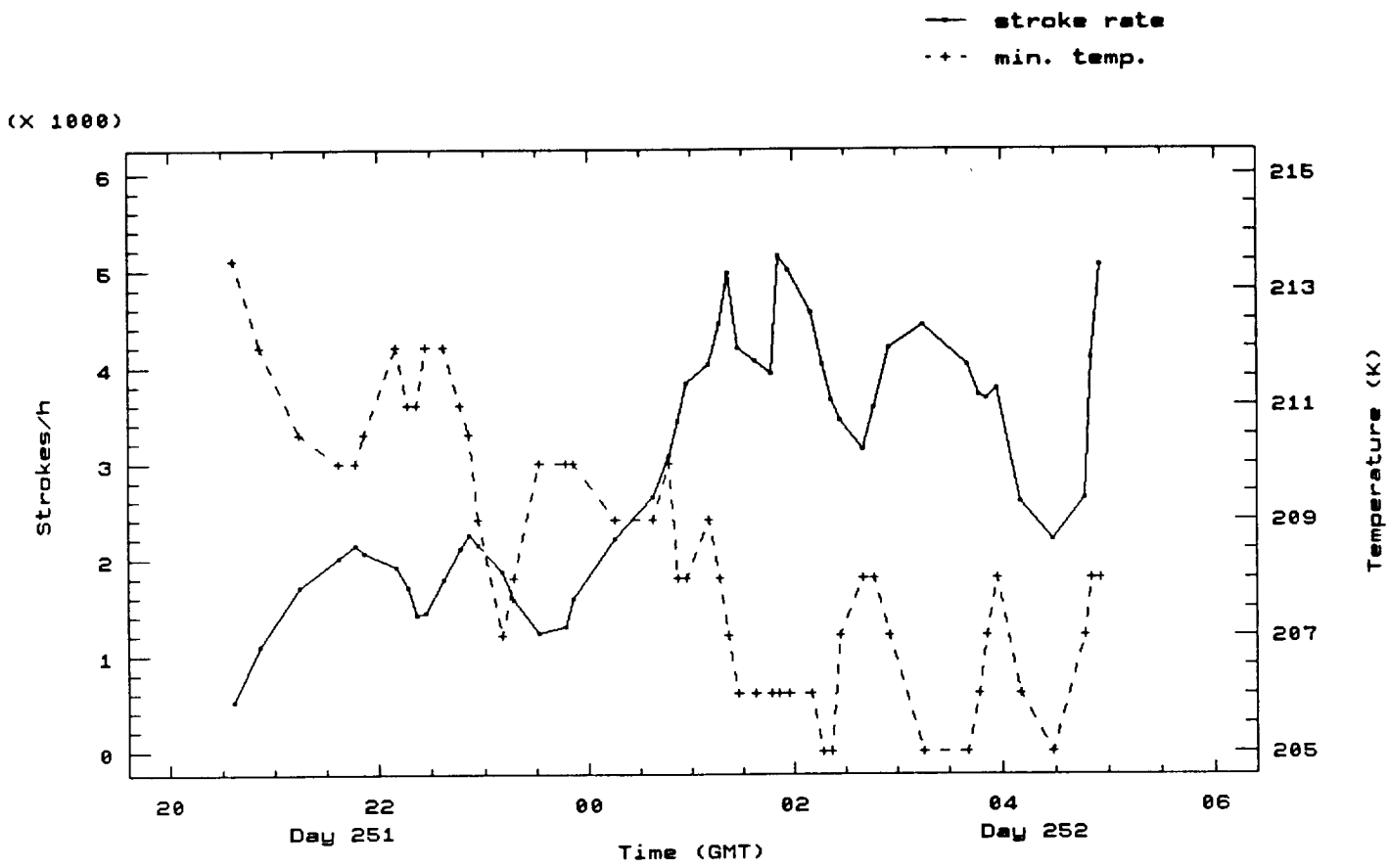
stroke rate
min. temp.
(X 1000)
Strokes/h
Temperature (K)
215
213
211
209
207
205
6
5
4
3
2
1
0
20
22
00
02
04
06
Day 251
Day 252
Time (GMT)

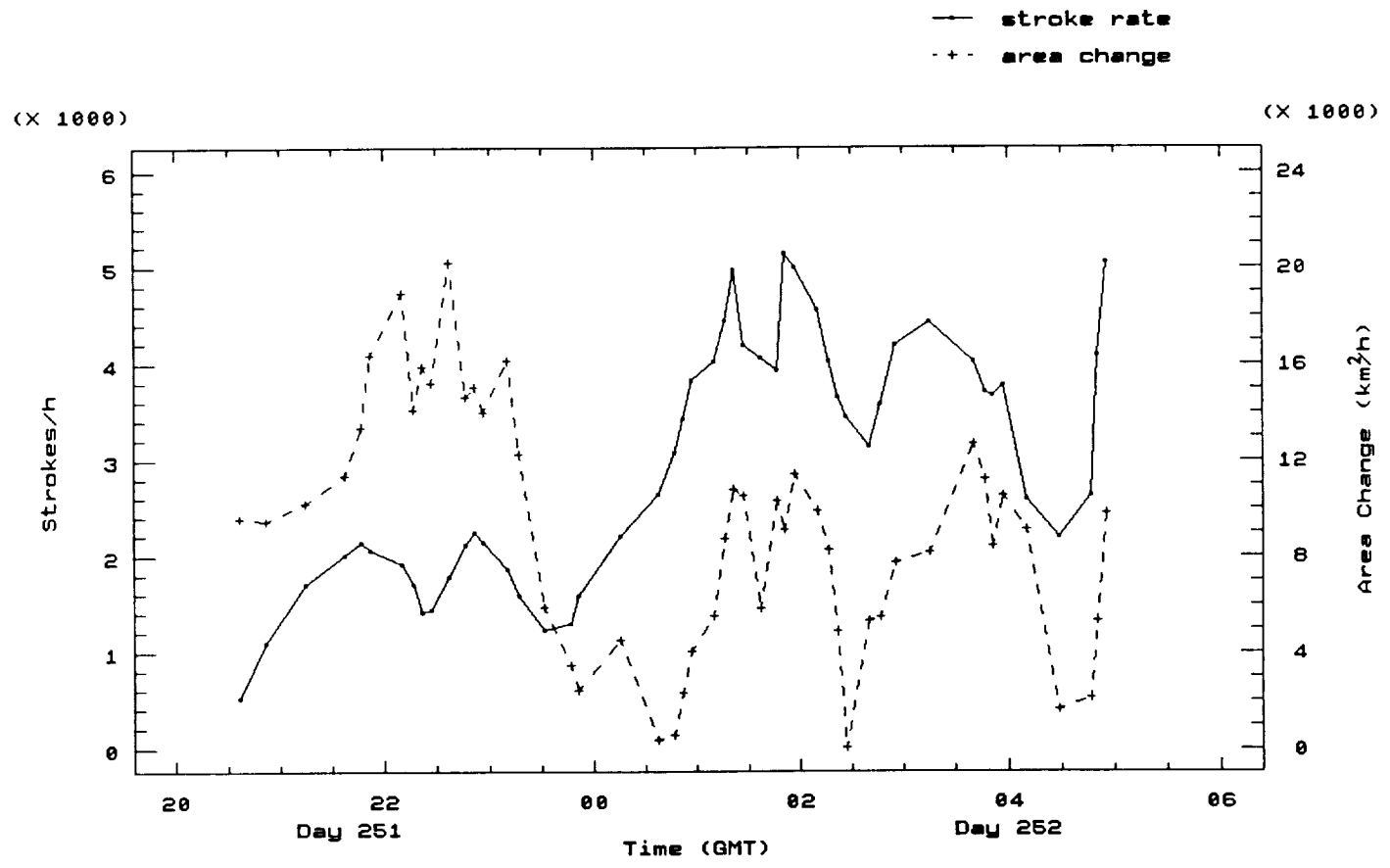
stroke rate
area change
(X 1000)
(X 1000)
Strokes/h
Area Change (km²/h)
24
20
16
12
8
4
0
6
5
4
3
2
1
0
20
22
00
02
04
06
Day 251
Day 252
Time (GMT)

Figure 20

confirmed by the correlation between the smoothed *dA/dt* values and stroke rate: it is actually a -0.22. If one excludes the hours before 00 GMT, however, the correlation jumps to about 0.65. In Study One, where the periods of time covered are shorter, these correlations range from +0.40 to -0.47, with no clear trend emerging.

For all of the anvils measured in these two case studies, we also computed divergence. Unfortunately, in our calculations divergence proved to be sensitive to the size of the area measured and underwent a rapid decrease after anvil formation, regardless of the trend in stroke rate. An example is shown in Figure 21. After the initial decline, divergence closely parallels changes in *dA/dt* and adds little to the information gained by looking solely at anvil growth.

In order to obtain a better understanding of how minimum anvil temperatures and anvil growth relate to lightning, we have made composites of these two variables relative to peaks in stroke rate. In order to obtain relatively isolated and sustained changes in electrical activity, these peaks were defined as relative maximums in flashrate that exhibited a sustained rise and then a fall over a forty minute periods centered on the maximum. In Study One, these criteria resulted in the selection of 8 maxima from six anvils, two of the peaks being secondary maxima. In Study Two, only one convective area was measured but this area showed four relative maxima over the 8.5 hour period.

A value of 1.0 was assigned to the maximum stroke rate and all other flash rates were scaled accordingly. Relative to these maxima, minimum temperatures and *dA/dt* were calculated in either direction at intervals of 6 minutes. Because some peaks occurred close to the time when the anvil first formed or when measurement was terminated, there was a limit to how far forward or back in time measurement could be computed for temperature and dA/dt. For Study One the interval computed turned out to be 30 minutes prior to the maximum to 42

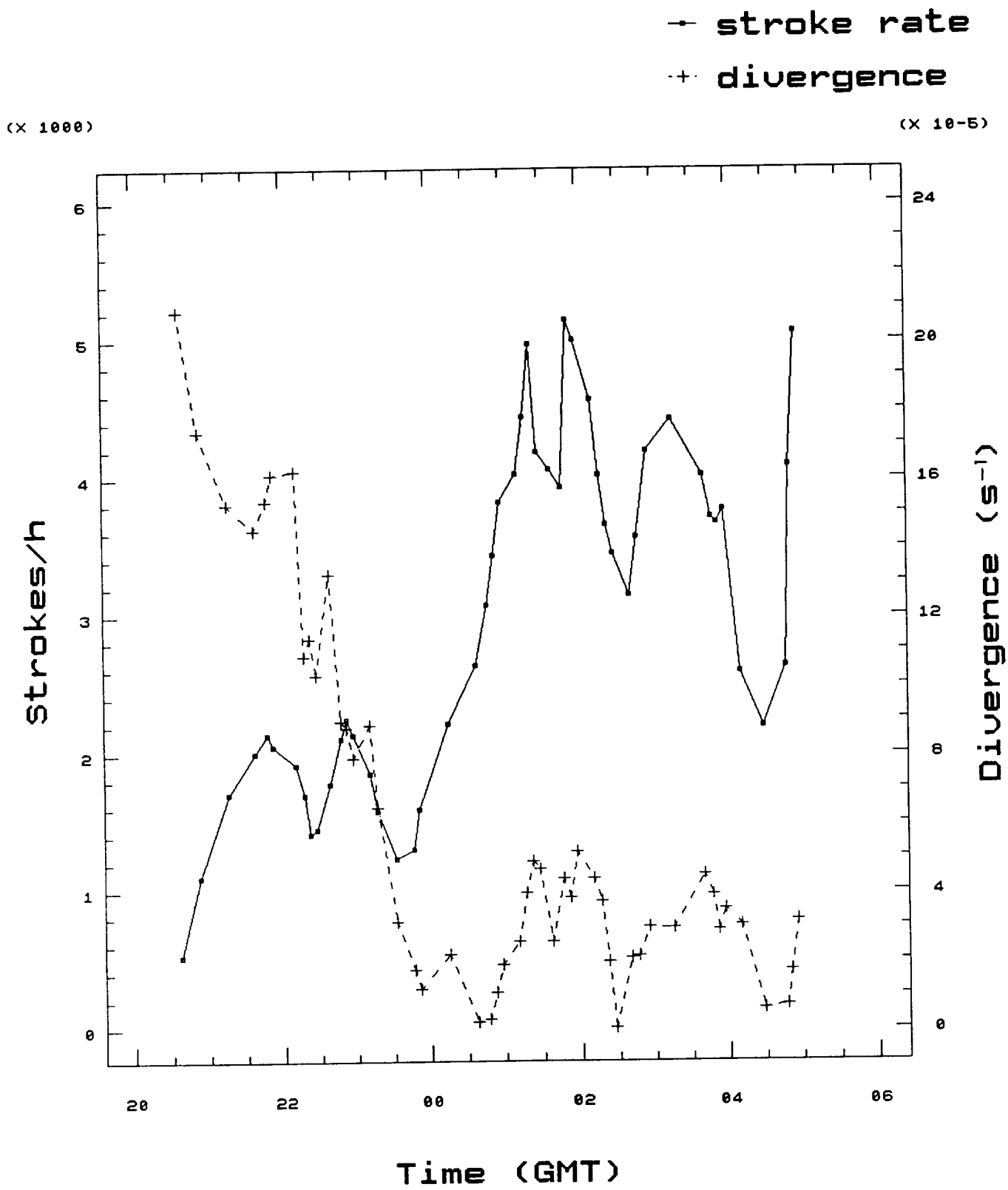
stroke rate
divergence
(X 1000)
(X 10-5)
Strokes/h
Divergence (s-1)
Time (GMT)
0
1
2
3
4
5
6
0
4
8
12
16
20
24
20
22
00
02
04
06

Figure 21

minutes after the peak. For Study Two, the intervals were 48 minutes on both sides. Minimum temperatures were normalized by setting the warmest temperature to 1.0 and the coldest to zero. *dA/dt* was normalized by setting the largest positive value to 1.0 and the largest negative value (if any) to -1.0 and scaling the remaining values accordingly. The results for Case Study 1 and 2 can be seen in Figure 22a,b (minimum temperature) and 23a,b (*dA/dt*), respectively.

In respect to lightning the stroke rate curve is flatter for Study Two. Many of the peaks in Study One were the result of very steep climbs from a base of zero near the beginning of the storm's lifecycle, while the peaks in the second study were mostly fluctuations superimposed on a relatively high base rate of activity. In absolute terms, Study Two also had much higher flash rates. The variation between composited base and peak rates in Study Two is 1007/h to 1456/h, compared to 139/h to 416/h for Study One. In both cases, we see a steady fall of temperature as stroke rate increases. Over the 30 minutes following peak stroke rate, minimum temperature either continues to fall or remains about the same.

In absolute terms, the minimum temperatures found in both samples were similar as well. Average minimum temperatures relative to the lightning maxima ranged from 209.7 to 205.6 K for Study 1 and 209.9 to 207.4 for Study 2. This range agrees well with tropopause temperature at 00 GMT, September 8 (Figure 17), which ranged from 209 to 205 K across the study area. For individual anvils showing at least some electrical activity, we found a range in Study 1 of 218 to 198 K. The less varied sample in Study 2 showed extremes of 212 and 205. By way of comparison, our findings from the climatological study in the previous section showed lightning first occurring around 243 K and present in almost all samples for minimum temperatures less than 210 K. It is notable that our compositing sample did not include any relatively warm (around

Study One

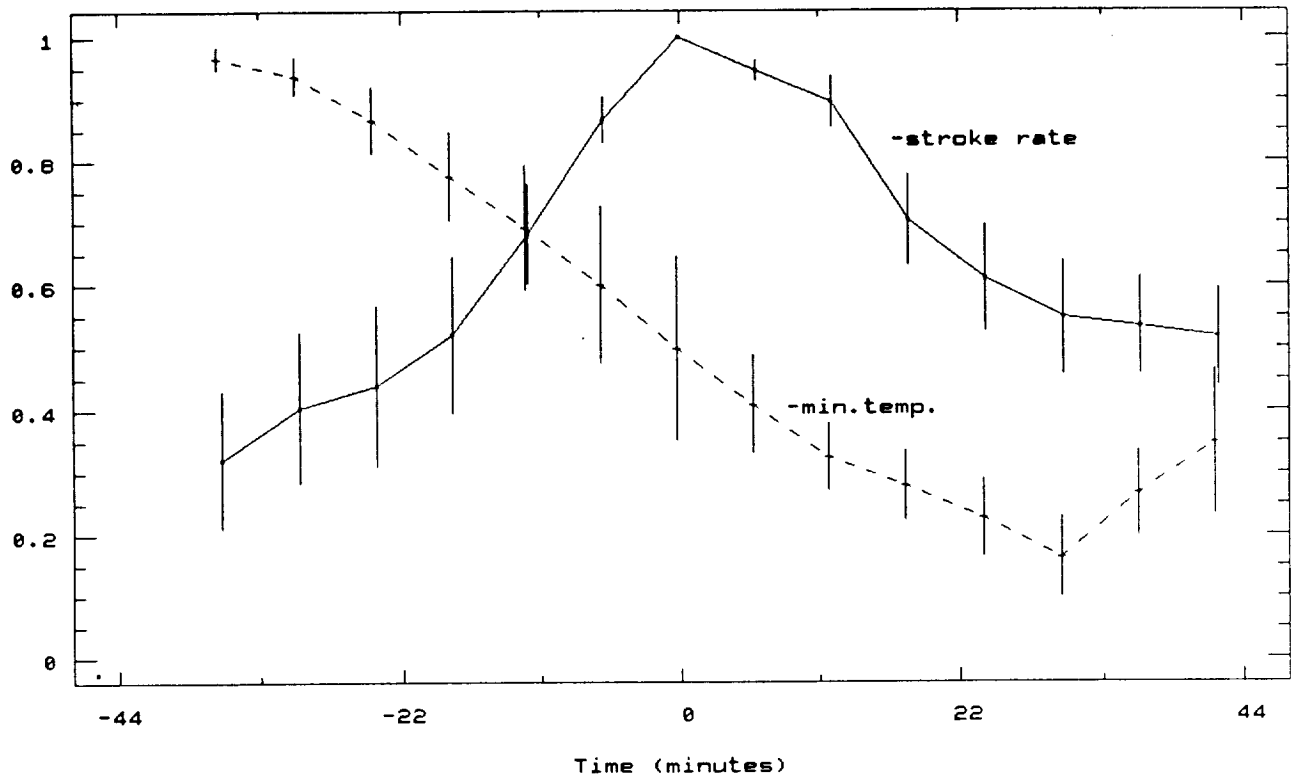

Study Two

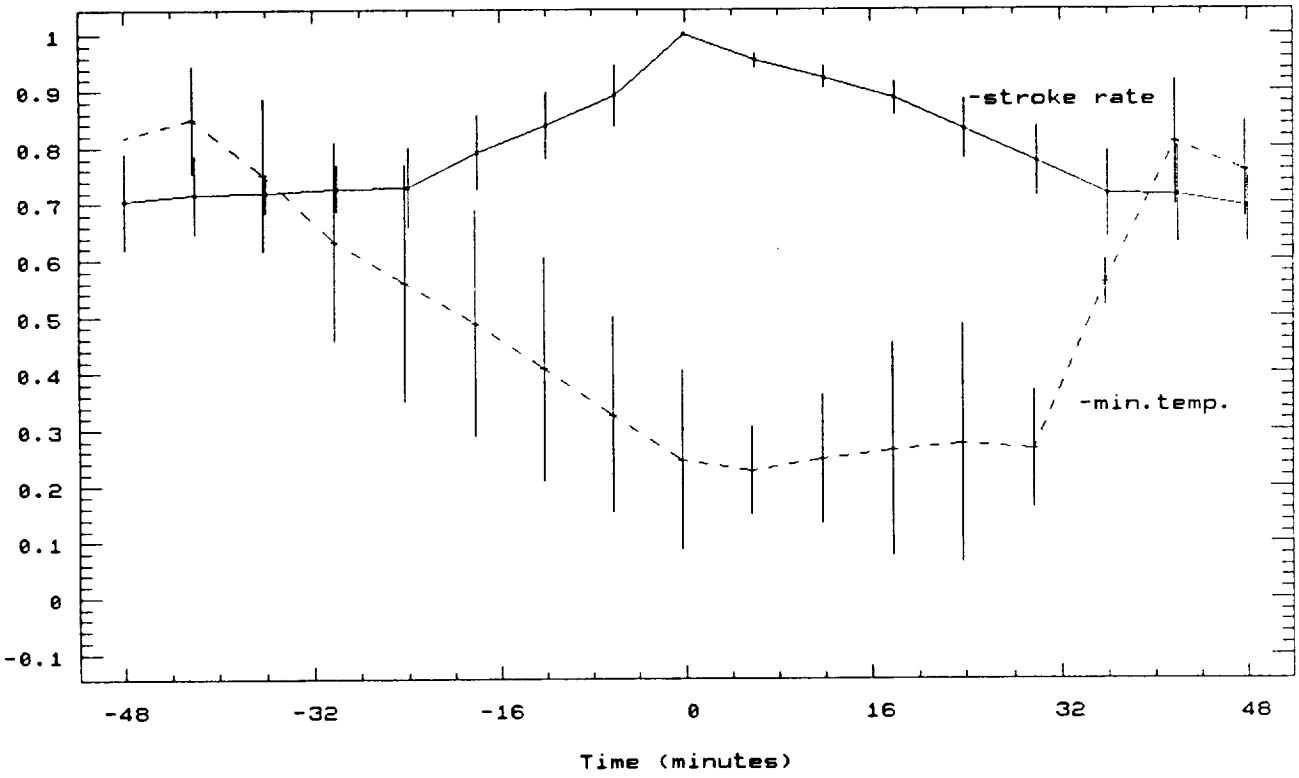

Figure 22

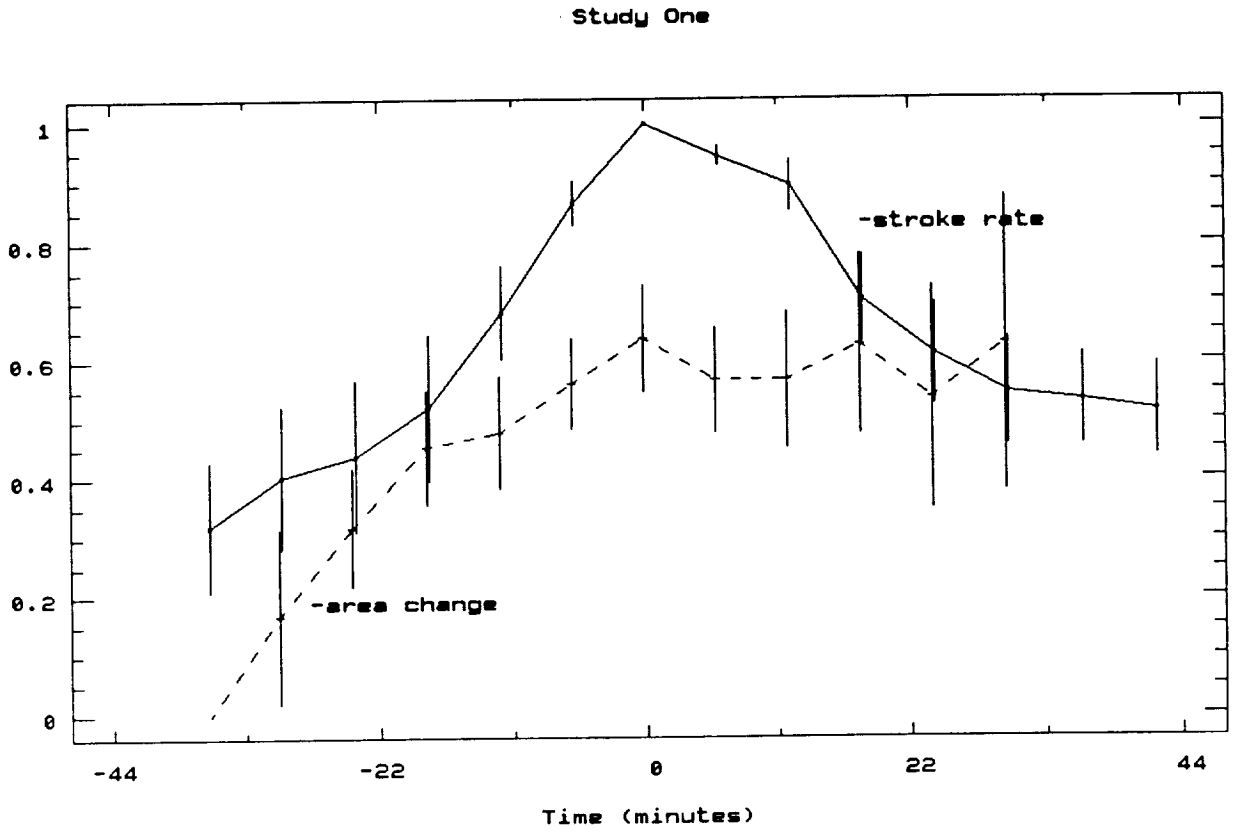
Study One
1
0.8
0.6
0.4
0.2
0
-stroke rate
-area change
-44
-22
0
22
44
Time (minutes)

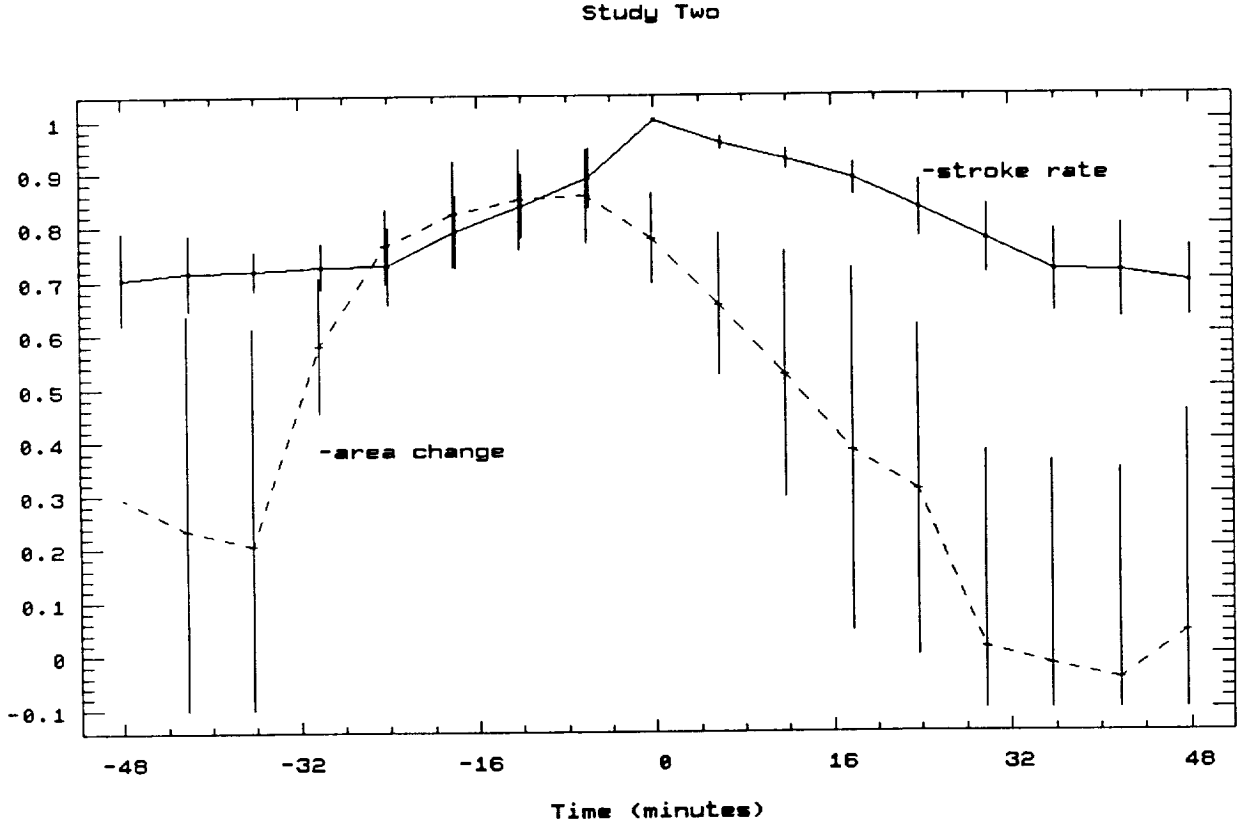
Study Two
1
0.9
0.8
0.7
0.6
0.5
0.4
0.3
0.2
0.1
0
-0.1
-stroke rate
-area change
-48
-32
-16
0
16
32
48
Time (minutes)

Figure 23

240 K) lightning producing clouds.

The lag we have found between cloud top temperatures and stroke rate may correspond to a similar finding by Marshall and Winn (1982);Ziegler et al.(1986). Using time lapse photography, the authors show a five minute lag between peak flash rates and observed cloud top heights in a isolated mountain thunderstorm. Although the lag time was much shorter than ours, so also was the scale of the clouds.

For anvil growth rate (Figure 23), the greatest increase occurs during the early increase in stroke rate. Twenty or twenty-five minutes prior to the lightning peak, area tends to level off. Thereafter, the growth rate in Study One remains almost steady, but drops precipitously for Study Two. As the error bars indicate, however, there is wide variation in the behavior of *dA/dt* 30 minutes before and 15 minutes after the lightning peak.

The slight lag of lightning compared with anvil growth rate is also supported in the literature. Rust et al.(1981) report that the total flash rate coarsely followed the changes in maximum updraft speed determined by Doppler radar. Goodman and MacGorman (1986) find that the most rapid expansion of the anvil cloud shield colder than 221 K occurs during the increase of flash rates to their peak. This characterization is especially apt for Study Two, a storm similar to their sample of MCC's.

What do these findings about anvil and lightning relationships suggest about the physical processes in the cumulonimbus relative to lightning? We can assume first of all that minimum anvil temperatures are roughly a measure of cloud top heights averaged over the 10 km instantaneous field of view of the satellite sensor. We may also associate anvil growth with the thunderstorm updrafts via the volume flux of air into the outflow region of the thunderstorm. Our results, then, indicate that the volume flux via the updraft and the growth of cloud tops are in some way temporally tied to charge separation and

generation of lightning. It would appear that in the mature stage of an updraft--when the core speed is large and cloud tops are growing--stroke rate increases. Subsequently, some critical point may be reached in the intensity of the weakening updraft which is no longer as conducive to electrical charge generation. In the anvil growth curve this is reflected in a leveling off or decline in the volume flux into the anvil.

Why minimum anvil temperatures should lag behind the peak in anvil growth is not completely clear. One reason might have to do with dynamics of the updraft. Although the maximum growth of the 226 K area would take place as or soon after the updraft core passes though this temperature level, the maximum cloud tops occur somewhat later as the core approaches the very top of the anvil (e.g. see Adler and Mack, 1986). This delay might be further lengthened by the resolution of the IR sensor. Although overshooting tops may begin to decline some minutes after the fall in *dA/dt* according to our "bubble" view of the updraft, the spreading out of the area of elevated tops may form a cold dome that becomes detectable in the infrared. Not until the larger cold dome begins to decay do we get an actual rise in IR temperatures.

As pointed out in our description of the Study Two storm, contributions to anvil growth appear to have come from a number of active areas, more than one of which might be in existence at any one time. These areas are evidenced by their colder temperatures and associated centers of lightning. If one center of anvil growth is in decline while another is contributing to anvil expansion, the combined effect on anvil growth rate may explain why the maximum *dA/dt* slightly preceeds peak flash rates in Study Two, but not in Study One. If these centers of growth were completely independent from one another, the results of the compositing might have been very ambiguous. On the contrary, the emergence of relationships that agree for both studies suggests a certain synchronicity among the growth, temperature change, and lightning frequency of these centers which

may be the result of a common forcing mechanism.

4.3 Conclusions

Broadly speaking, the studies presented here suggest a similar result: satellite measurements of cold cloud--either their minimum temperature, their fractional coverage or their growth--have a relationship to the flashrate and, in a more limited way, to the polarity and numbers of return strokes. Where we could compare results between diverse regions (i.e. Marshall and NSSL), our results, as far as we could tell, varied little by location.

With data obtained from NSSL and Marshall for a wide variety of storms over a period of several months, we found lightning, especially positive strokes, to be correlated with fractional cloud coverage, especially for cloud at or below 213 K. Regressions based on these coverages and minimum temperatures show r-squared's up to 0.66. Additional evidence for the dependence of lightning on temperature can be seen in the sharp rise in flashrates for cloud colder than 242 K.

In the case studies we have seen that minimum temperature declines and anvil growth rates rises as stroke rate increases. What happens thereafter is less clear. Growth rates level off or decline; temperatures do not appear to rise until a half-hour after peak flash rates but better IR satellite resolution might reveal that decay of smaller scale features such as overshooting tops occurs more closely to the time of peak flash rates. Like fractional cloud coverage and minimum temperatures in our LLP studies, anvil temperature change and growth rates may have a good statistical relationship with the actual flash rates. From a small sample of case studies, however, we can only establish qualitative relationships.

A number of studies using modeling or actual data from individual storms have shown that the charging mechanisms most likely to be responsible for

thunderstorm electrification work within a preferred temperature range (e.g. Ziegler et al., 1986). Others have shown the close proximity of lightning source regions to the updraft and high radar reflectivities (Ray, et al., 1987). Our results seem to confirm these relationships. Significant flashrates (more than a few strokes an hour) are found only when cloud tops reach a certain temperature level. Thereafter, falling cloud top temperatures and increasing rates of updraft-induced anvil expansion are coincident with the increase in flash rate. Our statistics suggest that cloud temperature and coverage information from even a single summer IR satellite image are sufficient to make a useful estimate of the flashrate associated with the measured cloud.

5.0 Recommendations for Future Work

There are some obvious possibilities for future lightning research based on what we have presented here. The connections we have drawn in this report between lightning and satellite cloud could very possibly be improved if comparisons were made on a storm-by-storm basis over a large sample. In such an approach, it would be worthwhile to categorize the storms according to some objective criteria. For example, some of differences between the behavior of our Study One and Two set for storms may be due to differences in the relative sizes and lifetimes of the storms detailed in Table 4. Other bases of comparisons might be a multi-cell/supercell or linear (squall-line)/clustered (MCC) convection contrast. If lightning is closely related to updraft strength and location, and cloud heights and temperatures, then there may be ways in which lightning phenomenology varies depending on the configuration of these related characteristics.

In this work, we did not pay close attention to stroke location. Making a precise determination of location relative to satellite features would have required quality-controlled data not available at the time. Obtaining such data should be less of a problem in the future. Having them will allow other satellite-observable features such as overshooting tops and individual temperature features to be tracked relative to centers of lightning activity. In what quadrant of the storm does lightning usually occur? How does shear location and magnitude affect lightning behavior? We still have little understanding of how severe lightning relates in time and space to other severe weather phenomena. Satellite comparisons should help create an integrated picture.

Studies of lightning and radar reflectivities are another possibility. We have begun to acquire a picture of where lightning occurs relative to centers of

reflectivity. It would be helpful to extend these results so that reflectivities can be related more directly to flashrate; and, alternatively, lightning frequency and location can be an additional input into remote rainfall estimation schemes.

Finally, the extention of existing lightning networks to cover virtually the entire U.S. makes a vast quantity of accessible data available to the future researcher. Geographical and topographical comparison should be possible on a wider scale and on a better statistical base than ever before.

LIST OF ILLUSTRATIONS

10 /s). Positive vorticity is stippled. 00 GMT, 8 September 1985.

Figure 15: 200 mb streamlines and isotachs (m/s). Areas of speed exceeding 25 m/s are stippled. 00 GMT, 8 September 1985.

Figure 16: Sounding of temperature and dewpoint temperature at Green Bay, Wisconsin, plotted on a skew-T, log P diagram. Winds (with speeds in m/s) are plotted on the right side. The inset, upper center, show temperature and dewpoint temperature for Peoria, IL. 00 GMT, 8 September 1985.

Figure 17: Tropopause temperature (C). 00 GMT, 8 September 1985.

Figure 18: Thunderstorm outlines. Each contour outlines cumulonimbus cloud at the time of an image. Outlines were sketched on tracing paper laid over a photographic print. The nominal interval between successive images is one-half hour. (a) 2130 GMT, 7 September to 0200 GMT, 8 September, 1985. (b) 0231 to 1131 GMT, 8 September, 1985.

Figure 19: As for Figure 18, except 2000 GMT, 8 September to 0300 GMT, 9 September and 0400 to 0500 GMT, 9 September, 1985. Note change in scale. The line of crosses marks successive positions of the brightness-weighted center of the second Minnesota storm.

Figure 20: The solid line in both plots shows smoothed lightning stroke rate (strokes/h) associated with the Study Two anvil over time (GMT). The error bars show one standard error. Plot (a) also shows anvil minimum temperature (K) at each infrared image time while Plot (b) shows smoothed rate of anvil expansion (km /h). The time period covered is 2030 GMT, September 8 to 0500 GMT, September 9, 1985. Strokes rates and anvil expansion rates were smoothed using a 3 term running average. Anvil expansion rates were calculated using the 226 K infrared isotherm. Points on the curves compared in each plot were offset slightly on the time scale to allow the error bars to be distinguished from one another.

Figure 21: Same as Figure 20, except for divergence and stroke rate.

Figure 22: Normalized composites of smoothed stroke rate versus minimum anvil temperature for (a) the six anvils of Study One and, (b) the main anvil of Study Two. The error bars show one standard error. The maximum stroke rate observed in connection with each anvil was set arbitrarily to 1.0 and all other rates converted to fractions of this rate. Times along the x axis are relative to the time of the peak stroke rate. Minimum temperatures normalized between 0 (lowest temperature observed over the 80 minute period) and 1 (highest temperature observed) are shown at times relative to the peak flash rate.

Figure 23: Same as Figure 21 except that the normalized composite is for smoothed stroke rate versus smoothed anvil rate of expansion. The largest positive rate was set to 1.0 while the largest negative rate was set to -1.0.

Table 1: NSSL and Marshall statistics for basic variables--sample size (n), mean, standard deviations and maximum and minimum values for study samples of: fractional cloud coverages (*f273,f243,f213*), the mean brightness gradient (*gdmean*), minimum IR temperature (*tmin*), total number of strokes in 60 and 30 minutes intervals (*n60,n30*), number of positive strokes in 30 minutes intervals (*n30p*), number of return strokes (*nr*), and magnitudes of negative and positive strokes (*i30n,i30p*).

Table 2: NSSL and Marshall correlations coefficients between the basic variables (the same as those listed under Table 1). The shaded area highlights the coefficients discussed in detail in the text.

Table 3: Diurnal variations of basic lightning variables at NSSL and Marshall. Sample size, mean, maximum and minimum values for *n30*, *n30p*, *nr*, *i30n*, and *i30p*.

Table 4: Case study anvil measurement and associated electrical features.

REFERENCES

Adler, R.F. and R.A. Mack, 1986: Thunderstorm cloud top dynamics as inferred from satellite observations and a cloud top parcel model. *J. Atmos. Sci.*, 43, 1945-1960.

Adler, R.F., M.J. Markus, and D.D. Fenn, 1985: Detection of severe midwest thunderstorms using geosynchronous satellite data. *Mon. Wea. Rev.*, 113, 769-781.

Adler, R.F., and A.J. Negri, 1987: A satellite infrared technique to estimate tropical convective and stratiform rainfall. Submitted to *J. Clim. Appl. Meteor.*

Battan, L.J., 1965: Some factors governing precipitation and lightning from convective clouds. *J. Atmos. Sci.*, 22, 79-84.

Brook, M., M. Nakano, and P. Krehbiel, 1982: The electrical structure of the Hokuriku winter thunderstorm. *J. Geophys. Res.*, 87, 1207-1215.

Cherna, E.V., and E.J. Stansbury, 1986: Sferics rate in relation to thunderstorm dimensions. *J. Geophys. Res.*, 91, 8701-8707.

Clifton, K.S., and C.K. Hill, 1980: Low-light-level television measurements of lightning. *Bull. Amer. Meteor. Soc.*, 61, 987-992.

Goodman, S.J., and D.R. MacGorman, 1986: Cloud-to-ground lightning activity in mesoscale convective complexes. *Mon. Wea. Rev.*, 114, 2320-2328.

Holle, R.L., and M.W. Maier, 1982: Radar echo height related to cloud-ground lightning in south Florida. *Preprints 12th Conf. Sev. Loc. Storms*, Amer. Meteor. Soc., San Antonio, 330-333.

Kitterman, C.G., 1980: Characteristics of lightning from frontal system thunderstorms. *J. Geophys. Res.*, 85, 5503-5505.

Krider, E.P., R.C. Noggle, and M.A. Uman, 1976: A gated, wideband magnetic direction finder for lightning return strokes. *J. Appl. Meteor.*, 15, 301-306.

Lee, A.C.L., 1986: An experimental study of the remote location of lightning flashes using a VLF arrival time difference technique. *Quart. J. Roy. Meteor. Soc.*, 112, 203-229.

Lo, C.S., W.R. Barchet, and D.W. Martin, 1982: Vertical mass transport in cumulonimbus clouds on Day 261 of GATE. *Mon. Wea. Rev.*, 110, 1994-2004.

Lopez, R.E., and R.L. Holle, 1986: Diurnal and spatial variability of lightning activity in northeastern Colorado and central Florida during the summer. *Mon. Wea. Rev.*, 114, 1288-1312.

Lyons, W.A., K.G. Bauer, R.B. Bent, and W.H. Highlands, 1985: Wide area real-time thunderstorm mapping using LPATS--the lightning position and tracking system. *Second AMS Conference on Aviation Weather Systems*, Ed., Amer. Meteor. Soc., Montreal.

MacGorman, D.R., M.W. Maier, and W.D. Rust, 1984: Lightning strike density for the contiguous United States from thunderstorm duration records. *Publication NUREG/CR-3759*, Ed., Nuclear Reg. Com., Washington, D.C., 26pp.

Mach, D.M., D.R. MacGorman, W.D. Rust, and R.T. Arnold, 1986: Site errors and detection efficiency in a magnetic direction-finder network for locating lightning strikes to ground. *J. Atmos. Oceangr. Tech.*, 3, 67-74.

Maier, M.W., and E.P. Krider, 1982: A comparative study of the cloud-to-ground lightning characteristics in Florida and Oklahoma thunderstorms. *Preprints 12th Conf. Sev. Loc. Storms*, Ed., Amer. Meteor. Soc., San Antonio, 334-337.

Marshall, T.C. and W.P. Winn, 1982: Measurements of charged precipitation in a New Mexico thunderstorm: lower positive charge centers. *J. Geophys. Res.*, 87, 7141-7157.

Mazur, V., J.C. Gerlach and W.D. Rust, 1984: Lightning flash density versus altitude and storm structure from observations with UHF- and S-Band radars. *Geophys. Res. Let.*, 11, 61-64.

Mazur, V., W.D. Rust and J.C. Gerlach, 1986: Evolution of lightning flash density and reflectivity structure in a multicell thunderstorm. *J. Geophys. Res.*, 91, 8690-8700.

Ogawa, T., 1982: The lightning current. *Handbook of Atmospherics. Vol.1*, Ed. H. Volland, CRC Press, Boca Raton, FL, 23-63.

Orville, R.E., R.W. Henderson, and L.F. Bosart, 1983: An east coast lightning detection network. *Bull. Amer. Meteor. Soc.*, 64, 1029-1037.

Orville, R.E., R.A. Weisman, R.B. Pyle, R.W. Henderson, and R.E. Orville jr., 1987: Cloud-to-ground lightning flash characteristics from June 1984 through May 1985. *J. Geophys. Res.*, 92, 5640-5644.

Peckham, D.W., M.A. Uman, and C.E. Wilcox, 1984: Lightning phenomenology in the Tampa Bay area. *J. Geophys. Res.*, 8, 11789-11805.

Piepgrass, M.V., E.P. Krider, and C.B. Moore, 1982: Lightning and surface rainfall during Florida thunderstorms. *J. Geophys. Res.*, 87, 11193-11201.

Ray, P.S., D.R. MacGorman, and W.D. Rust, 1987: Lightning location relative to storm structure in a supercell storm and a multicell storm. *J. Geophys. Res.*, 92, 5713-5724.

Reap, R.M., 1986: Evaluation of cloud-to-ground lightning data from the western United States for the 1983-84 summer seasons. *J. Clim. Appl. Meteor.*, 25, 785-799.

Rust, W.D., D.R. MacGorman, and R.T. Arnold, 1981: Positive cloud-to-ground

lightning flashes in severe storms. *Geophys. Res. Let.*, 8, 791-794.

Rust, W.D., W.L. Taylor, and D.R. MacGorman, 1981: Research on electrical properties of severe thunderstorms in the Great Plains. *Bull. Amer. Meteor. Soc.*, 62, 1286-1293.

Schütte, T., O. Salka and S. Israelsson, 1987: The use of the Weibull distribution for thunderstorm parameters. *J. Clim. Appl. Meteor.*, 26, 457-463.

Sikdar, D.N., and C.E. Anderson, 1970: Convective transport of mass and energy in severe storms over the United States--an estimate from a geostationary altitude. *Tellus*, 22, 522-531.

Stansbury, E.J., and J.S. Marshall, 1978: Sferics at two stations compared with radar-observed precipitation. *Atmos. Ocean*, 16, 281-292.

Wallace, J.M., 1975: Diurnal variations in precipitation and thunderstorm frequency over the conterminous United States. *Mon. Wea. Rev.*, 103, 406-419.

Williams, S.F., H.M. Goodman, K.R. Knupp, and J.E. Arnold, 1987: Space/COHMEX Data Inventory Document, *NASA Tech. Memo. 4006*, NASA, Washington, D.C. 20546, 480 pp.

Ziegler, C.L., P.S. Ray, and D.R. MacGorman, 1986: Relations of kinematics, microphysics and electrification in an isolated mountain thunderstorm. *J. Atmos. Sci.*, 43, 2098-2114.

APPENDIX A

LISTING OF 1985 OKLAHOMA NSSL LIGHTNING NETWORK DATA

day	time	f273	f243	f213	gdmean	tmin	n60	n30	nr	n30p	i30n	i30p
135	1201	4.00	0.00	0.00	0.3	266	0	0		0		
136	1	55.17	2.64	0.00	0.9	234	0	0		0		
136	1201	11.75	0.00	0.00	1.1	244	0	0		0		
137	0	35.85	22.73	7.62	1.0	203	50	31	2.71	2	-98.88	450.85
137	1201	29.96	6.90	0.00	1.0	223	0	0		0		
138	1	46.41	10.97	0.00	1.1	225	0	0		0		
138	1201	45.16	1.26	0.00	0.6	230	0	0		0		
139	1	16.24	0.79	0.00	1.8	234	0	0		0		
139	1202	26.99	2.21	0.00	1.4	224	0	0		0		
140	1	63.54	35.06	4.72	1.9	205	648	347	2.71	6	-117.98	276.20
140	1201	55.38	20.34	0.73	1.5	211	275	141	2.61	1	-212.06	503.90
141	0	73.97	55.19	8.57	1.3	206	1015	559	2.74	11	-147.37	209.20
141	1201	70.56	32.40	0.00	0.9	218	5	4	2.25	1	-46.77	155.10
142	1	46.23	17.29	0.00	1.9	218	20	5	1.60	0	-190.88	
142	1201	41.84	13.90	0.00	1.4	214	22	13	1.54	2	-111.62	139.05
143	1	43.53	11.12	0.04	1.4	227	7	3	2.33	0	-127.93	
143	1201	15.29	0.00	0.00	1.1	244	3	2	1.50	0	-37.35	
144	1	18.83	12.17	0.00	1.9	215	17	8	1.88	0	-160.01	
144	1201	7.10	0.00	0.00	0.9	255	0	0		0		
145	1201	0.01	0.00	0.00	2.0	271	0	0		0		
146	1	17.46	10.94	1.38	2.2	207	33	19	1.63	4	-106.89	205.63
146	1201	13.56	1.03	0.00	1.8	227	0	0		0		
147	0	29.17	19.84	2.48	2.3	202	551	280	2.13	16	-143.17	264.70
148	1201	48.73	34.84	8.13	0.8	206	1080	549	2.89	9	-171.22	267.96
149	1201	21.32	15.69	1.70	1.1	209	162	80	2.49	6	-190.84	552.55
153	0	24.36	15.30	0.63	2.0	211	406	210	2.50	18	-126.41	219.21
153	1201	25.03	3.06	0.00	1.5	220	46	24	1.88	1	-139.17	46.90
154	1	15.79	8.81	2.13	2.0	206	358	241	2.67	23	-134.44	87.83
154	1201	73.40	23.92	0.00	1.1	221	83	42	2.00	0	-176.11	
155	0	67.93	57.79	25.96	0.9	199	1391	746	2.43	55	-154.13	228.71
156	0	85.15	70.56	12.67	0.7	200	834	444	2.32	41	-147.16	237.58
158	0	23.72	6.35	0.00	2.3	222	14	8	4.88	0	-315.40	
158	1201	0.65	0.00	0.00	2.0	248	0	0		0		
159	0	0.28	0.00	0.00	2.5	255	0	0		0		
159	1201	4.44	0.00	0.00	1.3	244	0	0		0		
160	1201	87.76	48.04	14.73	1.3	204	163	102	1.75	12	-148.60	372.30
161	0	29.41	5.64	1.14	2.5	204	289	185	2.49	13	-118.56	59.35
161	1200	56.90	21.16	8.71	1.4	199	1247	659	2.43	22	-147.61	188.12
162	1201	48.70	28.58	1.22	1.3	210	73	32	2.06	5	-152.27	290.20
163	0	10.30	0.01	0.00	1.6	242	12	10	1.30	2	-57.75	287.60
163	1201	39.81	8.12	0.00	0.6	216	26	13	1.92	1	-80.62	180.50
164	0	1.38	0.00	0.00	1.6	251	2	1	1.00	0	-38.70	
164	1201	19.12	0.00	0.00	0.9	245	0	0		0		
165	1	28.64	9.74	0.68	2.3	211	12	8	1.80	0	-101.61	
165	1205	37.02	11.83	0.00	1.5	215	23	3	1.00	1	-448.95	194.50
170	0	27.70	6.43	0.00	1.5	221	15	12	1.25	0	-275.03	
170	1201	2.09	0.00	0.00	0.9	261	0	0		0		
171	1	1.40	0.60	0.00	3.6	218	0	0		0		
171	1201	11.34	1.51	0.00	1.8	221	0	0		0		
172	1201	30.95	14.23	1.15	1.7	211	57	18	2.11	1		
173	0	32.86	26.28	6.92	1.5	201	1056	615	2.64	71		
174	1	0.74	0.01	0.00	3.1	239	11	5	2.40	0	-86.30	
174	1201	6.91	4.69	0.35	1.3	212	43	26	2.62	7		
175	0	25.20	19.65	7.55	1.7	201	420	258	2.31	51		
175	1200	15.84	0.55	0.00	2.1	235	2	1	1.00	1		121.30
176	0	5.91	2.92	0.00	2.0	216	2	2	1.50	0		
180	1	0.00	0.00	0.00		276	0	0		0		
183	1	24.29	4.22	1.32	1.5	209	5	4	1.00	3	-122.30	469.97
183	1201	46.91	4.65	0.00	1.4	226	15	6	1.33	0	-140.62	
184	1	35.05	15.48	3.36	2.0	204	369	189	2.89	0	-133.31	
184	1200	45.25	27.60	3.15	1.1	206	354	206	2.56	5	-156.37	210.52
185	0	10.48	5.70	1.18	2.5	206	70	35	2.23	2	-97.42	126.15
185	1201	13.66	4.40	0.00	2.5	222	96	56	2.25	0	-157.35	
186	0	14.64	9.57	0.40	2.3	210	323	141	2.44	3	-140.06	190.93
186	1201	0.89	0.00	0.00	2.9	250	0	0		0		
187	1	0.24	0.08	0.00	5.6	224	4	2	1.50	0	-83.00	
187	1201	0.00	0.00	0.00		276	0	0		0		
188	1	0.15	0.00	0.00	3.3	254	0	0		0		
188	1201	2.46	0.00	0.00	2.2	251	0	0		0		
189	1	0.02	0.00	0.00	2.5	266	0	0		0		
189	1201	7.96	2.70	0.31	1.7	211	0	0		0		

day	time	f273	f243	f213	gdmean	tmin	n60	n30	nr	n30p	f30n	f30p
190	1	11.02	1.77	0.00	2.8	215	45	24	2.75	0	-145.26	
190	1201	17.47	2.80	0.00	1.7	223	0	0		0		
191	0	24.31	8.76	0.00	1.9	221	38	17	2.88	0	-111.88	
191	1201	19.63	1.58	0.00	1.7	228	0	0		0		
192	0	12.73	7.90	0.08	3.0	213	0	0		0		
192	1201	1.55	0.00	0.00	1.8	255	33	25	2.80	0	-98.24	
193	0	0.42	0.00	0.00	2.3	254	0	0		0		
193	1201	25.66	4.02	0.00	1.8	226	0	0		0		
194	0	10.15	0.23	0.00	2.1	235	0	0		0		
194	1201	24.13	1.30	0.00	1.6	227	0	0		0		
195	0	23.45	0.97	0.02	1.2	213	7	3	1.67	0	-112.23	
195	1201	25.46	3.18	0.00	1.9	224	1	0		0		
196	0	32.52	19.78	7.00	2.1	205	202	94	2.56	18	-127.86	290.54
196	1201	47.17	13.87	0.00	1.7	222	0	0		0		
198	1	16.55	8.05	1.37	2.7	203	204	136	2.40	1	-123.41	94.40
198	1201	6.07	0.08	0.00	1.9	232	35	21	3.33	1	-248.40	103.40
199	1	3.40	1.45	0.01	3.0	213	20	11	2.00	0	-74.76	
199	1201	32.47	11.85	5.11	1.6	201	208	97	2.55	2	-206.31	320.80
200	1	11.84	1.30	0.10	2.0	211	74	40	1.95	0	-133.56	
200	1201	41.66	25.98	7.10	1.1	203	105	41	2.12	2	-214.24	457.65
201	3	21.08	9.63	2.16	3.2	203	695	354	2.48	2	-150.23	106.75
201	1201	33.11	6.46	0.06	1.6	213	59	26	2.50	0	-203.33	
205	1	44.89	18.13	1.89	2.5	206	389	216	2.83	2	-153.96	153.50
205	1201	33.00	3.91	0.00	1.3	217	2	1	1.00	1		135.90
206	1	64.16	46.56	10.60	1.9	203	1928	1075	2.95	17	-146.06	204.12
206	1201	57.21	20.99	0.06	1.5	212	43	28	2.29	2	-170.29	404.25
207	1	31.55	15.05	1.36	2.2	206	183	93	2.66	3	-113.33	108.93
207	1201	21.81	3.73	0.00	1.7	222	30	17	2.00	0	-186.19	
208	1	17.19	2.46	0.26	2.6	204	71	37	2.89	0	-119.58	
208	1201	11.73	0.55	0.00	1.6	227	0	0		0		
209	1	3.76	0.88	0.00	3.1	221	17	10	1.90	0	-95.89	
209	1201	26.09	8.33	0.00	1.7	215	941	506	3.27	8	-167.50	191.66
210	1	25.85	6.66	0.08	1.8	209	37	21	1.95	1	-99.01	108.30
210	1201	70.74	34.06	0.00	1.0	215	50	28	2.07	3	-161.69	244.17
211	0	29.07	7.67	1.87	1.6	201	427	286	2.26	1	-121.87	114.60
211	1231	22.64	5.23	0.00	1.3	214	163	69	2.32	2	-222.72	433.10
212	1201	29.73	6.84	1.74	1.5	204	579	340	2.73	10	-155.28	256.71
213	1	11.18	7.97	4.21	3.1	204	662	383	2.84	3	-158.32	92.17
213	1201	9.36	2.50	0.00	2.1	217	232	101	3.20	1	-166.68	223.10
214	0	1.06	0.01	0.00	2.8	242	91	51	1.90	0	-95.53	
214	1201	40.95	4.40	0.00	1.6	227	3	2	1.50	0	-55.70	
215	1	22.33	3.93	0.60	1.7	206	205	121	2.59	1	-129.53	55.10
215	1201	36.61	18.36	10.32	1.9	196	1675	852	3.14	10	-152.78	241.42
221	0	0.14	0.02	0.00	6.6	236	9	4	2.00	0	-94.12	
221	1201	18.55	1.41	0.00	1.9	233	32	13	1.46	2	-102.95	399.75
222	0	30.47	23.94	14.22	1.5	196	5448	2915	3.21	28	-148.88	175.40
222	1201	32.31	1.85	0.00	1.7	225	4	1	1.00	0	-67.20	
223	1	4.85	0.73	0.00	3.6	228	71	39	2.10	0	-149.17	
223	1201	17.20	0.15	0.00	1.1	240	0	0		0		
224	0	18.07	4.27	0.62	2.0	208	248	155	3.13	0	-133.57	
224	1201	26.04	0.06	0.00	0.9	241	2	2	1.00	1	-63.30	319.10
225	0	24.66	11.15	0.28	2.9	209	386	196	2.27	3	-143.67	150.40
225	1201	40.93	8.56	0.00	1.5	218	6	2	1.50	0	-117.30	
226	1	56.42	37.00	10.02	1.8	200	2529	1437	2.79	45	-141.61	245.15
226	1201	74.85	31.31	0.00	1.1	218	16	8	1.63	5	-102.30	264.70
227	1	55.81	23.23	2.02	1.6	204	449	255	3.43	11	-168.53	178.35
227	1201	12.59	1.08	0.00	1.1	234	0	0		0		
228	1	5.77	2.55	0.02	1.4	213	22	9	1.33	0	-70.88	
228	1201	1.83	0.03	0.00	2.0	238	12	8	2.00	0	-151.49	
229	0	2.84	2.02	0.43	2.8	210	24	11	1.27	0	-116.68	
229	1201	17.07	6.71	0.00	1.8	217	631	362	2.63	1	-161.48	251.10
230	0	8.35	4.19	2.26	2.1	208	956	554	3.28	2	-195.77	68.45
230	1201	7.10	0.09	0.00	1.3	218	136	65	2.03	0	-182.26	
231	1	37.43	17.89	0.35	1.5	208	877	502	3.35	16	-103.34	98.05
236	1	41.48	26.01	10.43	1.3	201	1862	1051	2.64	24	-135.29	162.73
236	1200	40.16	12.26	0.00	1.5	221	99	64	2.48	0	-147.09	
237	0	1.29	0.02	0.00	2.6	241	9	6	1.67	0	-137.53	
237	1200	0.34	0.00	0.00	2.5	258	0	0		0		
239	1	0.98	0.34	0.00	3.1	218	4	4	1.25	0	-90.55	
239	1201	12.31	7.74	0.00	1.8	214	191	106	2.16	3	-128.26	220.63
242	1	0.23	0.00	0.00	1.6	262	0	0		0		

day	time	f273	f243	f213	gdmean	tmin	n60	n30	nr	n30p	i30n	i30p
242	1201	4.82	0.00	0.00	1.7	255	0	0		0		
243	1	2.25	1.31	0.00	4.0	214	0	0		0		
243	1201	0.00	0.00	0.00		277	0	0		0		
244	1201	6.86	1.36	0.00	1.7	228	0	0		0		
245	1	7.08	0.14	0.00	3.1	227	2	1	1.00	0	-72.90	
245	1201	9.51	2.98	0.00	1.8	218	16	7	1.71	0	-110.60	
246	1	9.37	4.08	0.00	2.2	216	66	39	3.15	0	-91.58	
246	1201	10.98	0.00	0.00	1.4	244	0	0		0		
247	1	10.69	1.29	0.00	2.0	230	6	5	1.40	2	-47.87	223.80
247	1201	26.59	6.48	0.05	1.8	213	75	29	1.72	0	-229.78	
248	1	10.73	1.30	0.03	2.0	211	95	56	2.73	5	-153.72	373.32
248	1201	0.04	0.00	0.00	0.8	271	0	0		0		
249	0	5.09	1.92	0.00	3.2	224	90	56	2.30	2	-146.63	118.90
249	1201	7.47	0.44	0.00	2.1	227	0	0		0		
250	1	12.19	5.35	0.65	2.5	206	31	19	2.47	0	-154.10	
250	1201	17.24	0.01	0.00	2.1	243	0	0		0		
251	0	18.50	7.17	0.00	2.7	219	8	4	1.50	0	-71.08	
251	1201	0.13	0.00	0.00	1.0	269	0	0		0		
252	1	15.32	9.15	0.98	2.5	206	778	429	3.05	17	-144.54	88.90
252	1201	22.74	1.98	0.00	1.5	229	0	0		0		

APPENDIX B

LIST OF 1985 NASA-MARSHALL LIGHTNING NETWORK DATA

day	time	f273	f243	f213	tmin	n60	n30	nr	n30p	i30n	i30p
178	2300	71.	33.	13.38	206	455	214	3.0	0	-43.05	
192	1101	44.	0.	0.00	254	1	1	1.0	0	-2.70	
192	2300	44.	20.	0.67	210	32	18	1.8	0	-11.99	
193	1101	0.	0.	0.00	273	1	1	1.0	0	-6.00	
193	2300	26.	3.	0.00	223	37	19	1.7	0	-22.39	
194	1101	28.	0.	0.00	261	1	0		0		
194	2300	44.	16.	0.00	223	51	30	1.8	0	-25.76	
195	1101	0.	0.	0.00	284	2	1	1.0	0	-1.80	
196	1101	43.	0.	0.00	261	1	0		0		
197	2300	71.	45.	3.95	212	90	40	2.1	1	-20.88	18.70
198	1101	0.	0.	0.00	286	0	0		0		
198	2301	0.	0.	0.00	286	2	0		0		
199	1101	0.	0.	0.00	284	0	0		0		
199	2301	0.	0.	0.00	278	0	0		0		
200	1101	0.	0.	0.00	288	0	0		0		
200	2301	0.	0.	0.00	278	0	0		0		
201	1101	0.	0.	0.00	287	1	0		0		
201	2301	0.	0.	0.00	284	0	0		0		
202	1101	5.	0.	0.00	246	6	4	1.3	0	-4.13	
203	2301	68.	41.	11.59	206	1103	610	2.7	5	-48.34	25.84
204	2301	73.	37.	0.00	223	6	4	1.8	0	-27.03	
205	1101	56.	2.	0.00	234	1	0		0		
205	2301	47.	2.	0.00	239	2	1	4.0	0	-12.10	
206	1101	0.	0.	0.00	275	1	1	1.0	0	-1.20	
206	2301	1.	0.	0.00	268	6	3	3.7	0	-14.37	
207	1101	98.	44.	0.00	214	46	24	1.8	3	-53.77	33.97
207	2301	100.	71.	39.76	199	110	34	2.2	2	-56.68	42.00
208	1101	100.	24.	0.00	223	0	0		0		
208	2301	63.	19.	0.00	218	3	1	1.0	0	-0.20	
209	1101	85.	0.	0.00	252	1	0		0		
209	2301	32.	1.	0.00	226	9	9	2.1	0	-67.30	
210	1101	19.	0.	0.00	262	0	0		0		
210	2301	26.	0.	0.00	247	3	3	2.3	0	-14.20	
211	2301	66.	32.	5.08	208	45	29	3.0	0	-57.16	
212	1101	0.	0.	0.00	274	0	0		0		
212	2301	22.	3.	0.00	229	48	31	3.0	0	-56.65	
213	1101	58.	32.	0.00	214	10	5	2.0	1	-10.90	21.40
213	2300	61.	54.	37.67	201	920	501	2.8	9	-63.38	77.60
214	1101	0.	0.	0.00	284	0	0		0		
214	2301	0.	0.	0.00	277	2	2	1.0	0	-5.45	
215	1101	0.	0.	0.00	279	0	0		0		
215	2301	74.	0.	0.00	240	0	0		0		
216	1101	41.	0.	0.00	250	3	2	1.0	0	-2.55	
216	2301	0.	0.	0.00	272	1	0		0		
217	1101	19.	0.	0.00	266	2	2	1.0	0	-1.45	
218	1101	52.	0.	0.00	241	0	0		0		
219	2359	96.	0.	0.00	244	2	2	1.5	0	-9.70	
219	1101	94.	1.	0.00	236	11	6	2.5	0	-148.53	
219	2300	25.	0.	0.00	242	4	2	1.5	0	-31.50	
220	1101	0.	0.	0.00	273	0	0		0		
220	2300	4.	0.	0.00	237	0	0		0		
221	1101	0.	0.	0.00	286	0	0		0		
221	2300	1.	0.	0.00	255	6	2	3.0	0	-23.05	
222	1101	0.	0.	0.00	288	0	0		0		
222	2301	11.	0.	0.00	245	1	0		0		
223	1101	0.	0.	0.00	269	1	0		0		
223	2300	6.	1.	0.00	233	1	1	1.0	0	-28.00	
224	1101	0.	0.	0.00	289	0	0		0		
224	2300	0.	0.	0.00	279	0	0		0		
225	1101	0.	0.	0.00	286	0	0		0		
225	2301	0.	0.	0.00	286	0	0		0		
226	1101	1.	0.	0.00	263	0	0		0		
226	2300	41.	15.	0.20	212	13	6	1.7	0	-5.77	
227	1101	40.	0.	0.00	255	3	2	4.5	0	-13.75	
228	2300	100.	96.	14.73	210	0	0		0		
229	1101	0.	0.	0.00	278	0	0		0		
229	2300	0.	0.	0.00	278	2	1	1.0	0	-8.10	
230	1101	0.	0.	0.00	284	0	0		0		
230	2301	0.	0.	0.00	290	2	1	1.0	0	-8.10	
231	1101	0.	0.	0.00	288	0	0		0		
232	1101	64.	12.	0.00	233	5	3	4.3	0	-18.50	

day	time	f273	f243	f213	tmin	n60	n30	nr	n30p	i30n	i30p
232	2301	30.	18.	0.00	221	136	86	2.6	1	-53.69	28.80
233	1101	0.	0.	0.00	285	0	0		0		
233	2300	1.	0.	0.00	267	0	0		0		
234	1100	0.	0.	0.00	281	0	0		0		
234	2300	36.	0.	0.00	250	0	0		0		
235	1100	51.	0.	0.00	250	0	0		0		
235	2300	32.	0.	0.00	252	1	0		0		
236	1100	98.	35.	0.00	214	276	172	2.6	1	-50.61	10.40
236	2300	100.	100.	15.18	208	42	20	2.5	4	-17.41	87.65
237	1100	63.	3.	0.00	241	1	1	1.0	0	-8.50	
238	2300	91.	49.	0.00	221	0	0		0		
239	1100	78.	22.	0.00	231	0	0		0		
239	2301	5.	0.	0.00	243	14	10	1.3	1	-51.01	81.20
240	1101	0.	0.	0.00	288	0	0		0		
240	2301	0.	0.	0.00	280	0	0		0		
241	2301	0.	0.	0.00	286	0	0		0		
242	1101	0.	0.	0.00	283	0	0		0		
242	2301	35.	13.	0.00	227	198	115	2.9	2	-45.50	25.85
243	1101	0.	0.	0.00	279	0	0		0		
243	2301	0.	0.	0.00	281	0	0		0		
244	1101	0.	0.	0.00	285	0	0		0		
244	2301	0.	0.	0.00	288	0	0		0		
245	1100	0.	0.	0.00	285	0	0		0		
245	2301	3.	0.	0.00	254	0	0		0		
246	1101	0.	0.	0.00	275	0	0		0		
246	2301	30.	8.	0.00	218	3	0		0		
247	1101	0.	0.	0.00	276	0	0		0		
247	2301	3.	0.	0.00	265	1	0		0		
248	1101	24.	1.	0.00	241	5	3	3.3	0	-12.73	
248	2300	96.	12.	0.00	229	0	0		0		
249	1100	33.	0.	0.00	261	0	0		0		
249	2300	4.	0.	0.00	268	0	0		0		
250	1100	10.	0.	0.00	269	0	0		0		
250	2300	3.	1.	0.00	233	8	3	1.7	0	-8.80	
251	1100	0.	0.	0.00	290	0	0		0		
251	2300	6.	1.	0.00	229	60	24	2.1	0	-23.30	
253	1101	0.	0.	0.00	286	0	0		0		
253	2300	66.	37.	0.00	216	222	174	2.8	3	-62.37	30.30
254	1101	2.	0.	0.00	265	0	0		0		
254	2301	0.	0.	0.00	286	3	3	1.3	0	-6.23	
255	1101	0.	0.	0.00	285	0	0		0		
255	2301	0.	0.	0.00	283	0	0		0		
256	1101	8.	0.	0.00	262	0	0		0		
256	2301	0.	0.	0.00	277	0	0		0		
257	1101	32.	0.	0.00	254	0	0		0		
257	2301	88.	5.	0.00	236	0	0		0		
258	1101	61.	1.	0.00	241	0	0		0		
258	2301	34.	0.	0.00	250	0	0		0		
259	1101	9.	0.	0.00	258	0	0		0		
259	2300	0.	0.	0.00	256	0	0		0		
260	1101	0.	0.	0.00	273	0	0		0		
260	2301	0.	0.	0.00	288	0	0		0		
261	1101	0.	0.	0.00	284	0	0		0		
261	2301	0.	0.	0.00	287	0	0		0		
262	1101	0.	0.	0.00	283	0	0		0		
262	2301	0.	0.	0.00	289	0	0		0		
263	1101	0.	0.	0.00	284	0	0		0		
263	2301	0.	0.	0.00	289	0	0		0		
264	1101	0.	0.	0.00	280	0	0		0		
264	2301	0.	0.	0.00	279	0	0		0		
265	1101	0.	0.	0.00	281	0	0		0		
265	2301	0.	0.	0.00	279	0	0		0		
266	1101	82.	16.	0.00	228	0	0		0		
266	2301	100.	67.	0.00	221	2	0		0		
267	1101	15.	0.	0.00	247	0	0		0		
267	2301	12.	0.	0.00	255	0	0		0		
268	1101	0.	0.	0.00	277	0	0		0		
268	2301	1.	0.	0.00	260	2	0		0		
269	1101	76.	15.	0.00	218	109	50	3.2	0	-58.01	
269	2301	0.	0.	0.00	280	0	0		0		
270	1101	12.	0.	0.00	265	0	0		0		

day	time	f273	f243	f213	tmin	n60	n30	nr	n30p	l30n	l30p
270	2301	0.	0.	0.00	281	0	0		0		
271	1100	0.	0.	0.00	276	0	0		0		
271	2301	0.	0.	0.00	285	0	0		0		
272	1101	19.	0.	0.00	254	0	0		0		
272	2301	1.	0.	0.00	271	0	0		0		
273	1101	7.	0.	0.00	256	0	0		0		